KASTAMONU UNIVERSITY JOURNAL OF ENGINEERING AND SCIENCES

e-ISSN 2667-8209

CİLT : 05 SAYI 01
VOL : 05 ISSUE 01

KASTAMONU UNIVERSITY JOURNAL OF ENGINEERING AND SCIENCES

e-ISSN 2667-8209

Kastamonu Üniversitesi Mühendislik ve Fen Bilimleri Dergisi

Kastamonu University Journal of Engineeering and Science

Kastamonu Üniversitesi Mühendislik ve Fen Bilimleri Dergisi Hakemli bir dergidir ve yılda 2 defa yayınlanır

Kastamonu Üniversitesi Mühendislik ve Fen Bilimleri Dergisi

Kastamonu University Journal of Engineeering and Science

Cilt: 5	No:1	Haziran 2019	Vol: 5	Issue: 1	June 2019	E-ISSN:2667-8209

Kastamonu Üniversitesi Mühendislik ve Fen Bilimleri Dergisi

Kastamonu University Journal of Engineeering and Science

Cilt: 5	No:1	Haziran 2019	Vol: 5	Issue: 1	June 2019	E-ISSN:2667-8209

Kastamonu Üniversitesi Mühendislik ve Mimarlık Fakültesi 37100- Kastamonu / TÜRKİYE

Tel: +(90)366 2802901 Fax: +(90)366 2802900

Web: http://dergipark.ulakbim.gov.tr/kastamonujes

e-mail: kujes@kastamonu.edu.tr

Bu dergi yılda iki defa yayınlanır. **This journal is published two times in a year.**

(Haziran-Aralık) **(June-December)**

Kastamonu University Journal of Engineeering and Science
Indexed and Abstracted in: Dergipark

Kastamonu Üniversitesi Mühendislik ve Fen Bilimleri Dergisi

Kastamonu University Journal of Engineeering and Science

Cilt: 5	No:1	Haziran 2019	Vol: 5	Issue: 1	June 2019	E-ISSN:2667-8209

İÇİNDEKİLER/ CONTENTS

Kastamonu University
Journal of Engineering and Sciences
e-ISSN 2667-8209
http://dergipark.gov.tr/kastamonujes

Kinetic Study on Copper Leaching in Electroplating Waste Sludge Using Ammonium Nitrate Solution

Gediz Uğuz[1*], Feza Geyikçi[1]

[1]*Department of Chemical Engineering, Ondokuz Mayıs University, Samsun, Turkey*

ARTICLE INFO

Received: March:29.2019
Reviewed: April:30.2019
Accepted: May:22.2019

Keywords:
Ammonium nitrate,
Copper,
Kinetic model,
Leaching,
Waste sludge.

Corresponding Author:
[*]E-mail:gedizuguz55@gmail.com

ABSTRACT

The electroplating process, which is based on coating the surface of materials with electric current and various heavy metals, has a significant share in the industry. Heavy metals such as copper iron, which is present in the resulting slurry of electroplating process, threaten the environmental health. For this reason, these threats must be eliminated or minimized. In this study, electroplating waste sludge (EWS), which is an oxidized copper waste sludge, is leached with alkali reagents called ammonium nitrate solution (ANS). The effects of parameters on the leaching were examined, and a kinetic model was developed. As a result of the study, the leaching rate increased with increasing concentration of reagent solution, temperature, and stirring speed, as well as decreasing dimension of the solid particle and solid to reagent solution ratio. It was determined that the leaching reaction followed the mixed kinetic controlled model, which includes two different leaching processes together with reaction below 303 K to 323 K and diffusion above 323 K to 343 K. The activation energies were calculated as 84.62 and 28.85 kJ/mol, respectively.

Anahtar Kelimeler:
Amonyum nitrat
Bakır
Kinetik model
Çözeltme
Atık çamur

ÖZ

Malzemelerin yüzeyinin elektrik akımı ve çeşitli ağır metallerle kaplanmasına dayanan elektro kaplama işlemi sektörde önemli bir paya sahiptir. Elde edilen galvanik işlem bulamacında bulunan bakır demir gibi ağır metaller çevre sağlığını tehdit eder. Bu nedenle, bu tehditler ortadan kaldırılmalı veya en aza indirilmelidir. Bu çalışmada, oksitlenmiş bakır atık çamuru olan galvanik atık çamur (EWS), amonyum nitrat çözeltisi (ANS) adı verilen alkali reaktiflerle süzülüyor. Parametrelerin liç üzerindeki etkileri incelenmiş ve kinetik bir model geliştirilmiştir. Çalışma sonucunda, leaktif oranı, reaktif çözeltisinin konsantrasyonu, sıcaklık ve karıştırma hızının yanı sıra katı partikül ve katı maddenin reaktif çözelti oranının azaltılması ile birlikte artmıştır. Liç reaksiyonunun, 303 K ila 323 K'nin altındaki reaksiyonla ve 323 K ila 343 K'nin üzerindeki difüzyonla birlikte iki farklı liçleme prosesini içeren karışık kinetik kontrollü modeli takip ettiği belirlenmiştir. Sırasıyla, aktivasyon enerjileri 84.62 ve 28.85 kJ / mol olarak hesaplanmıştır.

1. Introduction

There are many objects composed of various materials in our surroundings and these objects range from small and simple parts up to large and complex parts respectively such as from accessories to machinery parts. These parts are coated with additional material to protect against corrosion, improving some of their properties and beautifying the objects. Metal coating is one of the conventional techniques used for coating these various parts. This chemical process is carried out in the presence of an electrical field and is known as ‘’electroplating’’. In this process, the surface of the prewashed substances is coated with deposition of specific metals by rinsing in a coating bath. The concentration of the metal ions increases and the efficiency of the coating process decreases because of repeated recirculation of the bath liquids. Hence, the contaminated baths are required to change with a fresh solution [1, 2]. For this reason, large amounts

of liquid waste is generated called wastewater after this chemical process. These wastewaters contain harmful and toxic subtances such as heavy metals [3].

With the treatment of the wastewater, a large amount of waste sludge is produced and this valuable sludge is called EWS that is a complex mixture and hazardous solid waste, containing various heavy metals (Cu, Cr, Zn, Ni, Fe). In this respect, it is referred to be a potential valuable resource. For humans, exposure to these heavy metals can cause various diseases such as cancer, hypertension and renal dysfunction. These valuable heavy metals can be effectively cleared from the sludge with certain methods, then the filtered sludge and the remaining heavy metals can be reused.

It has importance that the to perform economic recycling and recovery of heavy metals from the sludge to the highest level, in order to have sustainable development, which emphasizes both the preservation of the environment and with the reusable resources.

In recent years, there are many techniques which have been developed for the recycling and reusability of heavy metals. Leaching, electrolysis, solvent extraction, membrane separation, ion exchange, and microbiological methods are among such these methods. In industrial practices these traditional methods are limited to such factors as economic and technical difficulties [4, 5, 6, 7, 8, 9, 10].

Recovery of heavy metals offers industrialists many advantages such as balancing the cost of treatment, minimizing hazardous waste and protecting resources and avoiding the encumbrance of responsibility for producing hazardous waste [11]. Leaching is a hydrometallurgical method for dissolving of heavy metals from various sources with leaching reagents, solvents or lixiviants by the use of strong acids such as HCl, HNO_3, and H_2SO_4. Acids are generally used as reagents in extractions from oxidized copper ores. Most of the heavy metals will dissolve between 1.5-2.0 pH. Because certain pH range can be provided by strong acid solutions, strong acids are used in acidic leaching process [12, 13, 14, 15, 16]. Veglio et al., (2003) used leaching with 0.15 M sulfuric acid for less than 10 minutes at 323 K to recover Cu metal, which is 9.2-17.8% oxide in the galvanic waste sludge in a laboratory scale study and they yielded between 94% and 96% [17]. Miškufova et al., (2006) extracted Cu, Zn, Cr metals in galvanic sludge at room temperature with 0.25 M sulfuric acid for 10 min at room temperature and obtained 90% Cu, 85% Zn and 25% Cr yield [18]. However, the disadvantage of this reagent is the dissolvability of other metals with the copper. The disadvantage causes some impurities in high consumption of acid. Contrarily, alkaline leaching with ammonia solutions have some advantages as well. For example, the complex formation of ammonia with copper ions increases the leaching rate. Due to the ammonia, the copper can be selectively extracted from the copper ore and undesirable impurities are left in the residue [18, 19, 20]. NH_4NO_3 (ANS) consists of strong acid (HNO_3) and weak base (NH_3) composition displaying, salt character. In the aqueous medium, and ions formed by the ionization reaction of NH_4NO_3 and NH_3 and by the hydrolysis reaction of ammonium. These reactions play an important roles in leaching process because ions provide protons by required for the dissolution of sludge. Thus, ammonia complexes with copper ions, which increases the leaching rate [20, 24]. The copper in the EWS is in the form of CuO. Copper amine the complexes ($Cu(NH_3)_2^{2+}$) form with NH_3 during the leaching reaction. Accordingly, the copper ions do not precipitate in the solution. It can be leached into the reagent solution.

Recently alkaline leaching has gained importance for recovery of copper. Leaching with alkaline bacteria, ammonia or a combination of the two clearly indicated that copper recovery was remarkably better [21]. Glycine, one of the simplest amino acids, has been emerging as an efficient and environmental-friendly lixiviant for copper leaching. In the present study, an alkaline glycine–peroxide lixiviant system was used to leach copper from chalcopyrite concentrate by a suite of kinetic studies under different conditions [22]. A systematic study has been made of the effects of glycine concentration, temperature, dissolved oxygen, particle size, stirring speed, on the leaching kinetics of chalcopyrite in alkaline glycine from which a power law rate model has been derived to model the shrinking core [23].

The aims of this study is define suitable leaching conditions for EWS and investigate leachability of copper from EWS using ANS and develop suitable kinetic model. The effects of experimental six parameters including time, particle size, stirring speed, solid/liquid ratio, ANS concentration and temperature were investigated on the leaching of EWS.

2. Material and Method

EWS that contains valuable heavy metals used for leaching experiments was provided from metal plating plant in Amasya, Turkey. Ammonium was purchased from Sigma- Aldrich.

A glass beaker was used as a leaching reactor. A mechanical stirrer and a heater respectively were used to obtain desired stirring speed and temperature. Temperature was provided by a heater in the reactor. HANNA HI 8341 pH-meter was used for controlling the pH. The required the addition of an amount of EWS desired particle size into the ANS of given properties. After a given period of time, about a 5 mL of sample was taken from the beaker. After sampling, about a 5 mL of fresh ANS was immediately added to the beaker due to almost balancing solid to reagent soluiton ratio. The amount of dissolved copper was determined by the Perkin Elmer model AAS.

Percent copper recovery was calculated by the following equation:

$$\%\,\text{Copper Recovery} = \frac{M_{C\text{-}L}}{M_{C\text{-}0}} \text{ x } 100 \quad (1)$$

where $M_{C\text{-}L}$ is the weight of copper in the sludge and $M_{C\text{-}0}$ is the weight of copper in the leaching solution.

Spectrometer Blue model ICP –OES was used for chemical analysis of EWS which contains oxides of Cu, Zn, Mg, Al, Pb, Sn ions. The JEOL JSM-7001F model SEM was used to view morphology of EWS before the leaching process. Rigaku Smart Lab model XRD device was used to define morphology of EWS sludge before leaching process. The EWS was dried 24 hours in an oven at 200 ˚C for removing water. Then, it was sieved to get appropriate particle size for experiments.

3. Result and Discussion

3.1. Material Characterisations

Results from the chemical analysis are given in Table 1.

Table 1. Chemical composition of EWS

Component	% Composition
Cu	10.448
Zn	2.513
Mg	1.022
Al	0.212
Sn	0.051
Pb	0.001

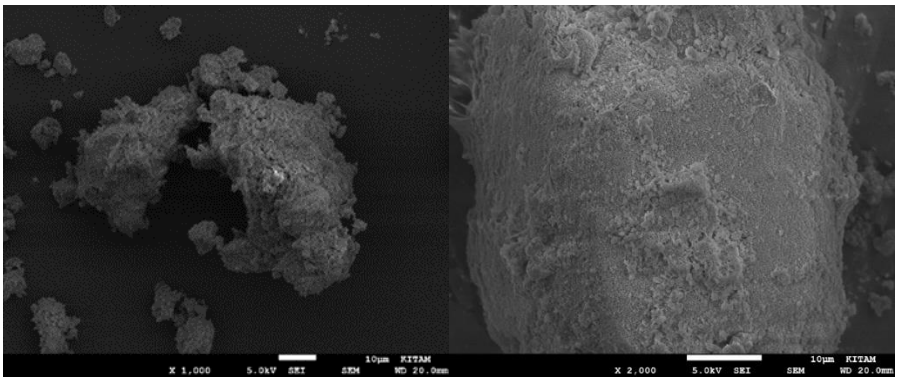

Figure 1. SEM images of EWS sludge before leaching process

Before the leaching process, the SEM images are shown in Figure 1. The XRD pattern of the sample before leaching is illustrated as Figure 2. and the phases are identified in the EWS.

The SEM images of the EWS sludge taken at different magnification levels are shown in Fig. 1. It can be seen from the figure that the EWS consisted of aggregated small particles in an irregular shape and it is an agglomerate of fine floccules of metal compounds. It is considered that the particles agglomerated during filtration and drying process of EWS. The particles size distribution of the EWS is uniform in homogeneous shapes.

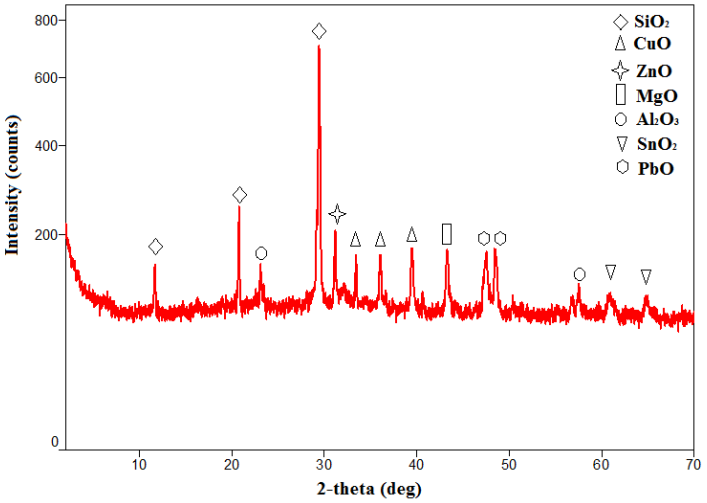

Figure 2. XRD of EWS sludge before leaching process

Figure 2. shows that there are metal phases in the electroplating waste sludge (EWS). Presence of copper oxide can be seen in the Figure 2.

3.2. Reactions of Leaching

Acids are generally used as reagents for extracting from oxidized copper ores [12, 13]. However, the disadvantage of this reagent is the dissolution of other metals with copper. The disadvantage causes some impurities in high consumption of acid.

Contrarily, alkaline leaching with ammonia solutions has some advantages to it, too. For example, ammonia complexes with copper ions, which increases the leaching rate. Due to the ammonia, the copper can be extracted from the copper ore and undesirable impurities would be left in the residue.

It was explained that NH_4NO_3 (ANS) consists of strong acid (HNO3) and weak base (NH3) composition and shows salt character. In the aqueous medium, and ions formed by the ionization reaction of NH4NO3 and NH3 and by the hydrolysis reaction of ammonium are shown below.

$$NH_4NO_3 \rightarrow NH_4^+ + NO_3^- \quad (2)$$

$$NH_4^+ + H_2O \leftrightarrow NH_3 + H_3O^+ \quad (3)$$

These reactions play important roles in leaching process because NH_4^+ ions provide protons by H_3O^+ required for the dissolution of sludge. The copper in the EWS is in the form of CuO. When EWS is added into ANS, the reactions occur according to the following flow of reaction:

$$CuO + 2\,H_3O^+ \rightarrow Cu^{2+} + 3\,H_2O \quad (4)$$

Copper amine complexes ($Cu(NH_3)_2^{2+}$) form with NH_3 during the leaching reaction. In that way, the copper ions do not precipitate in the solution. The copper amine complex formation reaction can be written as follows:

$$Cu^{2+} + 2NH_3 \leftrightarrow Cu(NH_3)_2^{2+} \quad (5)$$

$$Cu(NH_3)_2^{2+} + 2NH_3 \leftrightarrow Cu(NH_3)_4^{2+} \quad (6)$$

$$2CuO + 4NH_4NO_3 \rightarrow 2\,Cu^{2+} + 4NH_3 + 2H_2O + 4\,NO_3^- \text{ ‘’} \quad (7)$$

[18, 19, 20, 24].

3.3. Effects of Leaching Parameters

3.3.1. Particle size of solid (PS)

The effect of PS was studied with different particle size of sludge as -500+250, -250+125, -125+63, -63+45 and -45 µm. The values of concentration of reagent solution, temperature, solid to reagent solution ratio, stirring speed and pH were kept at 3 M, 323 K (50° C), 2 g solid/0.5 L reagent solution, 140 rpm and 7.1 pH respectively. The results were provided in Figure 3. It is observed that if the particle size decreases, the rate of leaching increases.

A sample of each fraction of the EWS was taken and treated with king water [(v/v) 3:1 HCl: HNO_3] then was solubilized and analyzed on the AAS analyzer [24]. The Cu values for each fraction are given in Table 2.

Table 2. Percentage of Cu for each EWS fraction

Particle size (µm)	Cu (%)
-500+250	10.528
-250+125	10.468
-125+63	10.508
-63+45	10.498
-45	10.448

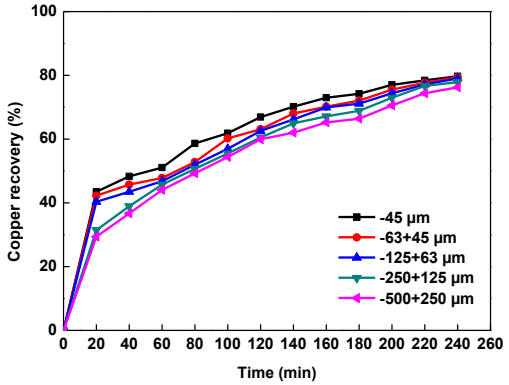

Figure 3. Effect of PS on leaching

Studies examining leaching parameters and their effects were investigated. In order to optimize the leaching conditions to be used, a range is set for each parameter. To examine the effect of a parameter, other parameters must be kept constant. In this study, firstly effect of particle size was examined. For this purpose, since the effects of the other parameters are not known, the values in the middle of the values in the selected range were taken. Once the best particle size was determined, this particle size was used when the effects of other parameters were examined. The impact of the other parameters was also determined in the same way.

3.3.2. Concentration of reagent solution (C)

ANS is used as reagent solution in experiments. The experiments were carried out using from 1, 2, 3, 4 and 5 M of ANS. In these experiments, the values of temperature, solid to reagent solution ratio, particle size, stirring speed and pH were all kept at 323 K, 2 g solid/0.5 L reagent solution, 45 µm, 140 rpm and 7.1 pH respectively. The effect of concentration of reagent solution on the rate of leaching is shown in Figure 4.

After 240 minutes, the percentage of the copper leaching from the sludge was 76.1%, 76.9%, 80.6%, 82.0 % and 83.1% at 1, 2, 3, 4, and 5 M of concentration, respectively. It can be seen from these results that If the ANS concentration increases, the rate of copper leaching increase.

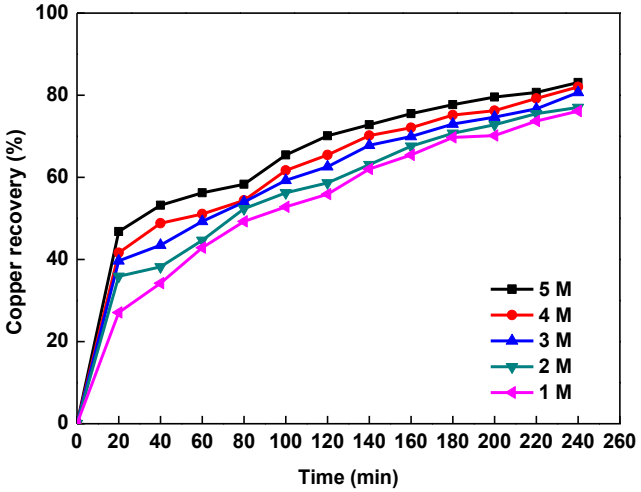

Figure 4. Impact of the concentration of reagent solution on leaching

3.3.3. Stirring speed (SS)

The impact of the stirring speed was determined by testing 100, 120, 140, 160, 180 rpm while the values of concentration of reagent solution, temperature, solid to reagent soluiton ratio, particle size and pH were kept constant at 5 M, 323 K, 2 g solid/0.5 L reagent solution, 45µm and 7.1 pH, respectively. The results are given in Figure 5. After 240 minutes, the percentage of copper leaching from the sludge increased from 76.9 % to 85.9 % when the stirring speed increased from 100 to 180 rpm. The results show that the SS is an important parameter for the leaching of the sludge.

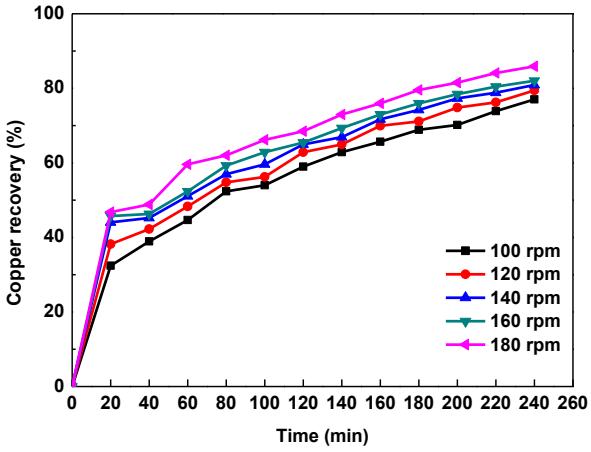

Figure 5. Effect of stirring speed on leaching

3.3.4. Solid to reagent solution ratio (S:R)

The experiments were carried out at five solid to reagent solution ratio in the range of 1g solid/0.5 L reagent solution to 3g solid/0.5 reagent solution L. The values of concentration of reagent solution, particle size, temperature stirring speed and pH were kept constant at 5 M, 45 µm, 323 K, 180 rpm and 7.1 pH respectively. It can be seen at Figure 6, the leaching rate decreases with increasing S:R. At a solid to solution ratios of 1g solid/0.5 reagent solution L, 91% of copper was leached after 240 minutes, whereas at solid/liquid ratios of 1g solid/0.5 L, 87.4% of copper was leached.

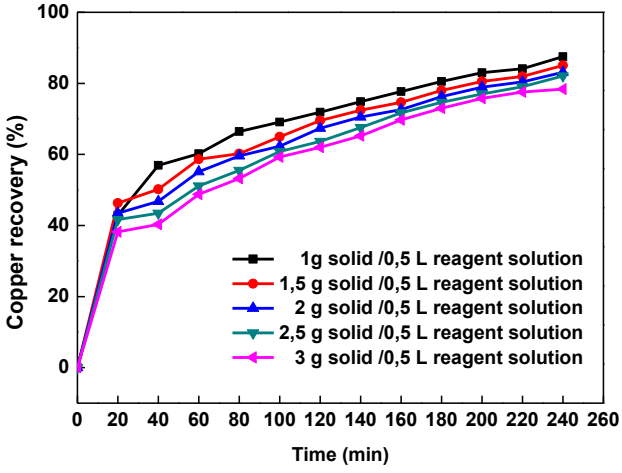

Figure 6. The impact of solid to reagent solution ratio on leaching

3.3.5. Temperature (T)

The experiments were actualized at different temperatures between at 303 K to 343 K. The values of concentration of reagent solution, solid to reagent soliton ratio, particle size, stirring speed and pH were kept constant at 5 M, 2 g solid/0.5 L reagent solution, 45 µm, 180 rpm and 7.1 pH respectively. The leaching rate increases with increasing temperatures. The reaction temperature is an important factor on the experiments. At a temperature of 303 K, 82.0% of copper was leached after 240 minutes, whereas at a temperature of 343 K, 89.5% of copper was leached.

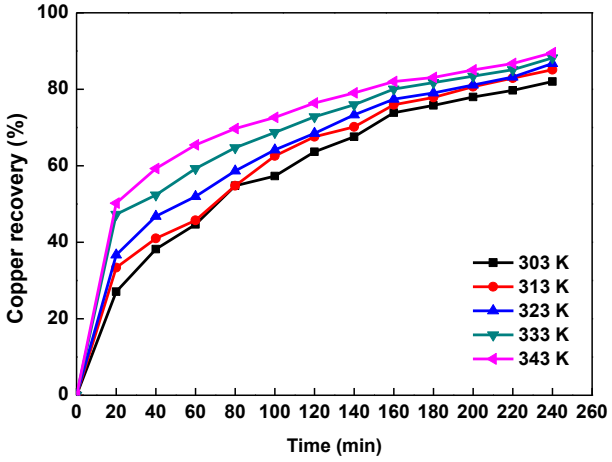

Fig. 7. Effect of reaction temperature on leaching

3.3.6 Leaching time (t)

The effect of leaching time on the leaching of EWS is shown in Figure 8. Clearly, the percentage of copper increased rapidly with increasing time. At nearly 20 min, 50% percentage of copper was achieved and this increased to 93% after 240 minutes. It can be seen from Figure 8. after 40 minutes leaching time, percentage of copper increases rather slowly. 40 minutes was found optimum for experiments.

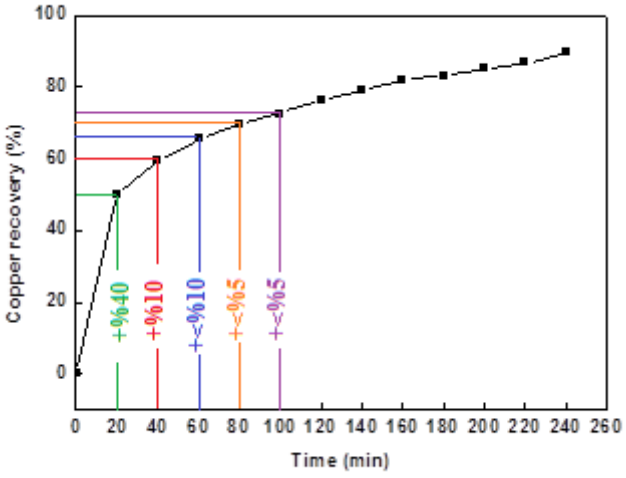

Fig. 8. The impact of leaching time on the leaching

3.4. Kinetic Study

The leaching process is a basic unit operation, and the reaction that takes place during this process with the mixture of solid and solution reactants is heterogeneous. The reaction occurring between the fluid and solid surfaces during the leaching process is described by the following reaction:

$$aA_{(fluid)} + bB_{(solid)} \xrightarrow[process]{\text{Leaching}} cC_{(liquid\ and\ solid\ products)} \quad (8)$$

The most effective factors are the particle shape and size, since the leaching process is a process based on the solubility of particles. This process can be regarded as homogenous if the size of the particles is small enough and the solids content in the solution is low. Accordingly, rate laws of kinetic models are convenient to explain the leaching experiments in classic homogeneous systems. However, this model alone is not considered to be sufficient to explain the reactions occurring in the leaching medium.

Hence, non-catalytic heterogeneous reaction models are utilized while kinetic description of leaching processes is done [25, 26, 27, 28]. It is possible for the heterogeneous process to be diffused or chemically controlled. In the shrinking core model, the size of the particle does not change during the reaction, and the diffusion phenomenon occurs along a product layer formed on the outer surface of the particle. Non-reacting solids and formed products allow a porous layer to thicken. In the shrinking particle model, the size of the particle shrinks during the reaction and the diffusion phenomenon occurs along a fluid film layer formed on the outer surface of the particle. Simple equations are derived using these models and can be written as follows Table 3 [25, 26].

Table 3. Kinetic equations of SCM and SPM

Model	Kinetic Equation		Explain	References
SCM	$k_d t=1-3(1-x)^{(2/3)}+2(1-x)$	(9)	Controlled by the diffusion	[30]
SPM	$k_r t = 1-(1-x)^{1/3}$	(10)	Controlled by the reaction	[30]
SPM	$k_p t = 1-(1-x)^{2/3}$	(11)	Controlled by the surface diffusion	[30]

In Table 3, where x is the conversion fraction of solid particle, k_P is the rate constant for diffusion through the liquid film, k_d is the rate constant for diffusion through the product layer, k_r is the apparent rate constant for the surface chemical reaction, and t is the reaction time. At the same time, t/t^* is equal to Eq 9., Eq 10., Eq 11. To identify the kinetic parameters and rate-controlling step of the leaching of sludge in ANS, the data found in the experiments were determined based on the SCM using the rate expression given in Eqs. (9) through (11).

By applying Eqs. (9) through (11) to the experimental data found, the rate constants were calculated accordingly. The rate constant values determined from the graphical apse and ordinate layout used for the curve slopes calculating from example of Fig. 9. For each parameter, the rate constants given in Table 4.

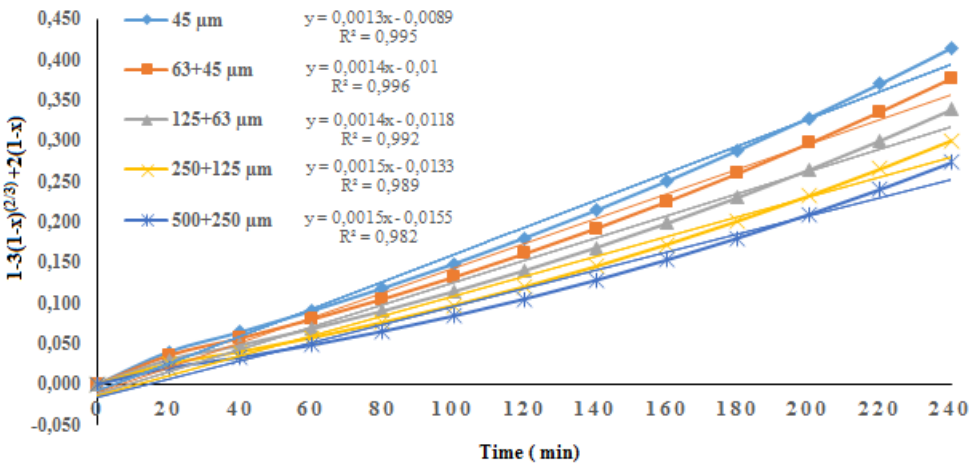

Fig 9. The graphical apse and ordinate layout used for the curve slopes calculating rate constant.

Table 4. The rate constants, k_r,k_d, k_p for kinetic models and correlation coefficient values

Model	**SCM**		**SPM**			
Place of Phenomenon	**Diffusion through the product layer**		**Surface Chemical Reaction**		**Surface diffusion through**	
Equations	**$1-3(1-x)^{(2/3)}+2(1-x)$**		**$1-(1-x)^{1/3}$**		**$1-(1-x)^{2/3}$**	
Parameter	**k_r (min^{-1})**	**R^2**	**k_d (min^{-1})**	**R^2**	**k_p (min^{-1})**	**R^2**
Particle size (µm)						
-500+250	0,0013	0,995	0,0014	0,940	0,0021	0,902
-250+125	0,0014	0,996	0,0014	0,942	0,0022	0,901
-125+63	0,0014	0,992	0,0014	0,919	0,0021	0,868
-63+45	0,0015	0,989	0,0014	0,905	0,0021	0,850
-45	0,0015	0,982	0,0014	0,878	0,0021	0,816
Concentration (M)						
1	0,0013	0,995	0,0014	0,953	0,0022	0,919
2	0,0014	0,995	0,0014	0,916	0,0021	0,888
3	0,0015	0,993	0,0014	0,932	0,0022	0,864
4	0,0016	0,989	0,0015	0,906	0,0022	0,847
5	0,0016	0,979	0,0015	0,871	0,0022	0,799
Stirring speed (rpm)						
100	0,0013	0,995	0,0016	0,909	0,0021	0,888
120	0,0014	0,993	0,0014	0,904	0,0021	0,870
140	0,0015	0,990	0,0015	0,899	0,0021	0,846
160	0,0016	0,989	0,0014	0,920	0,0022	0,836
180	0,0018	0,989	0,0013	0,931	0,0023	0,831
Solid to reagent solution ratio						
1.0:0.5	0,0019	0,982	0,0016	0,882	0,0023	0,804
1.5:0.5	0,0017	0,988	0,0015	0,891	0,0022	0,820
2.0:0.5	0,0016	0,991	0,0015	0,902	0,0022	0,838
2.5:0.5	0,0016	0,994	0,0015	0,921	0,0022	0,866
3.0:0.5	0,0015	0,993	0,0014	0,923	0,0022	0,874
Temperature (K)						
303	0,0018	0,994	0,0017	0,958	0,0026	0,916
313	0,0019	0,995	0,0017	0,861	0,0025	0,920
323	0,0020	0,996	0,0017	0,942	0,0025	0,888
333	0,0020	0,989	0,0017	0,902	0,0024	0,826
343	0,0020	0,973	0,0017	0,861	0,0023	0,769

As shown in Figure 7, the leaching reaction of sludge was quite sensitive to temperature. Therefore, to define the rate-determining step of this process, the mixed kinetic models were tested using the experimental data [19, 20, 24, 25, 29]. Mixed kinetic models was found that the following model could be more useful to show the kinetics of the dissolution of sludge in ANS.

$$1\text{-}2(1\text{-}x)^{1/3} + (1\text{-}x)^{2/3} = k_m t \quad (12)$$

where k_m is the rate constant for the MKM. The rate constants calculated and their correlation coefficients are shown in Table 5. The following mathematical model can be suggested to determine effects of parameters:

$$k_m = k_0 (PS)^p (C)^c (SS)^r (S:R)^s \exp(-Ea/RT) \quad (13)$$

where PS, C, SS, S:R, Ea, R, and T represent the particle size, concentration, stirring speed, solid to reagent solution ration, activation energy, universal gas constant and temperature, respectively.

The constants p, c, r and s are the reaction order for relating parameters, and k_0 is the frequency or preexponential factor. Combining Eqs. (12) and (13), the following equation is obtained:

$$1 - 2(1-x)^{1/3} + (1-x)^{2/3} = k_m t$$

$$1 - 2(1-x)^{1/3} + (1-x)^{2/3} = k_0 (PS)^p (C)^c (SS)^r (S:R)^s \exp(-Ea/RT)t \quad (14)$$

The constants p,c, r, and s were estimated from the apparent rate constant. The plots of ln(k_m) vs ln(PS), ln(k_m) vs ln(C), ln(km) vs ln(SS) and ln(km) vs ln(S:R) were constructed using the values given in Table 5. for each parameter. The slopes of the straight lines in the graphs obtained assign the reaction order for each parameter. The values of the constants p, c, r and s were determined to be -10.43, 4.64, 1.46 and 4.32 respectively. The activation energy of leaching was calculated from the Arrhenius equation. The Arrhenius plot of the reaction is shown in Figure 9. The presence of the two lines in Figure 9 shows the presence of two different models in the process.

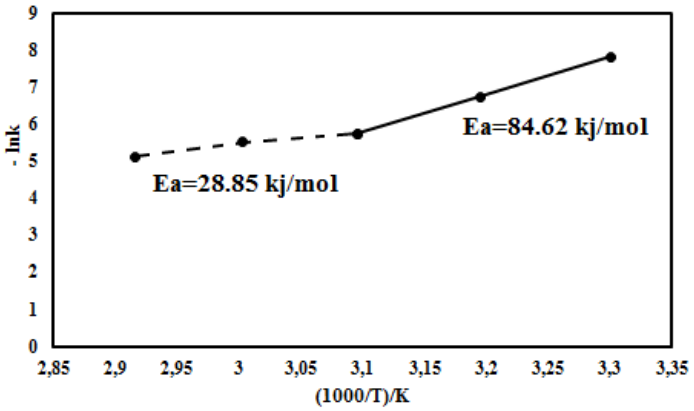

Fig 10. Arrhenius plot for leaching process

The lines in Figure 10. shows the variations between 303 K to 323 K the first zone (surface reaction) and 323 K to 343 K the second zone (product layer diffusion). At temperatures below 323 K (i.e., the first zone), the activation energy and the preexponential factor were calculated to be 84.62 kJ/mol and 1,51 x 10^{11} s^{-1}, respectively. At temperatures above 323 K (i.e., the second zone), these values were determined to be 28.85 kJ/mol and 142 s^{-1}, respectively.

The activation energy of a diffusion controlled process is usually below 40 kJ/mol, while for a chemically controlled reaction this value is usually greater than 40 kJ/mol [25]. Therefore, the value of the activation energy of a leaching reaction may be used to predict the rate controlling step of the process. According to the activation energies values determined in this study, the rate of process is controlled by the surface chemical reaction in the first zone (i.e., less than 323 K) and by the diffusion through the product layer in the second zone (i.e., greater than 323 K). In the product layer (the second zone), reaction first occurs at the exterior surface of the particle. The reaction interface, then proceeds

towards the core of the particle as the reaction moves, leaving a product layer and an inner core of the unreacted solid. When the chemical reaction at the interface has a insignificant resistance to the progress of the reaction compared with diffusion through the ash layer, the overall rate is controlled by the latter since the slowest process in the whole reaction determines the rate controlling step. It can be obtained spherical particles [28]. SEM analysis of the product layer diffusion in Figure 11.

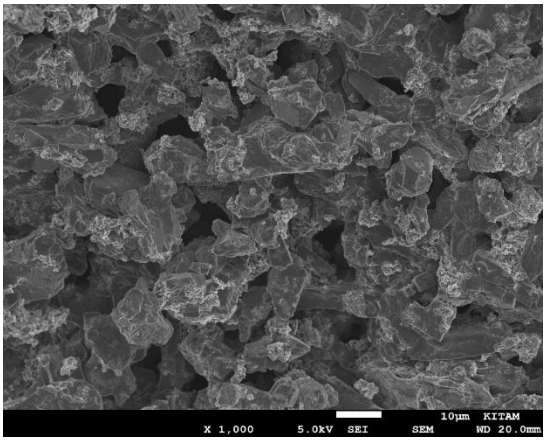

Figure 11. SEM Analysis of formation of spherical particles in product layer diffusion

As a result, the kinetic expressions be written as follows:

$$1 - 2(1-x)^{1/3} + (1-x)^{2/3} = 1.51 \times 10^{11} (PS)^{-10.43} (C)^{4.64} (SS)^{1.46} (S:R)^{4.32} \exp(10178/T).t \quad (15)$$

(for 303 K to 323 K)

$$1 - 2(1-x)^{1/3} + (1-x)^{2/3} = 142.3 (PS)^{-10.43} (C)^{4.64} (SS)^{1.46} (S:R)^{4.32} \exp(3471/T).t \quad (16)$$

(for 323 K to 343 K)

Table 5. The rate constant, km, for MKM and correlation coefficients

Model	**MKM**	
Equations	**$1 - 2(1-x)^{1/3} + (1-x)^{2/3}$**	
Parameter	**k_m (min^{-1})**	**R^2**
Particle size (µm)		
-500+250	0,0006	0,9901
-250+125	0,0006	0,9907
-125+63	0,0007	0,9900
-63+45	0,0007	0,9905
-45	0,0007	0,9925
Concentration (M)		
1	0,0006	0,9901
2	0,0006	0,9923
3	0,0007	0,9907
4	0,0007	0,9904
5	0,0008	0,9903
Stirring speed (rpm)		
100	0,0006	0,9900
120	0,0007	0,9920

140	0,0007	0,9902
160	0,0008	0,9908
180	0,0009	0,9910
Solid to solution ratio (g/L)		
1.0:0.5	0,0009	0,9900
1.5:0.5	0,0008	0,9912
2.0:0.5	0,0008	0,9937
2.5:0.5	0,0008	0,9907
3.0:0.5	0,0007	0,9926
Temperature (K)		
303	0,0004	0,9926
313	0,0012	0,9907
323	0,0032	0,9937
333	0,0040	0,9912
343	0,0060	0,9900

It is generally known that there is an increase in solubility due to an increase in ambient temperature in a solution process. Experimental studies with ammonium nitrate (NH_4NO_3) show that the increase in the dissolution efficiency of Cu^{2+} is due to the increase in temperature.

According to the results obtained from the experimental studies, it can be said that the particle size decreases and the Cu^{2+} dissolution efficiencies increase. As the particle size shrinks, the surface area increases and thus it is thought that EWS increases the dissolution efficiency by reacting with the solvent in the medium. The purpose of stirring in the leaching process is to homogenize the leaching medium and increase the unit-time contact of the solvent-soluble material. It has therefore determined that in the experimental results, the Cu^{2+} dissolution efficiency increases due to the increase of the stirring speed. It can be said that the dissolution efficiency will increase due to the increase in contact at the unit time.

ANS is used to leach the EWS and it can easily dissolve in the ANS. Experimental results showed that as the amount of NH_4NO_3 consumed increased, the dissolution of EWS also increased (Fig. 4.). The amount of NH_4NO_3 consumed is directly related to the NH_4NO_3 concentration. The highest copper recovery conditions were determined as concentration of ANS, 5 M; temperature, 343 K; particle size -45 μm; solid to liquid ratio, 1:0.5 g/L; stirring speed, 180 rpm and pH of the reagent solution 7.1.

4. Conclusions

At the end of this study, the leaching kinetics of EWS were studied using ANS as the leaching solution. The effects of parameters on the copper leaching process from the sludge were examined, and kinetic models were determined. It was observed that the leaching rate increased with increasing concentration, temperature and stirring speed, meanwhile decreasing the particle size and solid to solution ratio. It was also found that the investigated leaching reaction followed the mixed kinetic model. The leaching rate is controlled by chemical reaction at temperatures between 303 K and 323 K (Ea = 84.62 kJ/mol), while it is controlled.

4. References

[1] Akbal, F., Camcı, S., (2011). Copper, chromium and nickel removal from metal plating wastewater by electrocoagulation. Desalination, 269:214-220.

[2] Hosseini, S.S., Bringas, E., Tan, N.R., Ortiz, I., Ghahramani, M., Shahmirzadi, M.A.A., (2016). Recent progress in development of high performance polymeric membranes and materials for metal plating wastewater treatment: A review. Journal of Water Process Engineering, 9:78-110.

[3] Al-Shannag, M., Al-Qodah, Z., Bani-Melhem, K., Qtaishata, M., R., Alkasrawi M., (2015). Heavy metal ions removal from metal plating wastewater using electrocoagulation:Kinetic study and process performance. Chemical Engineering Journal, 260:749-756.

[4] Magalhães M., J., Silva J., E., Castro F.,P., Labrincha, J.,A., (2004). Role of the mixing conditions and composition of galvanic sludges on the inertization process in clay-based ceramics. Journal of Hazardous Materials, 106:169-176.

[5] Sophia, A.C., Swaminathan, K., (2005). Assessment of the mechanical stability and chemical leachability of immobilized electroplating waste. Chemosphere, 58:75-82.

[6] Chung, S., Kim S., Kim, J.O., Chung, J., (2014). Feasibility of combining reverse osmosis-ferrite process for reclamation of metal plating wastewater and recovery of heavy metals. Industrial & Engineering Chemistry Research, 53:15192-15199.

[7] Chena, D., Hou, J., Yao, L.H., Jin, H.M., Qian, G.R., Xu, Z.P., (2010). Ferrite materials prepared from two industrial wastes: Electroplating sludge and spent pickle liquor. Separation and Purification Technology, 75:210-217.

[8] Li, C., Xie, F., Ma, Y., Cai, T., Li, Huang, H., Z., Yuan, G., (2010). Multiple heavy metals extraction and recovery from hazardous electroplating sludge waste via ultrasonically enhanced two stage acid leaching. Journal of Hazardous Materials, 178:23-833.

[9] Gomez, M., R., Cerutti, S., Sombra, L., L., Silva, M., F., Martinez, L.D., 2007. Determination of heavy metals for the quality control in argentinian herbal medicines by ETAAS and ICP-OES. Food and Chemical Toxicology, 45:1060-1064.

[10] Sua, R., Lianga, B., Guana, J., (2016). Leaching effects of metal from electroplating sludge under phosphate participation in hydrochloric acid medium. Procedia Environmental Sciences, 31:361-365.

[11] Chang, C.J., Liu, J.C., (1998). Feasibility of copper leaching from an industrial sludge using ammonia solutions. Journal of Hazardous Materials, 58:121–132.

[12] Parhi, P.K., Sethy, T.R., Rout, P.C., Sarangi, K., (2015). Selective dissolution of copper from copper-chromium spent catalyst by baking-leaching process. Journal of Industrial and Engineering Chemistry, 21:604-609.

[13] Habbache, N., Alane, N., Djerad, S., Tifouti L., (2009). Leaching of copper oxide with different acid solutions. Chemical Engineering Journal, 152:503-508.

[14] Arzutuğ, M.E., Kocakerim, M.M., Copur, M., (2004). Leaching of Malachite Ore in NH3-Saturated Water. Industrial & Engineering Chemistry Research, 43:4118-4123.

[15] Bingöl, D., Canbazoglu, M., (2004). Dissolution kinetics of malachite in sulphuric acid. Hydrometallurgy, 72:159-165.

[16] Sarı, B., (2005). Metal sanayi atık çamurlarında ağır metal gideriminde biyoliç yönteminin kullanılması. Doktora Tezi, Çukurova Üniversitesi Fen Bilimleri Enstitüsü, Adana.

[17] Veglio, F., Quaresima, R., Fornari, P., Ubaldini, S., (2003). Recovery of Valuable Metals From Electronic and Galvanic Industrial Wastes By Leaching and Electrowinning. Waste Management, 23:245-252.

[18] Miškufova, A., Havlik, T., Laubertova, M., Ukašík, M., (2006). Hydrometallurgical Route For Copper, Zinc And Chromium Recovery From Galvanic Sludge Acta Metallurgica Slovaca, 12:293-302.

[19] Blanco, L.J.L., Zapata, V.F.M., Garcia, D.D.J., (1999). Statistical Analysis of Laboratory Results of Zn Wastes Leaching. Hydrometallurgy, 54:41-48.

[20] Ekmekyapar, A., Aktas, E., Kunkul, A., Demirkıran, N., (2012). Investigation of Leaching Kinetics of Copper from Malachite Ore in Ammonium Nitrate Solutions. The Minerals, Metals & Materials Society and ASM International, 43:764-772.

[21] Yin, S., Wang, L., Wu, A., Kabwe, E., Chen, X., Yan, R., (2018). Copper recycle from sulfide tailings using combined leaching of ammonia solution and alkaline bacteria. Journal of Cleaner Production, 189:746-753.

[22] Shin, D., Ahn, J., Lee, J., (2019). Kinetic study of copper leaching from chalcopyrite concentrate in alkaline glycine solution. Hydrometallurgy, 183:71-78.

[23] Tanda, B.C., Eksteen, J.J., Oraby, A.E., O'Connor, G.M., (2019). The kinetics of chalcopyrite leaching in alkaline glycine/glycinate solutions. Minerals Engineering, 135:118-128.
[24] Köseler M., (2012). Mikrodalga etkisinde adatepe (karaçam) lateritik cevherinin liçing şartlarinin belirlenmesi. Yüksek Lisans Tezi, Selçuk Üniversitesi Fen Bilimleri Enstitüsü, Konya.
[25] Ermis, İ., U., (2011). Stronsiyum sülfat konsatresinden liçing yöntemleriyle amonyum sülfat ve stronsiyum karbonat üretimi. Doktora Tezi, Selçuk Üniversitesi Fen Bilimleri Enstitüsü, Konya.
[26] Aras, A., 2003. Koyulhisar sfalerit konsantresinin asidik ferrik klorürlü ortamda liçing şartlarını belirleme. Yüksek Lisans Tezi, Selçuk Üniversitesi Fen Bilimleri Enstitüsü, Konya.
[27] Crundwell, F.K., (1995). Progress in the mathematical modelling of leaching reactors. Hydrometallurgy, 39:321-335.
[28] Moustafa A.F., (2017). Isothermal reduction process and kinetic of nanomaterials in reducing atmosphere: A review. Journal of Analytical and Applied Pyrolysis, 127:126–139.
[29] Mondal, S., Paul, B., Kumar, V., Singh, D.K., Chakravartty, J.K., (2015). Parametric optimization for leaching of cobalt from Sukinda ore of lateritic origin – A Taguchi approach. Separation and Purification Technology, 156:827-834.
[30] Levensipel, O., Chemical Reaction Engineering Third Edition, John Wiley & Sons, 1974, 569

Kastamonu University
Journal of Engineering and Sciences
e-ISSN 2667-8209
http://dergipark.gov.tr/kastamonujes

Genome-Wide Determination, Characterization and Bioinformatics Analysis of Cold Shock Protein (*CSP*) Genes In Atlantic Salmon (*Salmo salar*), Carp (*Cyprinus carpio*) and Rainbow Trout (*Oncahorynchus mykiss*)

Büşra Özkan [a], Buket Ustaoğlu [a], Tevfik Hasan Can [a], Mehmet Cengiz Baloglu [a], Yasemin Celik Altunoglu [a] *

[a] *Department of Genetics and Bioengineering, Faculty of Engineering and Architecture, Kastamonu University, Kastamonu, Turkey*

ARTICLE INFO

Received: May:11.2019
Reviewed: May:15.2019
Accepted: May:30.2019

Keywords:
Atlantic Salmon
Carp
Rainbow Trout
Bioinformatics
Cold Shock Protein

Corresponding Author:
*E-mail: yasemincelikbio@gmail.com

ABSTRACT

Atlantic salmon (*Salmo salar*) is the symbol of the underwater world; carp (*Cyprinus carpio*) is a freshwater fish that gives its name to the Cyprinidae family and rainbow trout (*Oncorhynchus mykiss*) is a species of Salmonidae family, like as salmon. These three types of fish are important in the world because they are made of fish farming. The cold shock proteins (CSP) were first described in *Escherichia coli* and are the conserved proteins that have the activity to protect the organism against cold temperatures. They can be characterized by general stress response in fish. There is no comprehensive study related to the identification of CSPs in fish genomes. In this study, determination, characterization and bioinformatics analysis of CSPs were carried out in the genomes of salmon, carp and rainbow trout. The study results represent preliminary knowledge about understanding of the effects of these proteins in cold tolerance in economically important fish species.

Anahtar Kelimeler:
Somon Balığı
Sazan Balığı
Gökkuşağı Alabalığı
Biyoinformatik
Soğuk Şoku Proteini

ÖZ

Atlantik somonu *(Salmo salar*) sualtı dünyasının simgesidir; sazan balığı (*Cyprinus carpio*), sazangiller (Cyprinidae) familyasına adını veren tatlı su balığıdır ve gökkuşağı alabalığı (*Oncorhynchus mykiss*) somon gibi Salmonidae ailesine ait bir balık türüdür. Bu üç balık türü dünyada en çok çiftçiliği yapılan balık türlerinden olduğu için önemlidir. Soğuk şoku proteinleri (CSP) ise ilk kez *Escherichia coli*'de tanımlanmış olup organizmayı soğuğa karşı koruma aktivitesine sahip olan korunmuş proteinlerdir. Bunlar, balıklardaki genel stres tepkisi ile karakterize edilebilir. Balık genomlarında CSP proteinlerinin tanımlanması ile ilgili kapsamlı bir çalışma yoktur. Bu çalışmada, Atlantik somonu, sazan balığı ve gökkuşağı alabalığı genomlarında CSP proteinlerinin belirlenmesi, karakterizasyonu ve biyoinformatik analizleri gerçekleştirilmiştir. Çalışma sonuçları, ekonomik öneme sahip balık türlerinde bu proteinlerin soğuk toleransındaki etkilerinin anlaşılması için ön bilgi sunmaktadır.

1. Introduction

Atlantic salmon (*Salmo salar*) is a fish species of Salmonidae family, composed of 11 genera and 70 species, living in the North Atlantic Ocean, exhibiting a wide range of ecological adaptations and using a variety of marine and freshwater habitats [1]. Atlantic salmon is an icon and king in the underwater world. However, today, like many types of water, its survival has been threatened [2]. Therefore, it is one of the most important species for fish farming worldwide.

The carp (*Cyprinus carpio*) is a freshwater fish that gives its name to the cyprinids (Cyprinidae) family [3]. Common carps are native to Europe and Asia and have been introduced to all parts of the world except the poles. These are the third most common fish species worldwide [4] and the dates they spend as farm fishes are based on the Roman period. Carp is used as food in many areas, but is also considered harmful in several regions due to its ability to compete with local fish stocks [5]. Carp is an important food fish in most parts of the world, except in Australia and North America, where the fish are thought to be tasteless [6, 7].

The rainbow trout (*Oncorhynchus mykiss*) is native to North America, along the eastern North Pacific region, through the Aleutic Islands from Mexico and the Kamchatka Peninsula [8]. The rainbow trout is classified as *Oncorhynchus mykiss*, and Salmonidae, which is of the same breed as the Pacific salmon and which contains various trout (Salvelinus sp.), such as Atlantic salmon (*Salmo salar*), Arctic char (*Salvelinus alpinus*), Arctic grayling (*Thymallus arcticus*) and whitefish (Coregonus sp.) belongs to the family. The rainbow trout may tolerate a wide range of water temperatures and other environmental variables, such as water quality, but require high levels of oxygenated water and develop at water

temperatures of 13-18° C. They are very valuable nutrients and can be grown with a pigmented (red) or non-pigmented (white) meat depending on their nutrition. Rainbow trout is the most common farm trout in the world, which has been cultured for hundreds of years [9].

All living cells are capable of responding to changes in the environment, such as temperature, pressure, osmotic stress, and oxygen availability. For example; at the cellular level, acclimation or adaptation in response to the temperature flow occurs with changes in metabolic rate, intracellular pH, ion concentration, membrane composition, and gene expression. An increase in temperature results in a specific heat shock response shared by all organisms, from bacteria to mammals. The heat shock response is featured by the synthesis of a number of highly conserved heat shock proteins. Cellular responses to a decrease in temperature have not been well studied and no conserved cold inducible protein set has been identified among all organisms. There are adaptive mechanisms used by many organisms in response to cold temperature. These include changes in membrane fluidity and changes in the protein translation mechanism of the cell [10]. Membrane fluidity decreases on temperature drop affecting membrane-related cellular functions. Organisms overcome this by reducing the degree of saturation in membrane phospholipids to achieve greater flexibility. This condition is described in *Escherichia coli*. As in Bacillus and Synechococcus, the synthesis and stability of membrane-bound desaturase is followed by a cold shock. Cold shock allows secondary structures to stabilize in RNA and DNA, leading to a decrease in the efficiency of translation, transcription and DNA replication. The harmful effects of cold shock are overcome by stimulation of cold shock proteins (CSP). CSPA, a major cold shock protein, was first identified from *E. coli* and has since been identified in various Gram-positive and Gram-negative bacteria, including homologs, psychrotrophic, psychophilic, mesophilic and thermophilic strains [11].

CSPs are among the most conserved proteins. The characteristic feature is that it comprises one or more cold shock domains (CSD) having nucleic acid binding properties. This condition equips these proteins with pleiotropic functions, such as the regulation of transcription, translation and splicing [12]. CSPs eliminate some of the harmful effects of temperature drop and thus help to adapt the cells. After the emergency cold shock response, the synthesis of CSPs is reduced and the synthesis of other proteins is increasing. This allows the cells to grow at low temperature, although at a lower rate. CSPs are known to be important during the cold shock response, but recent studies have shown that CSPs may play a wider role in the stress tolerance of bacteria [13].

A cold shock that reduces body temperature to the lower limit of the thermal range of an organism can cause severe inferior disorders and mortality. The magnitude of the cold shock response depends on both the temperature drop rate and the magnitude of the change according to the thermal tolerance limits [14, 15]. While the cold shock stress response is generally thought to be an adaptive response to maintain homeostasis, prolonged or severe temperature changes other than a certain tolerance change may ultimately result in mortality [16] or otherwise affect the health and condition of the organism [17].

CSPs are generally better defined in bacteria. Although there is no comprehensive study related to the identification of CSPs in fish genomes, they have been characterized by general stress response in fish [17]. When these three fish species are considered, *Salmo salar* is at the risk of extinction and *Salmo salar*, *Cyprinus carpio* and *Oncahorynchus mykiss* are the most consumed fishes in the world and this indicates the importance of these fishes. In this study, it was aimed to identify genes encoding for CSP in *Salmo salar*, *Cyprinus carpio and Oncahorynchus myciss* genomes and their settlements, phylogenetic relations, estimated biological roles, molecular functions, cellular settlements, target miRNAs and secondary structures and locations on chromosomes.

2. Material and Method

The NCBI (https://www.ncbi.nlm.nih.gov/) database was used to identify CSPs and BLASTP analysis (Protein Blast-Sequence Comparison) was performed from the NCBI database. The presence of protein sequences in the CSP family was checked by Pfam domain analysis and various physical and chemical parameters were calculated using the Expasy Prot Param Tool (https://web.expasy.org/protparam/). pH range, molecular weights, variability states and isoelectric effect (pI) values were reached with this analysis.

The certain amino acid sequences were identified by the MEGA7 program [18] and were used for sequence alignment. Multiple sequence alignments were performed with ClustalW program. The exon-intron regions were determined by using the GSDS2.0 (http://gsds.cbi.pku.edu.cn/) database [19], using the genomic sequences and the CDS sequences of the CSP sequences. A phylogenetic tree was created by the Neighbor Joining method that gave the closest tree to the evolutionary process. For the phylogenetic tree, the Bootstrap 1000 value, which is a 1000 repetitive boot tab, was selected and the phylogenetic tree was generated with the desired analysis [20]. The resulting phylogenetic tree was visualized in ITOL and the relationship between evolutionary processes has been made more prominent. The database used as DNA motif screening tool (MEME) [21] was used to identify protected motifs. In the analysis, the maximum number of motifs and the widths of the motifs were ≥ 2 and ≤ 300, respectively. Following the identification of the MEME motifs, the InterPro database and InterProScan were also scanned [22].

Functional analyzes of CSP protein sequences were performed using the Blast2GO program [23]. These functional analyzes were carried out in three steps. In the first step, maps were loaded with the sequences loaded in the program (BLASTp), and in the second step maps related to the BLAST results were prepared (MAPPING) and in the third step, the

information file was prepared for the sequences (ANNOTATION). With this program, three categories were created and biological functions, cellular content and molecular functions were determined by GO classification.

miRNAs were determined in order to identify miRNA-controlled gene targets in the *CSP* genes in Atlantic salmon, carp and rainbow trout and to understand the miRNA functions. For this, miRBase v20.0 (http://www.mirbase.org/) was used and previously known animal miRNA precursors were detected. The plant miRNA database was used to identify miRNAs targeting the *CSP* genes found in salmon, carp and rainbow trout. In addition, all known plant miRNAs were identified using the psRNA Target Server (https://plantgrn.noble.org/psRNATarget/) database to align the *CSP* gene transcripts in Atlantic salmon, carp and rainbow trout and defined miRNAs in these fishes. All known animal miRNAs and their target or targets were identified by the parameters described. The miRNA targets detected by computer screening were confirmed. BLASTX screening was also performed for the analysis of gene homologs. Using the protein sequences, the 3D structure of the CSPs was estimated by Phyre2 (http://www.sbg.bio.ic.ac.uk/phyre2/html/page.cgi?id=index). The reliability of the model was confirmed by other numerical data [24].

3. Results and Discussion

CSP genes from *Salmo salar*, *Cyprinus carpio* and *Oncorhynchus mykiss* were named as *SsaCSP*, *CcaCSP* and *OmyCSP*, respectively. According to the results, 86 genes for *SsaCSP*, 15 genes for *CcaCSP* and 60 genes for *OmyCSP* were identified. Carp, Atlantic salmon and rainbow trout have 2n = 58, 2n = 100 and 2n = 58 chromosomes, respectively. Based on the analysis of *Salmo salar* genome by using CSP sequences, chromosomal location of *SsaCSP* genes on 13th and 15th carp chromosomes are noteworthy and most of the *SsaCSP* genes located on these two chromosomes. This finding shows that the 13th and 15th chromosomes have an important role for the SsaCSP family members (**Figure 1**). *CcaCSP* gene family members were only on 8 chromosomes of carp. In this family, the maximum gene placement was located in the scaffold. Since the localizations of the genes in this family are largely in the scaffold, it is unclear which chromosome plays a role for CSPs (**Figure 1**). Gene placement of *OmyCSP* gene family on 9th and 16th on chromosomes was quite remarkable. On the 9th and 16th chromosome pairs, there were 23 and 21 *CSP* genes, respectively. The other chromosomes had an average of 1-2 *CSP* genes. This table clearly shows that the 9th and 16th chromosomes are directly related to CSPs. The presence of only 1 gene on scaffold provides stronger interpretations when compared to other gene families (**Figure 1**).

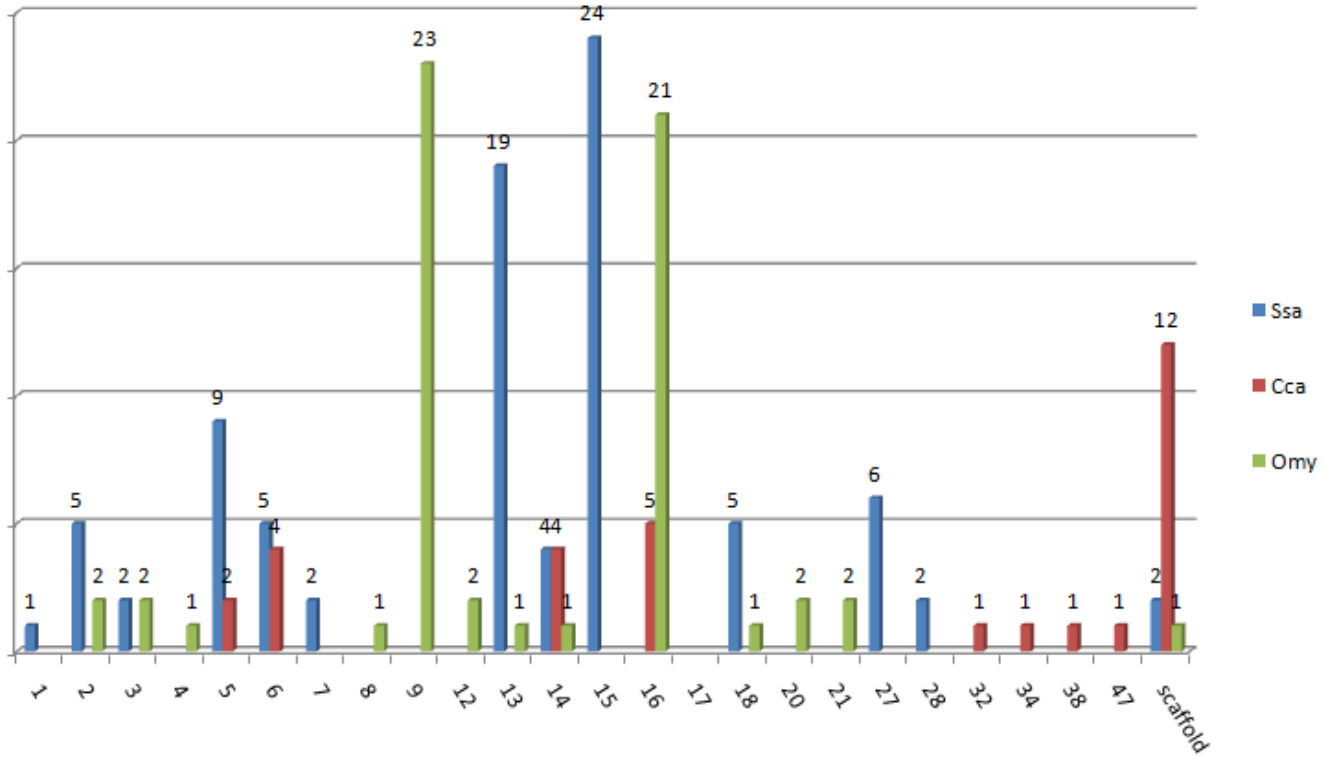

Figure 1. Chromosomal distribution of *SsaCSP*, *CcaCSP* and *OmyCSP* genes in Atlantic salmon, carp and rainbow genomes, respectively

The protein lengths determined for the SsaCSP family members were between 108-939 aa. The average molecular weight of this family members was 75 kDa. Thirty-eight SsaCSPs were acidic and 48 SsaCSPs were found to be basic. Although the number of proteins with basic character was greater than the number of proteins with acidic character, the average of pI values was 7.90 (**Table S1 in appendix**).

CcaCSPs had 101-315 aa in length and the average length of these proteins were 228 aa. The average molecular weight of this protein family in common carp was 25.5 kDa (Since a large amount of scaffold was detected in the *CcaCSP* gene family, it was not taken into account in the protein length and molecular weight average). Two of CcaCSP proteins were found to be acidic and 29 of CcaCSPs were basic. The number of proteins with basic character was more than the number of proteins with acidic character among CcaCSPs and the average of pI values was 8.97 (**Table S2 in appendix**).

The protein length determined for the OmyCSP family was between 130-1862 aa and the average length was 667 aa. The average molecular weight of this protein family was 73.9 kDa. Thirty-four of the OmyCSPs were acidic and 26 OmyCSPs were basic. However, the average of pI values was 7.48. This was due to the strong basic character of basic proteins among OmyCSPs (**Table S3 in appendix**). It can be concluded that CSPs from Atlantic salmon, carp and rainbow trout were mainly basic proteins.

Phylogenetic tree analysis was performed by using MEGA7 (Molecular Evolutionary Genetics Analysis) program to determine the evolutionary relationships among SsaCSP, CcaCSP and OmyCSPs. In this analysis, the Neighbor Joining Method was used. According to the phylogenetic tree analysis, SsaCSPs, CcaCSPs and OmyCSPs were categorized in 9, 8 and 5 main classes, respectively (**Figure 2**). Based on the phylogenetic distribution of the SsaCSP family, the highest number of proteins was found in the 7th class. The most of the CcaCSPs were determined in the 8th class. Besides, the highest number of proteins were defined in the 5th class when phylogenetic distribution of the OmyCSP family was analyzed.

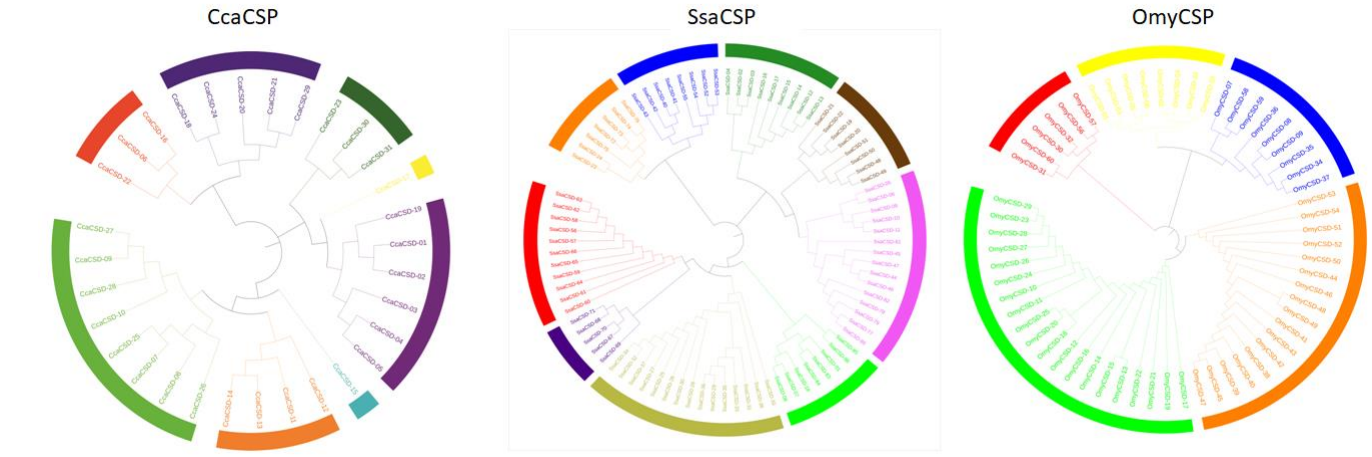

Figure 2. Phylogenetic distribution of Atlantic salmon, carp and rainbow trout CSPs drawn by the Mega7 program

In order to test the reliability of the phylogenetic tree, the motif compositions of the SsaCSP, CcaCSP and OmyCSPs were examined. Eighty-six for SsaCSP, 31 for CcaCSP and 60 for OmyCSP amino acid sequences of protein were loaded into the MEME database. A total of 20 different conserved motifs were identified for SsaCSP (**Table 1A**), CcaCSP (**Table 1B**), OmyCSP (**Table 1C**) proteins. Protected motifs, sequences and motif lengths of proteins were determined. According to those analysis, proteins containing similar motif patterns were found to be in the same cluster in the phylogenetic tree. In addition, motif patterns were similar in each of CSPs in s Atlantic salmon, carp and rainbow trout as species level, which can be attributed to the characteristic structure of the CSPs.

Table 1 Amino acid composition of the (A) *Salmo salar*, (B) *Common carp* and (C) *Oncorhynchus mykiss* CSP motifs

Motif no.	Sites	E-value	Amino acid sequence composition of motif	Width (aa)
(A)				
Motif 1	66	6.5e-1985	EVFYLTYGPDDIEKECHLPPQPKKSFYMZTNKHTGAVSAHN	41
Motif 2	81	4.9e-1196	NVRDGFGFIKCVDRDARMFFHFSD	24
Motif 3	63	6.9e-2193	FVSYSKLDMEGFRSLQEGEKVEFTFNESKRGLZQSAVTGPIGNRCVGTER	50
Motif 4	31	1.3e-1514	LLGYIATLKDNFGFIETANHDQEIFFHYSELCGDLENLELGDTVEYTLSK	50
Motif 5	31	1.2e-1498	NNGHTAFANGTAAGIRETGVVEKLLTSYGFIQCSERQARLFFHCSQYNGN	50
Motif 6	31	7.9e-1487	KCQNYSFGIVGMANKADCLQKGEMVKFQLCTVAQTGQKMACNVVPQRKAL	50
Motif 7	31	5.5e-1475	MRCQGVVCATKEAFGFIERADVVKEIFFHYSEFKGDLEALQAGDDVEFTI	50
Motif 8	31	1.3e-1206	LLEGDHVQFNISTDRRDKLERATNIDILPDTFHFTKESREM	41
Motif 9	31	1.2e-1446	RLLAQGTVIFEDISIEQFEGTVIKVIPKVPTKNQNDPLPGRICARISFTD	50
Motif 10	31	1.3e-1435	FSVILNQRTGKCSACNVRRVSEGPKPVATPRPDRLVNRLKSITLDDASAP	50
Motif 11	31	7.2e-1431	DMLSAQRNHAVRIKKLPKGTVSFHTQSEQRFVGVVEKEATAAITNNKSAS	50
Motif 12	31	1.5e-1341	NKVSAEKVTKVVAVNGVGQDVGETVMLGKVVRPLRSVDPSQTEYQGLIEL	50

Motif 13	31	2.1e-1336	LQELKIGDDVEFEVSSDRRTGKPIAVKLLKIKPEVLPEERISGQVGPDSH	50
Motif 14	24	1.1e-1075	MERVHSEPPLARNTASATSVVAIPRSFSVSHKKHKRTPLYQRSMSFDPGM	50
Motif 15	51	2.5e-842	LVIVRQPRGPDNSKGFNVERKTRQPGVID	29
Motif 16	31	5.1e-1127	VECVKDQFGFITYEVGESKKLFFHVKEVHDGLELQTGDEVE	41
Motif 17	24	5.4e-881	ASPFTVLHGYIHPVVSAIPTHLDGKSAPGQVPTGSVCYERN	41
Motif 18	29	1.9e-679	WKGFVEFTLPASPPAAFVSADLSSTSPVGLSLSPYGRSCDP	41
Motif 19	52	1.8e-529	KKKDKEAEEGVISYEDCGVKL	21
Motif 20	59	1.1e-357	EGQLHISDEVEFTVV	15
(B)				
Motif 1	26	5.8e-385	VIATKVLGTVKWFNVRNGYGFINRN	25
Motif 2	20	2.0e-478	RKYLRSVGDGETVEFDVVEGEKGAEAANVTGPGGVPVQGSK	41
Motif 3	12	5.4e-437	YPPYFVQRRYGRRPPYTNAPQRGEMTEGGEGDENQGGPDQGNKPMRQNYY	50
Motif 4	12	1.6e-417	GQNQEPRQRRYRRNFNYRRRRPQTTKPQDGKDSKAADASAEKSAAPEAEQ	50
Motif 5	12	1.1e-419	YAADRNRYRRFPRRRGPPRDYQENYQSDGEAREKREEEENVPEGEMQQQQ	50
Motif 6	17	1.0e-223	AAETQQPPQPAADAESPSSPAAAATAGDK	29
Motif 7	21	6.4e-169	KEDVFVHQTAIKKNN	15
Motif 8	12	1.6e-126	RGPPRPRPVREGEEDKENQDE	21
Motif 9	10	2.0e-126	VPVEGDEVTYKVCSIPPKHKKIQAVEVVITHLAPGTKHETW	41
Motif 10	9	1.5e-053	GLLPSPLPTKRTRTYSATVRA	21
Motif 11	11	2.9e-036	SAEPEESTSPDLSPLSPESASQPSSFPFP	29
Motif 12	12	1.4e-032	PTYPGRRR	8
Motif 13	7	6.1e-027	VQKRRKKGDRCYNCGGLDHH	20
Motif 14	5	3.2e-026	SREGVPLDPPVDVFVHQSKLH	21
Motif 15	3	6.7e-022	KCVDRDARMFFHFSEVLEESQLHISDEVEFTVVPDMLSAQRNHAVRIKKL	50
Motif 16	2	7.3e-022	NKGDCLQKGEMVKFQLCTVAQTGQKMACNIVPQRRALVECVKDQFGFITY	50
Motif 17	2	2.1e-020	NFGFIETANHDQEIFFHYSEVCGDVDNMDLGDTVEYTLSKGKGNKISAEK	50
Motif 18	2	6.8e-020	MGIRETGVVEKLLASYGFIQCSERQARLFFHCSQYNGNLQELKIGDDVEF	50
Motif 19	2	3.4e-019	TLDTGDKVNFYMETNKHTGAVSAHNIVLVKKKQSRCQGVVCATKEAFGFI	50
Motif 20	3	1.3e-017	KVPTKNQNDPLPGRISARINFTDKELLFGEKDTKSKVTLLEGDHVQFNI	49
(C)				
Motif 1	37	1.0e-1899	YLTYTPDDIEGNMHLDTGDKVSFYMETNKHTGAVSAHNIVLVKKKQMRCQ	50
Motif 2	37	2.9e-1817	DGTKCQNYSFGIVGMANKADCLQKGEMVKFQLCTVAQTGQKMACNVVPQR	50
Motif 3	37	5.6e-1859	TIKILNRTVNTKRLLGYIATLKDNFGFIETANHDQEIFFHYSELCGDLEN	50
Motif 4	52	3.3e-1577	AMRDGFGFIKCVDRDARMFFHFSEVLEEGQLHISDEVEFTVV	42
Motif 5	37	2.1e-1837	NNGHTAFANGTAAGIRETGVVEKLLTSYGFIQCSERQARLFFHCSQYNGN	50
Motif 6	37	7.6e-1781	NQNDPLPGRICARISFTDKELLFGEKDTKSKVTLLEGDHVQFNISTDRRD	50
Motif 7	37	2.6e-1769	MDMLSAQRNHAVRIKKLPKGTVSFHTQSEQRFVGVVEKEATAAITNNKSA	50
Motif 8	37	1.1e-1760	FGFITYEVGESKKLFFHVKEVHDGLELQTGDEVEFSVILNQRTGKCSACN	50
Motif 9	37	3.5e-1754	CATKEAFGFIERADVVKEIFFHYSEFKGDLEALQAGDDVEFTIKERNGKE	50
Motif 10	37	8.3e-1733	AEEGVISYEDCGVKLTVSYHVKDLEGATQPQAGDKVEFSINEVKRTGQQS	50
Motif 11	37	1.1e-1721	ATPRPDRLVNRLKSITLDDASAPRLVIVRQPRGPDNSKGFNVERKTRQPG	50
Motif 12	37	3.1e-1636	LQELKIGDDVEFEVSSDRRTGKPIAVKLLKIKPEVLPEERISGQVGPDSH	50
Motif 13	37	1.6e-1643	KGNKVSAEKVTKVVAVNGVGQDVGETVMLGKVVRPLRSVDPSQTEYQGLI	50
Motif 14	29	2.0e-1285	MGSPWKGFVEFTLPTSPPAAFISADLSSTSPIGLSLSPYGRSCFPVPTPL	50
Motif 15	27	6.8e-1225	MERVHSEPPLARNTAPSTSAVAIPRSFSVSHKKHKRTPLYQRSMSFDPGM	50
Motif 16	26	4.3e-966	SPFTVLHGYIHPVVSAIPTHLDGKSAPGQVPTGSVCYERNG	41
Motif 17	37	1.4e-931	DVRLLAQGTVIFEDISIEQFEGTVVKVIP	29
Motif 18	37	6.4e-710	RATNIDILPDTFHFTKESREM	21
Motif 19	45	1.5e-292	LELGTVEYTL	11
Motif 20	41	1.2e-257	VRRVSEGPKPV	11

Micro RNAs (miRNA) are products of a family of small non-coding RNAs. miRNAs break down the mRNA of the target gene to inhibit the expression of them [25]. miRBase v20.0 (http://www.mirbase.org/) was used and previously known animal miRNA precursors were downloaded. miRNAs targeting SsaCSP, CcaCSP and OmyCSP transcripts were evaluated in the miRNA database and then animal miRNAs were chosen. Two important parameters were used to identify these genes. The maximum expectation threshold was set to 3.0. The second parameter was the UPE maximum energy value. This value represents the energy required to open the secondary structure of the target region of the mRNA. According to the results, SsaCSP transcripts were targeted by 116 different miRNAs. Thirty-five different SsaCSP transcripts were targeted by these miRNAs. CcaCSP-31 was the most targeted transcript among CcaCSPs by the 13 miRNAs. miRNA targets of 14 different CcaCSP transcripts were identified. Besides, 25 of OmyCSP transcripts were targeted by 90 different miRNAs. Identification of miRNAs targeting CSP transcripts may be informative for functional genomics studies (**Figure 3**).

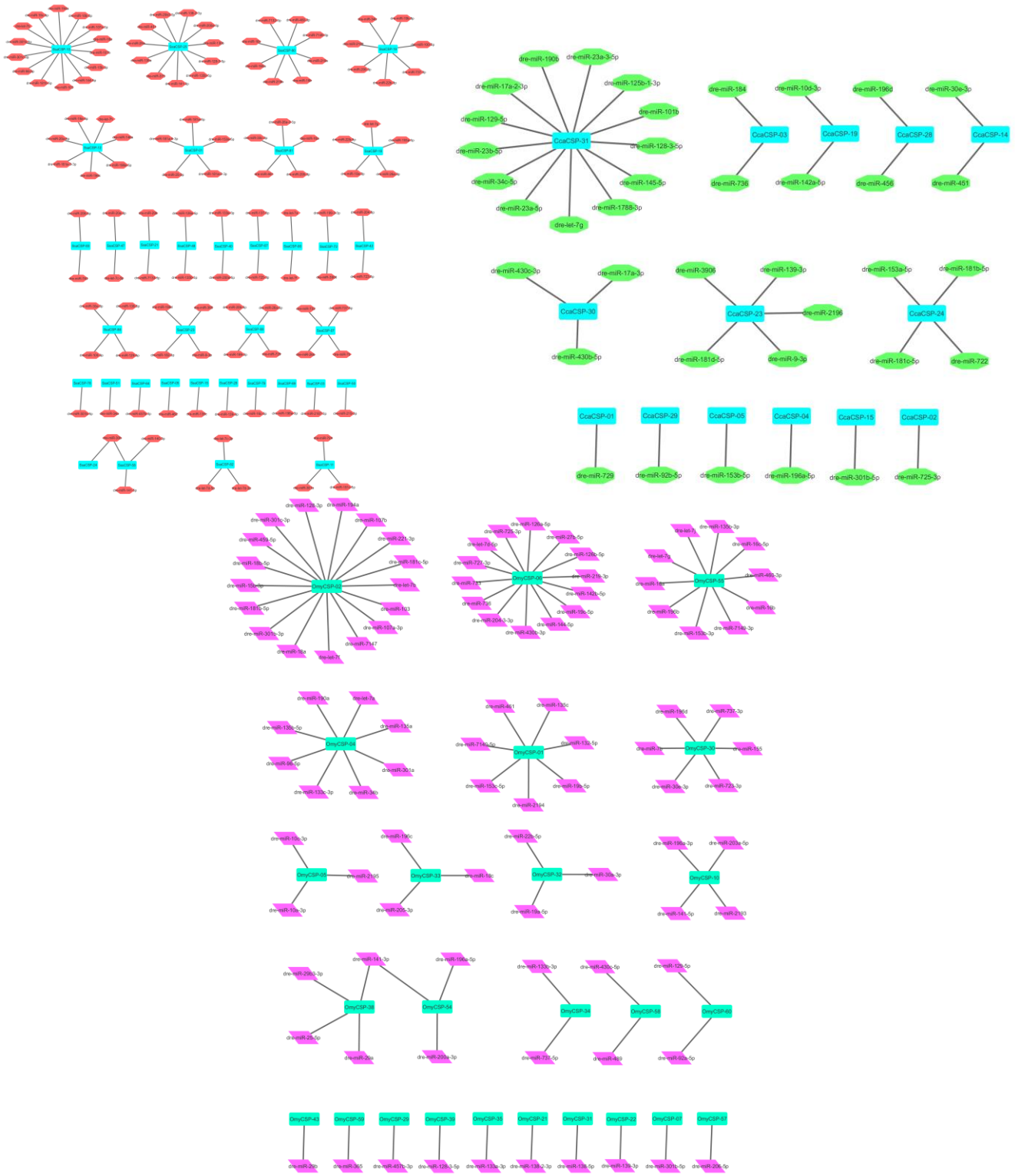

Figure 3. miRNA targets of SsaCSP, CcaCSP and OmyCSP transcripts

Using the Phyre2 database, BLASTP screening was performed for the CSPs found in the Protein Data Bank (PDB) and three-dimensional homology modeling of the SsaCSP, CcaCSP and OmyCSPs was performed. This database was used to estimate the structure, function, and analysis of mutations. There were 86 proteins for SsaCSP, 31 proteins for CcaCSP and 60 proteins for OmyCSP. A three-dimensional structure of 86 SsaCSP proteins was found in the similarity ratio of approximately 2 proteins with 90% reliability (**Figure 4**). A three-dimensional structure was determined from a total of 31 CcaCSPs in the similarity ratio of approximately 3 proteins with 90% reliability (**Fig. 4).** A three-dimensional structure was determined in the similarity ratio of 60 OmyCSP proteins with approximately 90% confidence in 1 protein (**Figure 4**). These protein models, which were estimated to have three-dimensional structures, might be useful in advanced studies for understanding of the function of CSPs in Atlantic salmon, carp and rainbow trout species. According to the 3-dimensional structure, OB (oligonucleotide binding) folding sites were found in CcaCSP protein. α-helix structures were generally

observed to be dominant in SsaCSPs. Rarely, β-layered structure was observed. There were also determined α-helix structures in OmyCSPs.

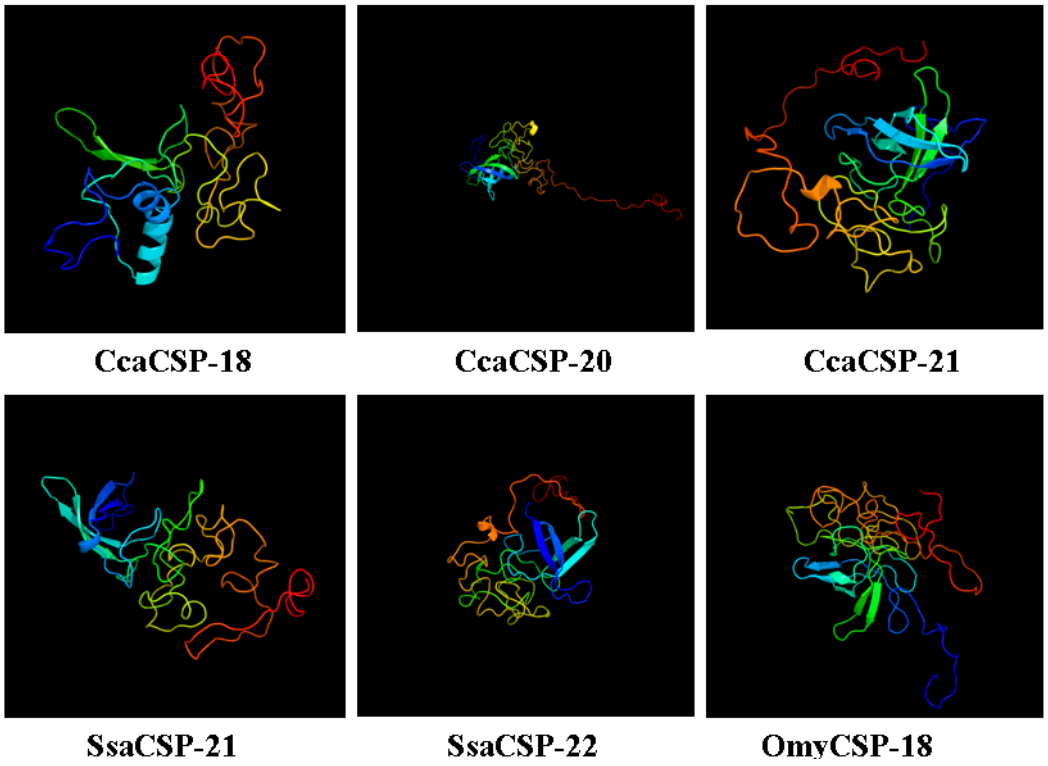

Figure 4. Predicted three-dimensional structure of SsaCSPs, CcaCSPs, OmyCSPs

Blast2Go program was used to understand the cellular localization, biological roles and molecular functions of SsaCSP, CcaCSP, OmyCSPs. In the light of the data obtained, the binding activity for SsaCSP, CcaCSP, OmyCSPs was determined as the molecular function. Binding to ATP, metal ions and cations were determined as the most binding activity for the SsaCSP, CcaCSP, OmyCSPs. SsaCSPs had function in biological regulation, metabolic and cellular processes. CcaCSPs were mainly located in the cell part and organelles and played important roles in metabolic and cellular processes and biological regulation. OmyCSPs had roles in metabolic and cellular processes and regulation of biological processes. (**Figure 5**).

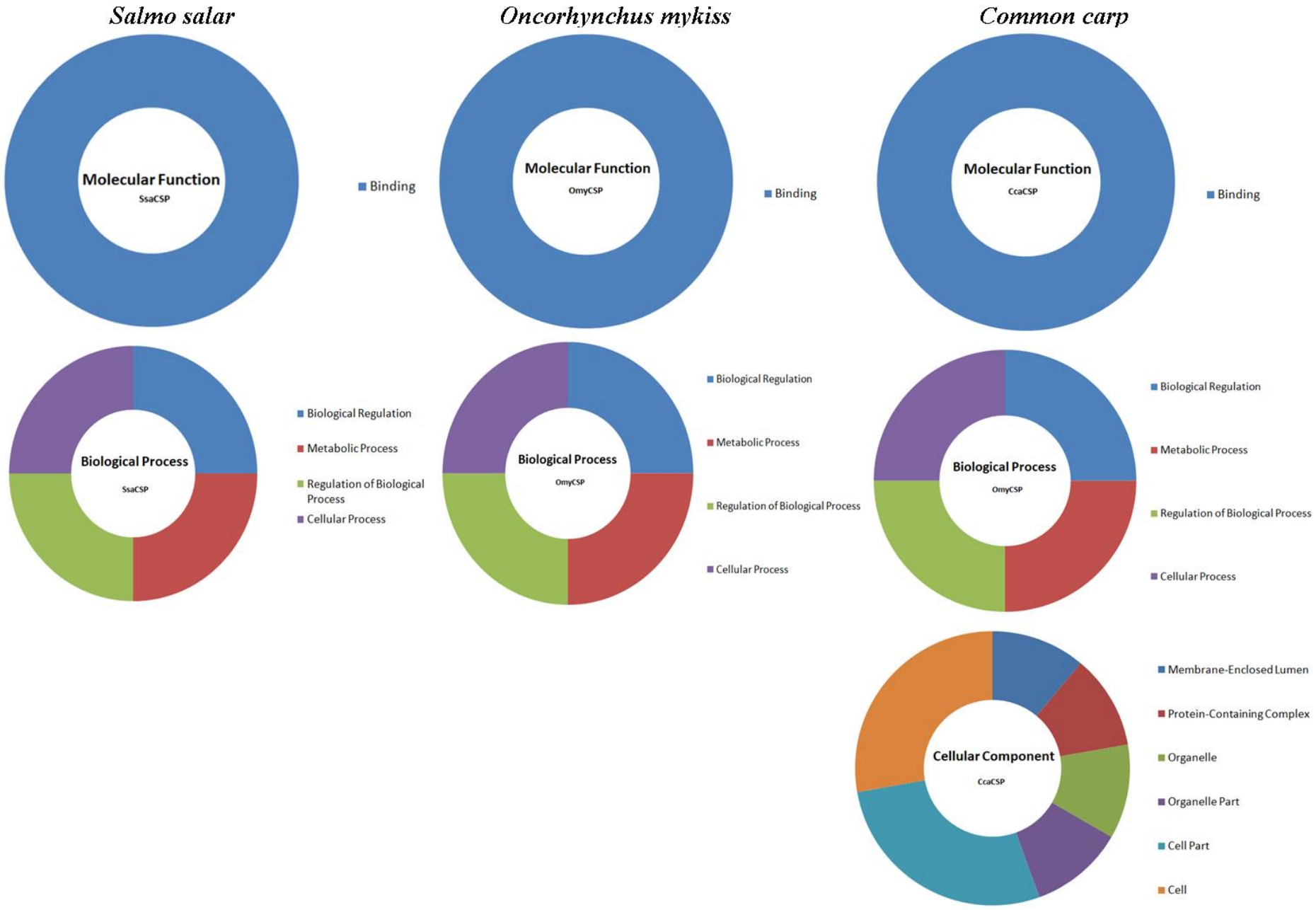

Figure 5. Functional analysis of SsaCSP, CcaCSP and OmyCSPs

Gene structure display server (http://gsds.cbi.pku.edu.cn/) was utilized to determine exon and intron structures of *SsaCSP*, *CcaCSP*, *OmyCSP* genes (**Figures 6**). All of the *SsaCSP*, *CcaCSP* and *OmyCSP* genes had introns. When the exon-intron structures of *SsaCSP*, *CcaCSP*, *OmyCSP* genes were compared in the phylogenetic trees, genes had similar exon-intron regions were found to be in the same phylogenic clusters in the trees.

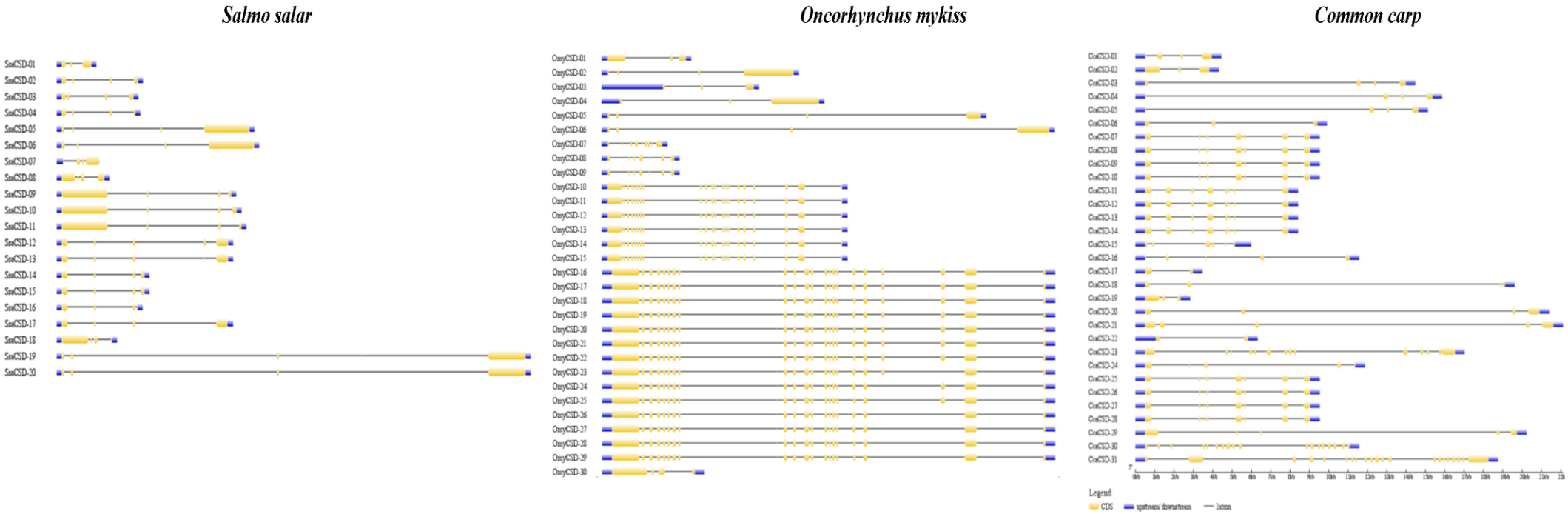

Figure 6. Exon-intron analysis of *SsaCSP*, *CcaCSP*, *OmyCSP* genes

As a result, there are not many studies on CSPs in fish. This protein region has been found in the zebrafish (*Danio rerio*), which is the model organism among fishes, but there is no similar study in the literature. The CSP family was found in a single-cell organism such as *Bacillus*, *Escherichia coli*. This includes CSPA, CSPC and CSPD family members in unicellular cells and is classified as CSPB, CSPC, and CSPD according to their function rather than CSP [11]. However, there is no such distinction in fish. It was found that these fish species were found in the *L. migrateria, ruets* and EST libraries. In the *L. migrateria* library, there were 43.481 motifs belonging to CSP. *Ruets* had 75 motifs. CSP was found in EST gene library with the number of 45.481. This shows the limited working area of CSPs in the fish. Current study represents the determination and characterization of CSP family members in these valuable fish species. This kind of gene identification studies open new perspectives to analyze functions of CSP family members in fishes. In addition, study results represent preliminary knowledge about understanding of the effects of these proteins in cold tolerance in these economically important fish species.

4. References

[1] Lien, S., Koop, B. F., Sandve, S. R., Miller, J. R., Kent, M. P., Nome, T., and Grammes, F. The Atlantic salmon genome provides insights into rediploidization. Nature, 533(7602), 200, 2016.
[2] Verspoor, E., Stradmeyer, L., & Nielsen, J. L. (Eds.). The Atlantic salmon: genetics, conservation and management. John Wiley & Sons, 2008.
[3] Kottelat, M. and J. Freyhof, Handbook of European freshwater fishes. Berlin, 2007, 646 pp.
[4] Courtenay, Walter R.; Welcomme, R. L., "International Introductions of Inland Aquatic Species". Copeia. 1989 (2): 520.
[5] Balon, Eugene K., "Probable Origin of Domestication", Domestication of the carp Cyprinus caprio L., Royal Ontario Museum, 1974, pp. 16–18.
[6] Banarescu, P., B. Coad., Cyprinids of Euroasia. in I Winfield, J Nelson, eds. Cyprinids Fishes, London: Chapman and Hall, 1991, Pp 127-155.
[7] McCrimmon, H., Carp in Canada. Fisheries Research Board of Canada, 1968.
[8] Fornshell, G. Rainbow trout—challenges and solutions. Reviews in Fisheries Science, 2002, 10(3-4), 545-557.
[9] Hardy, R. W., Rainbow trout, Oncorhynchus mykiss. Nutrient requirements and feeding of finfish for aquaculture, 2002,184-202.
[10] Thieringer, H. A., Jones, P. G., & Inouye, M., Cold shock and adaptation. Bioessays, 1998, 20(1), 49-57.
[11] Phadtare, S., Alsina, J., & Inouye, M., Cold-shock response and cold-shock proteins. Current opinion in microbiology, 1999, 2(2), 175-180.
[12] Lindquist, J. A., & Mertens, P. R., Cold shock proteins: from cellular mechanisms to pathophysiology and disease. Cell Communication and Signaling, 2018, 16(1), 63.
[13] Keto-Timonen, R., Hietala, N., Palonen, E., Hakakorpi, A., Lindström, M., & Korkeala, H., Cold shock proteins: a minireview with special emphasis on Csp-family of enteropathogenic Yersinia. Frontiers in microbiology, 2016, 7, 1151.
[14] Crawshaw, L. I., Physiological and behavioral reactions of fishes to temperature change. Journal of the Fisheries Board of Canada, 1977, 34(5), 730-734.
[15] Tanck, M. W. T., Booms, G. H. R., Eding, E. H., Bonga, S. W., & Komen, J., Cold shocks: a stressor for common carp. Journal of fish Biology, 2000, 57(4), 881-894.
[16] Fry, F. E. J., Effects of the environment on animal activity. Publ. Out. Fish. Res. Lab., 1947, 55(68), 1-62.1
[17] Donaldson, M. R., Cooke, S. J., Patterson, D. A., & Macdonald, J. S., Cold shock and fish. Journal of Fish Biology, 2008, 73(7), 1491-1530.
[18] Kumar, S., Stecher, G., & Tamura, K., MEGA7: molecular evolutionary genetics analysis version 7.0 for bigger datasets. Molecular biology and evolution, 2016, 33(7), 1870-1874.
[19] Hu B., Jin J., Guo A.Y., Zhang H., Luo J. and Gao G., GSDS 2.0: an upgraded gene feature visualization server. Bioinformatics, 2015, 31(8), 1296-1297.
[20] Saitou, N., & Nei, M., The neighbor-joining method: a new method for reconstructing phylogenetic trees. Molecular biology and evolution, 1987, 4(4), 406-425.
[21] Bailey, T. L., & Elkan, C., Fitting a mixture model by expectation maximization to discover motifs in bipolymers, 1994.
[22] Quevillon, E., Silventoinen, V., Pillai, S., Harte, N., Mulder, N., Apweiler, R., & Lopez, R., InterProScan: protein domains identifier. Nucleic acids research, 2005, 33(suppl_2), W116-W120.
[23] Conesa, A., & Götz, S., Blast2GO: A comprehensive suite for functional analysis in plant genomics. International journal of plant genomics, 2008.
[24] Kelley, L. A., & Sternberg, M. J., Protein structure prediction on the Web: a case study using the Phyre server. Nature protocols, 2009, 4(3), 363.
[25] Jones-Rhoades, M. W., & Bartel, D. P., Computational identification of plant microRNAs and their targets, including a stress-induced miRNA. Molecular cell, 2004, 14(6), 787-799.

Appendix

Table S1. Supplementary table for SsaCSPs

ID	NCBI Accession No.	Physical position on *Salmo Salar* genome			Protein length (aa)	Molecular weight (Da)	pI	Instability index	Stable or unstable
		Chromosome	Start position (bp)	End Position (bp)					
SsaCSP-01	XP_014063589.1	1	74,309,848	74,312,833	158	17480.85	8.82	53.35	unstable
SsaCSP-02	XP_014013043.1	2	14,826,588	14,834,258	262	28502.73	9.35	72.92	unstable
SsaCSP-03	XP_014013050.1	2	14,826,588	14,834,258	236	25961.05	9.62	74.30	unstable
SsaCSP-04	XP_014013059.1	2	14,826,588	14,834,258	145	15852.85	6.20	52.76	unstable
SsaCSP-05	XP_014022707.1	2	30,471,155	30,490,497	202	22117.74	6.86	59.61	unstable
SsaCSP-06	XP_014022716.1	2	30,471,155	30,490,497	195	21371.95	6.86	60.44	unstable
SsaCSP-07	NP_001133414.1	3	65.477.156	65.481.446	159	17459,82	9,26	55,65	unstable
SsaCSP-08	XP_014048617.1	3	65,477,156	65,481,446	159	17459.82	9.26	55.65	unstable
SsaCSP-09	XP_014055906.1	5	50,224,632	50,242,696	202	22170.89	8.35	64.51	unstable
SsaCSP-10	XP_014055908.1	5	50,224,632	50,242,696	195	21425.10	8.35	65.51	unstable
SsaCSP-11	XP_014055909.1	5	50,224,632	50,242,696	195	21425.10	8.35	65.51	unstable
SsaCSP-12	XP_014057001.1	5	65,451,183	65,467,908	285	31180.01	9.95	72.59	unstable
SsaCSP-13	XP_014057003.1	5	65,451,183	65,467,908	257	28094.38	9.92	75.81	unstable
SsaCSP-14	XP_014057004.1	5	65,451,183	65,467,908	252	27532.78	9.75	77.35	unstable
SsaCSP-15	XP_014057005.1	5	65,451,183	65,467,908	251	27475.73	9.75	77.13	unstable
SsaCSP-16	XP_014057007.1	5	65,451,183	65,467,908	226	24975.01	9.96	81.05	unstable

SsaCSP-17	XP_014057008.1	5	65,451,183	65,467,908	226	24975.01	9.96	81.05	unstable
SsaCSP-18	XP_014059274.1	6	33,682,575	33,687,644	159	17530.85	9.00	57.39	unstable
SsaCSP-19	XP_014060071.1	6	45,455,711	45,502,322	271	29388.34	8.64	66.63	unstable
SsaCSP-20	XP_014060072.1	6	45,455,711	45,502,322	267	29003.91	8.64	64.82	unstable
SsaCSP-21	XP_014060073.1	6	45,455,711	45,502,322	190	20665.36	8.35	79.73	unstable
SsaCSP-22	XP_014060074.1	6	45,455,711	45,502,322	190	20665.36	8.35	79.73	unstable
SsaCSP-23	XP_014062241.1	7	12,010,561	12,016,017	335	36643.33	10.19	80.82	unstable
SsaCSP-24	XP_014062242.1	7	12,010,561	12,016,017	331	36261.86	10.16	82.42	unstable
SsaCSP-25	XP_013990799.1	13	26.009.382	26.044.770	939	104041,31	6,95	36,08	stable
SsaCSP-26	XP_013990800.1	13	26.009.382	26.044.770	935	103541,7	6,71	36,28	stable
SsaCSP-27	XP_013990801.1	13	26.009.382	26.044.770	932	103234,39	6,95	36,05	stable
SsaCSP-28	XP_013990802.1	13	26.009.382	26.044.770	931	103226,31	6,71	35,64	stable
SsaCSP-29	XP_013990803.1	13	26.009.382	26.044.770	931	103041,08	a	35,01	stable
SsaCSP-30	XP_013990804.1	13	26.009.382	26.044.770	927	102726,7	6,52	35,84	stable
SsaCSP-31	XP_013990805.1	13	26.009.382	26.044.770	923	102226,08	6,45	34,55	stable
SsaCSP-32	XP_013990807.1	13	26.009.382	26.044.770	920	102028,06	7,08	35,79	stable
SsaCSP-33	XP_013990808.1	13	26.009.382	26.044.770	919	101726,47	6,31	34,75	stable
SsaCSP-34	XP_013990809.1	13	26.009.382	26.044.770	913	101221,15	7,08	35,75	stable
SsaCSP-35	XP_013990810.1	13	26.009.382	26.044.770	912	100919,55	6,31	34,71	stable

SsaCSP-36	XP_013990811.1	13	26.009.382	26.044.770	893	98906,31	6,31	34,38	stable
SsaCSP-37	XP_013990812.1	13	26.009.382	26.044.770	887	98718,27	7,33	33,44	stable
SsaCSP-38	XP_013990813.1	13	26.009.382	26.044.770	886	98159,58	6,46	34,37	stable
SsaCSP-39	XP_013990814.1	13	26.009.382	26.044.770	844	93877,73	6,46	32,04	stable
SsaCSP-40	XP_013991015.1	13	31.436.802	31.445.267	326	36365,72	9,71	60,63	stable.
SsaCSP-41	XP_013991016.1	13	31.436.802	31.445.267	322	35809,05	9,58	60,9	stable
SsaCSP-42	XP_013991017.1	13	31.436.802	31.445.267	305	33820,84	9,47	58,12	stable
SsaCSP-43	NP_001133216.1	13	31.436.802	31.445.267	301	33264,17	9,29	58,37	unstable
SsaCSP-44	XP_013997885.1	14	68.017.031	68.027.537	204	22532,07	6,66	65,79	stable
SsaCSP-45	XP_013997886.1	14	68.017.031	68.027.537	202	22084,52	6,18	64,7	stable
SsaCSP-46	XP_013997887.1	14	68.017.031	68.027.537	195	21284,65	6,18	64,47	stable
SsaCSP-47	XP_013997888.1	14	68.017.031	68.027.537	195	21298,72	6,39	63,69	stable
SsaCSP-48	XP_013999364.1	15	22.395.252	22.438.885	237	25670,05	8,88	68,03	stable
SsaCSP-49	XP_013999365.1	15	22.395.252	22.438.885	233	25285,62	8,88	65,98	stable
SsaCSP-50	XP_013999366.1	15	22.395.252	22.438.885	231	25069,28	8,75	68,36	stable
SsaCSP-51	XP_013999367.1	15	22.395.252	22.438.885	190	20669,44	8,97	73,19	stable
SsaCSP-52	XP_014001654.1	15	66,117,700	66,124,504	379	42113.05	9.57	70.43	unstable
SsaCSP-53	XP_014001655.1	15	66,117,700	66,124,504	378	42025.97	9.57	69.37	unstable
SsaCSP-54	XP_014001656.1	15	66,117,700	66,124,504	358	39568.17	9.34	68.87	unstable

SsaCSP-55	XP_014001657.1	15	66,117,700	66,124,504	357	39481.09	9.34	67.74	unstable
SsaCSP-56	XP_014001115.1	15	75.504.333	75.523.784	932	103181,39	6,52	34,55	stable
SsaCSP-57	XP_014001116.1	15	75.504.333	75.523.784	876	97304,57	6,45	32,3	stable
SsaCSP-58	XP_014001117.1	15	75.504.333	75.523.784	925	102374,48	6,52	34,5	stable
SsaCSP-59	XP_014001118.1	15	75.504.333	75.523.784	924	102283,35	6,52	33,89	stable
SsaCSP-60	XP_014001119.1	15	75.504.333	75.523.784	868	96406,53	6,44	31,58	stable
SsaCSP-61	XP_014001120.1	15	75.504.333	75.523.784	861	95599,61	6,44	31,51	stable
SsaCSP-62	XP_014001121.1	15	75.504.333	75.523.784	913	101168,15	6,55	34,23	stable
SsaCSP-63	XP_014001122.1	15	75.504.333	75.523.784	906	100361,24	6,55	34,17	stable
SsaCSP-64	XP_014001123.1	15	75.504.333	75.523.784	842	93586,37	6,46	31,09	stable
SsaCSP-65	XP_014001124.1	15	75.504.333	75.523.784	880	97804,18	6,61	32,11	stable
SsaCSP-66	XP_014001126.1	15	75.504.333	75.523.784	880	97804,18	6,61	32,11	stable
SsaCSP-67	NP_001167093.1	15	75.504.333	75.523.784	854	94950,98	6,13	30,69	stable
SsaCSP-68	XP_014001127.1	15	75,504,333	75,522,784	879	97291.55	6.12	32.38	stable
SsaCSP-69	XP_014001128.1	15	75,504,333	75,522,784	837	92965.65	6.12	30.16	stable
SsaCSP-70	XP_014001129.1	15	75,504,333	75,522,784	837	92965.65	6.12	30.16	stable
SsaCSP-71	XP_014001130.1	15	75,504,333	75,522,784	818	90952.41	6.10	29.70	stable
SsaCSP-72	NP_001133543.1	18	47.970.066	47.975.989	328	35950,69	9,94	81,7	unstable
SsaCSP-73	XP_014010961.1	18	47,970,066	47,974,989	339	37095.02	9.98	79.22	unstable

SsaCSP-74	XP_014010962.1	18	47,970,066	47,974,989	335	36713.55	9.94	80.78	unstable
SsaCSP-75	XP_014010963.1	18	47,970,066	47,974,989	332	36332.16	9.98	80.10	unstable
SsaCSP-76	XP_014010964.1	18	47,970,066	47,974,989	328	35950.69	9.94	81.70	unstable
SsaCSP-77	XP_014033333.1	27	19,676,671	19,691,042	204	22228.81	7.57	51.49	unstable
SsaCSP-78	XP_014033334.1	27	19,676,671	19,691,042	202	21919.48	6.65	53.78	unstable
SsaCSP-79	XP_014033335.1	27	19,676,671	19,691,042	195	21065.55	6.65	53.78	unstable
SsaCSP-80	XP_014033336.1	27	19,676,671	19,691,042	195	21079.62	7.02	52.99	unstable
SsaCSP-81	XP_014033337.1	27	19,676,671	19,691,042	175	19070.75	8.24	59.07	unstable
SsaCSP-82	XP_014033338.1	27	19,676,671	19,691,042	159	17347.53	8.12	53.21	unstable
SsaCSP-83	XP_014035109.1	28	13,878,289	13,888,222	158	17493.88	8.93	51.57	unstable
SsaCSP-84	XP_014035110.1	28	13,878,289	13,888,222	158	17493.88	8.93	51.57	unstable
SsaCSP-85	XP_014042228.1	scaffold	2,089	4,413	108	11519.15	6.05	25.02	stable
SsaCSP-86	XP_014039437.1	scaffold	13,179	15,319	167	17742.03	8.57	65.89	unstable

Table S2. Supplementary table for CcaCSPs

ID	NCBI Accession No.	Physical position on *Cyprinus carpio* genome			Protein length (aa)	Molecular weight (Da)	pI	Instability index	Stable or unstable
		Chromosome	Start position (bp)	End Position (bp)					
CcaCSP-01	XP_018925526.1	5	18,459,016	18,462,463	154	16856.21	9.30	60.69	unstable
CcaCSP-02	XP_018925532.1	5	18,459,016	18,462,463	154	16856.21	9.30	60.69	unstable
CcaCSP-03	XP_018931080.1	6	7,067,314	7,082,199	158	16923.21	8.91	71.16	unstable
CcaCSP-04	XP_018931086.1	6	7,067,314	7,082,199	158	16923.21	8.91	71.16	unstable
CcaCSP-05	XP_018931094.1	6	7,067,314	7,082,199	158	16923.21	8.91	71.16	unstable
CcaCSP-06	XP_018927839.1	6	11,490,177	11,499,086	201	22000.64	8.36	62.56	unstable
CcaCSP-07	XP_018963132.1	14	1,145,141	1,153,681	313	35663.85	9.58	66.21	unstable
CcaCSP-08	XP_018963133.1	14	1,145,141	1,153,681	312	35576.77	9.58	64.36	unstable
CcaCSP-09	XP_018963134.1	14	1,145,141	1,153,681	309	35076.16	9.44	65.76	unstable
CcaCSP-10	XP_018963135.1	14	1,145,141	1,153,681	308	34989.09	9.44	64.44	unstable
CcaCSP-11	XP_018964282.1	16	2,464,171	2,471,589	315	35914.01	9.56	67.45	unstable
CcaCSP-12	XP_018964283.1	16	2,464,171	2,471,589	314	35826.93	9.56	67.02	unstable
CcaCSP-13	XP_018964284.1	16	2,464,171	2,471,589	311	35383.38	9.42	69.05	unstable
CcaCSP-14	XP_018964285.1	16	2,464,171	2,471,589	310	35296.30	9.42	67.76	unstable
CcaCSP-15	XP_018964078.1	16	6,798,175	6,803,164	214	23815.09	9.78	68.96	unstable

Table S3. Supplementary table for OmyCSPs

ID	NCBI Accession No.	Physical position on *Oncorhynchus mykiss* genome			Protein length (aa)	Molecular weight (Da)	pI	Instability index	Stable or unstable
		Chromosome	Start *position* (bp)	End Position (bp)					
OmyCSP-01	XP_021481619.1	2	9,987,049	9,994,437	130	14105.98	9.44	61.44	unstable
OmyCSP-02	XP_021417535.1	2	23,615,665	23633142	202	22166.81	7.15	62.48	unstable
OmyCSP-03	XP_021437991.1	3	22,181,984	22195726	251	27291.40	9.66	82.57	unstable
OmyCSP-04	XP_021438459.1	3	33,644,075	33663929	195	21393.01	7.15	59.06	unstable
OmyCSP-05	XP_021454089.1	4	49,774,027	49809035	227	24494.67	8.53	70.08	unstable
OmyCSP-06	XP_021467181.1	8	8,446,940	8488379	227	24619.77	8.59	66.55	unstable
OmyCSP-07	XP_021470938.1	9	18,761,008	18766173	331	36214.33	10.10	83.29	unstable
OmyCSP-08	XP_021471492.1	9	36,175,698	36181996	379	42027.88	9.56	69.78	unstable
OmyCSP-09	XP_021471493.1	9	36,175,698	36181996	358	39483.00	9.31	68.18	unstable
OmyCSP-10	XP_021471853.1	9	45,229,012	45251043	940	104261.69	6.82	35.49	stable
OmyCSP-11	XP_021471854.1	9	45,229,012	45251043	936	103762.07	6.61	35.69	stable
OmyCSP-12	XP_021471856.1	9	45,229,012	45251043	933	103454.77	6.82	35.45	stable
OmyCSP-13	XP_021471857.1	9	45,229,012	45251043	932	103243.42	6.52	34.70	stable
OmyCSP-14	XP_021471858.1	9	45,229,012	45251043	932	103363.64	6.82	34.84	stable
OmyCSP-15	XP_021471859.1	9	45,229,012	45251043	928	102743.81	6.38	34.90	stable
OmyCSP-16	XP_021471860.1	9	45,229,012	45251043	928	102864.03	6.61	35.04	stable
OmyCSP-17	XP_021471861.1	9	45,229,012	45251043	924	102345.38	6.52	34.04	stable
OmyCSP-18	XP_021471862.1	9	45,229,012	45,251,043	921	102248.44	6.91	35.19	stable
OmyCSP-19	XP_021471863.1	9	45,229,012	45,251,043	920	101845.77	6.37	34.24	stable

OmyCSP-20	XP_021471864.1	9	45,229,012	45,251,043	914	101441.53	6.91	35.14	stable
OmyCSP-21	XP_021471865.1	9	45,229,012	45,251,043	913	101038.85	6.37	34.19	stable
OmyCSP-22	XP_021471866.1	9	45,229,012	45,251,043	894	99025.61	6.38	33.85	stable
OmyCSP-23	XP_021471867.1	9	45,229,012	45,251,043	888	98838.45	6.95	32.94	stable
OmyCSP-24	XP_021471868.1	9	45,229,012	45,251,043	887	98339.84	6.31	33.09	stable
OmyCSP-25	XP_021471869.1	9	45,229,012	45,251,043	868	96326.60	6.31	32.71	stable
OmyCSP-26	XP_021471870.1	9	45,229,012	45,251,043	845	93999.91	6.31	31.06	stable
OmyCSP-27	XP_021471871.1	9	45,229,012	45,251,043	838	93193.00	6.31	30.98	stable
OmyCSP-28	XP_021471872.1	9	45,229,012	45,251,043	826	91986.67	6.31	30.62	stable
OmyCSP-29	XP_021471873.1	9	45,229,012	45,251,043	819	91179.76	6.31	30.53	stable
OmyCSP-30	XP_021480819.1	12	72,079,696	72,083,911	159	17383.72	9.00	57.72	unstable
OmyCSP-31	XP_021481521.1	12	88,577,019	88,644,765	170	17851.11	8.24	57.48	unstable
OmyCSP-32	XP_021413690.1	13	39,520,408	39524430	159	17420.73	9.00	55.70	unstable
OmyCSP-33	XP_021417799.1	14	20,554,543	20563643	195	21253.67	6.00	66.08	unstable
OmyCSP-34	NP_001158512.1	16	34,115,146	34124611	301	33120.04	9.47	57.89	unstable
OmyCSP-35	XP_021420068.1	16	34,115,146	34124611	326	36221.59	9.82	60.19	unstable
OmyCSP-36	XP_021420069.1	16	34,115,146	34124611	322	35664.92	9.71	60.45	unstable
OmyCSP-37	XP_021420070.1	16	34,115,146	34124611	305	33676.71	9.62	57.65	unstable
OmyCSP-38	XP_021422074.1	16	49,176,543	49214631	939	104132.52	7.12	38.22	stable
OmyCSP-39	XP_021422075.1	16	49,176,543	49214631	935	103632.91	6.82	38.43	stable
OmyCSP-40	XP_021422076.1	16	49,176,543	49214631	932	103325.00	7.12	38.20	stable
OmyCSP-41	XP_021422078.1	16	49,176,543	49214631	931	103317.52	6.82	37.79	stable
OmyCSP-42	XP_021422079.1	16	49,176,543	49214631	1862	206431.79	6.78	37.49	stable

OmyCSP-43	XP_021422080.1	16	49,176,543	49214631	927	102817.91	6.61	38.01	stable
OmyCSP-44	XP_021422081.1	16	49,176,543	49214631	923	102317.29	6.52	36.73	stable
OmyCSP-45	XP_021422082.1	16	49,176,543	49214631	920	102119.27	7.29	37.97	stable
OmyCSP-46	XP_021422083.1	16	49,176,543	49214631	919	101817.68	6.38	36.94	stable
OmyCSP-47	XP_021422084.1	16	49,176,543	49214631	913	101312.36	7.29	37.95	stable
OmyCSP-48	XP_021422085.1	16	49,176,543	49214631	912	101010.76	6.38	36.91	stable
OmyCSP-49	XP_021422086.1	16	49,176,543	49214631	893	98997.52	6.39	36.63	stable
OmyCSP-50	XP_021422087.1	16	49,176,543	49214631	887	98837.54	7.58	35.71	stable
OmyCSP-51	XP_021422089.1	16	49,176,543	49214631	886	98237.78	6.46	36.08	stable
OmyCSP-52	XP_021422090.1	16	49,176,543	49214631	867	96224.54	6.49	35.77	stable
OmyCSP-53	XP_021422091.1	16	49,176,543	49214631	844	93955.93	6.46	33.84	stable
OmyCSP-54	XP_021422092.1	16	49,176,543	49214631	825	91942.69	6.49	33.47	stable
OmyCSP-55	XP_021428532.1	18	41,939,025	41955903	195	21093.57	6.39	57.79	unstable
OmyCSP-56	XP_021431664.1	20	16,564,828	16572932	158	17493.88	8.93	51.57	unstable
OmyCSP-57	XP_021431665.1	20	16,564,828	16572932	316	34969.74	9.06	51.60	unstable
OmyCSP-58	XP_021433847.1	21	42,643,840	42648716	333	36429.95	10.10	79.46	unstable
OmyCSP-59	XP_021433848.1	21	42,643,840	42648716	329	36048.48	10.07	81.05	unstable
OmyCSP-60	XP_021448749.1	scaffold	0,502	832	170	17851.11	8.24	57.48	unstable

Kastamonu University
Journal of Engineering and Sciences
e-ISSN 2667-8209
http://dergipark.gov.tr/kastamonujes

Advanced Road Materials in Highway Infrastructure and Features

Abdelwahab Z. Amaitik Altera [a], Oguzhan Yavuz Bayraktar [b], Mehmet Cetin *, [c]

[a] *Department of Engineering Management, Institute of Science, Kastamonu University, Kastamonu, Turkey*
[b] *Department of Civil Engineering,Faculty of Engineering and Architecture, Kastamonu University, Kastamonu, Turkey*
[c] *Department of Landscape Architecture, Faculty of Engineering and Architecture, Kastamonu University Kastamonu, Turkey*

ARTICLE INFO

Received: May:11.2019
Reviewed: May:14.2019
Accepted: May:22.2019

Keywords:
City road,
Highway,
Road materials,
Road planning,
Structure

Corresponding Author:
E-mail: mcetin@kastamonu.edu.tr

ABSTRACT

Highway is one of the most widely used parts of the transportation sector. It is especially important in natural conditions that do not allow other types of transport. Highway, which requires an important infrastructure investment, is noteworthy as difficult and long-lasting investments due to its high costs and long-term returns. Highway, while providing integration in the world on the one hand, on the other hand, as a developing sector within the framework of supplying interaction, needs to meet the needs of the global world. In this study, highway infrastructure and features will be presented. The expressway structure interfaces huge urban territories and rural systems all through the country. Highway gives the snappiest line from indicate A to B, suggesting that the people who must use this transport system ought to use the speediest and most direct course to pass by road. An average road system is fundamental for compelling improvement and headway in any country. At some point in the past emergency organizations were not open to the people who lived in remote zones in light of the way that there basically were not fitting ways.

Anahtar Kelimeler:
Şehir yolu,
Otoyol,
Yol malzemeleri,
Yol planlaması,
Yapı

ÖZ

Karayolu, taşımacılık sektörünün en çok kullanılan bölümlerinden biridir. Diğer taşıma türlerine izin vermeyen doğal koşullarda özellikle önemlidir. Önemli bir altyapı yatırımı gerektiren otoyol, yüksek maliyetleri ve uzun vadeli getirileri nedeniyle zor ve uzun ömürlü yatırımlar olarak dikkat çekmektedir. Otoyol, bir yandan dünyaya entegrasyon sağlarken, diğer yandan, etkileşimi sağlama çerçevesinde gelişen bir sektör olarak küresel dünyanın ihtiyaçlarını karşılamalıdır. Bu çalışmada, karayolu altyapısı ve özellikleri tanıtılacaktır. Otoyol yapısı, ülke genelinde devasa kentsel bölgelere ve kırsal sistemlere arayüzlük ediyor. Otoyol, en hızlı çizgiyi A'dan B'ye kadar gösterir; bu taşıma sistemini kullanması gereken insanların karayolunda en hızlı ve en doğrudan rotayı kullanmaları gerektiğini ileri sürmektedir. Ortalama bir yol sistemi, herhangi bir ülkede zorlayıcı iyileştirme ve ilerleme için temeldir. Aynı zamanda geçmişte acil durum örgütleri, temelde uygun olmayan yolların ışığında uzak bölgelerde yaşayan insanlara açık değildi.

1. Introduction

Highway, which has a share of 95% in freight and passenger transport all over the world, has been continuously updated and became widespread and has become one of the most important construction investments. As a result of the continuous increase in the world population, the development of industry and technology, the need for raw materials has increased and natural resources have started to decrease. Research on the economic use of existing limited resources has become widespread and has gained importance. Highway; the land is open to public use, bridges and areas. The highway can also be defined as the whole of the structures constructed for the purpose of bringing the natural ground to the desired heights (elevations) along a route determined in accordance with the predefined geometric standards and to enable the movement of the motor vehicles under the safety, comfort and desired speed conditions [1-18].

On a finished street, the zone between the leveling surface and the characteristic ground line is called, foundation. Framework; a dirt body shaped by the dirt brought from the outside in the filler areas of the street; in the part is regular ground. Nevertheless, the fillings made to shape the leveling surface in the part parts are likewise incorporated into the framework. Likewise; connect structures, viaducts, passages, ducts and holding dividers are additionally considered as foundation [3-18].

Seepage is a vital issue as it can make incredible harm water, street foundation and superstructure. At the point when the water comes into contact with the floor, it liberates the floor with the stop defrost impact and diminishes the conveying limit of the floor. With the base floor bringing down its bearing limit, the water must be avoided the street structure or expelled and expelled from the street structure, which will majorly affect the base floor and the superstructure. This can be accomplished with craftsmanship structures and an all around planned waste framework. [4-18].

So as to lessen the traffic loads exchanged from the vehicles to the framework, to transmit them to the foundation and to secure the foundation, the street structure which is commonly made out of covering, essential and sub-base layers is called Highway Superstructure [19-20].

2. Material and Method

The superstructures are partitioned into three gatherings as unbending (solid street), semi-inflexible and adaptable superstructure (black-top street) as indicated by their sort and development techniques. Contingent upon the ground floor, traffic, ecological conditions and financial conditions, the most reasonable ones are chosen and anticipated.

It is a sort of superstructure that conveys the hub loads on it with its very own solidness and the covering is structured as strengthened cement. The execution attributes of this kind of covering rely upon the properties of the solid sections, subbase and base layers shaping the covering, and the properties of the materials utilized in these layers [19-22]. Sub-base layer, solidifying impact that may harm the solid covering, swelling and shrinkage impact in soils demonstrating high volume change, siphoning impact in fine grained soils, solid piece with base layer or base layer. It is a layer of grains.

3. Results

The solid section layer is the legitimately influenced layer of traffic loads of the unbending superstructure. Longitudinal and transverse slant are the two most critical components to consider in solid chunks. Since the solid streets are harsh, because of the unpleasantness of the street, the longitudinal incline esteems can reach 7% [19-24]. In semi-unbending asphalts, not the same as the adaptable superstructures, it is utilized as a granular establishment or subbase balanced out with concrete reinforced granular establishment or bond. Bituminous base, folio and wear layers are laid over these layers [19-25].

Adaptable superstructure: It is an exceptionally normal kind of superstructure which is utilized and it is delivered from the materials with high quality and bearing quality from the base to the top, passing the traffic loads coming through different layers inside the structure, passing on them to a decent surface contact gave floor. It has high protection from total, adaptable rubbing esteems and high union opposition esteems in adaptable asphalts. This is on the grounds that the soundness of the covering decides the execution attributes of the superstructures. In the meantime, it needs to convey the traffic securely and financially [19-29].

Sub-base layer: It is the sub-base layer of the material layer balanced out with the base material of the base (street framework) and the base material of the settled grain or an appropriate fastener material. The principle task is to make a working stage for the development of bituminous layers. It isn't obligatory for the sub-base layer to be connected in territories where the ground layer is unblemished. Whenever financial and ecological components are mulled over, it is advantageous to utilize the materials, for example, rubble, slag and development squander in street construction [10, 11,14,15,19-22].

The fundamental layer; It is the layer which settles the superstructure of the superstructure, the slight leveling surface or the sub-base layer, which sets up the association between the base layer and the common ground which can be made out of at least one layers. The principle errand of the base layer is to spread the stresses brought about by the advances of the vehicles inside the cutoff points of the bearing limit of the base layer by giving a help to the covering layer. The cementitious or bitumen-reinforced blend can be either balanced out or painstakingly chosen granular

material, contingent upon the base layer. Bituminous blends are all the more broadly utilized in high traffic volumes [10, 11, 14, 15, 19-24].

The top layer of the superstructure that is straightforwardly presented to traffic loads is the covering layer. Because of the high pressure and tensile stresses because of traffic loads, the covering layer ought to have a higher modulus of flexibility than different layers of the superstructure. This layer comprises of two sections as wear and fastener, if essential. The wear layer must be developed in exceptionally high quality; other than being impervious to traffic, it is in charge of giving water impermeability and framing rubbing. The folio layer is a layer made of bigger totals than the wear layer so as to give comfort and economy in packing the covering layer on the off chance that it is thick [10-12, 14, 15, 19-25].

The covering layer must have a uniform moving surface with adequate unpleasantness so as to pass the traffic securely and serenely. It is additionally important to have seepage offices to forestall water sprinkles and little lakes out and about surface [10, 11, 13, 15, 19-26].

The transmission of traffic loads through the base and sub-base layers to the base floor resembles the traditional burden circulation inside the floors. That is, the adaptable superstructure experiences disfigurements under traffic loads, and each layer transmits the charge on it by spreading it somewhat further down. In this manner, the heap achieving the last base floor is halfway spread over a substantial zone. As the stretch qualities framed in the adaptable superstructure tumble down from the top layer of the street, it is alluring that the execution attributes of the materials to be utilized are adequate to meet these stresses. Since the covering layer made of black-top cement is straightforwardly presented to traffic and natural impacts, it is alluring to have highlights, for example, high versatility module, slip obstruction, impermeability property. On the off chance that adaptable asphalts are not very much structured, one of the accompanying two causes can prompt devastation of the street: [10, 11, 14, 15, 19-26]

1. Stresses happening in the street framework or in one of the layers shaping the superstructure surpass the limit pressure estimation of the material and the inside equalization falls apart.
2. High pressure stresses on one of the floor or street superstructure layers, and the event of generally unique settlements under the adjustment in dampness substance of the layer.

Adaptable asphalts have two kinds of covering, including surface coatings and solid black-top coatings [10, 11, 15, 19-25].

Surface coatings

This sort of covering is the kind of development of the folio and total. Black-top is splashed as a slim film on the base layer where the street will be made first. The pulverized stone with a specific degree is poured onto this black-top and compacted by a roller. Sticking is normally given by traffic loads ignoring the street in our nation. Be that as it may, this sort of covering isn't prescribed, particularly in light of the fact that the air temperature is high and the saltiness in winter can't indicate great quality [10, 11, 14, 16, 19-26].

Concrete asphalt (asphalt concrete) coatings

Solid black-top asphalts are gotten by blending in all respects deliberately decided bituminous fasteners, totals and elephants in consistent blending plants under severe control in temperature, mugginess and blend. Bituminous hot blend can be considered as a framework comprising of three stages as total, bituminous fastener and hole.

The total having an enough material from each total size to the totals from the coarse total to the persistent total and the hot blend arranged is likewise called black-top cement. Black-top solid blends are the most progressive sort of covering, overwhelming traffic streets, motorways, air terminal runways are connected and costs are very high [23-26].

In a decent covering, the accompanying highlights are looked for; [25-27]

- High dependability and yield esteem,
- High slip obstruction,
- High sturdiness,
- Sufficient surface harshness,
- Impermeability, adaptability,
- workability,
- Economy.

4. Discussions

Solidness: It is the opposition of the bituminous covering to the ceaseless powerful loads brought about by the traffic loads, the long haul static loads and the pressure, draw and shear compel brought about by the wheel impacts amid increasing speed or deceleration. The impacts of bitumen and total on dependability are as vital as the piece of the blend. The hardness of the bitumen, at the end of the day, is another factor influencing the security of the blend. At the point when the bituminous folio with a lower infiltration is utilized, the steadiness of the covering can be viewed as higher. For the strength of the covering, the greatest temperature to be seen out and about must be considered. Thinking about the traffic, condition and ground conditions, the ideal steadiness can be accomplished by utilizing the most reasonable total and bitumen proportion [21-28].

The yield obstruction is characterized as the pressure an incentive at which the perpetual distortion begins, in spite of the fact that the power on the covering stays consistent. It is conceivable to have data about the material by taking a gander at the connections among solidness and yield esteems. In spite of the fact that a high strength esteem is wanted, it tends to be said that with high solidness and low yield esteem is fragile material.

Slip obstruction: The slip opposition alludes to the required grinding power between the haggle cladding with the goal that the vehicles can stand safely amid braking and don't float because of the radiating power in the spaces. Slip obstruction for the most part increments with low black-top substance, high scraped area opposition total, pounded and harsh surface total, open and coarse evaluated blend. So as to guarantee the harshness of the covering surface and the impact of cleaning, it is of prime significance to shape the slip opposition [20-29].

The cleaning of the totals is the nonattendance of harshness of the totals on the outside of the covering, and the unpleasantness is diminished or lost by rolling. As the surface smoothness of the covering expands, driving solace increments, yet the slip obstruction likewise diminishes essentially. Surface harshness or absolute shear opposition of black-top coatings relies upon full scale and miniaturized scale unpleasantness. Miniaturized scale unpleasantness is identified with surface structure of total while large scale harshness is identified with grain size of total utilized in black-top mixture [30].

Toughness: The solidness is the protection from the impacts of traffic, water, air and temperature changes. As it were, the strength is the obstruction of a covering to scraped area, swelling, stripping and oxidation. Black-top cement should be steady just as steady. It is conceivable to acquire high toughness by utilizing high strip quality total and high bitumen rate. Since totals with high water assimilation have higher protection from stripping, they take greater need as far as solidness [31].

Adaptability: It is the capacity of the street body to oppose from breaking (versatility) to the sitting and breakdown developments happening on the base floor. It is additionally attractive to have the covering layer as adaptable as the base layer. The absence of adaptability causes street surface breaking. The proportion of mineral elephants in the blend; the extent, consistency and affectability of the bitumen (development) influence the adaptability. In any case, the steadiness with high versatility might be low [32].

Machinability: It is characterized as the proportion of the straightforwardness amid blending laying-pressure. Machinability as a rule, [33]

- Maximum grain measure,
- Amount of coarse total,
- Viscosity of black-top,
- Aggregate surface unpleasantness and crack,
- Intermediate measured material amount
- Use of squashed total

There are a few challenges amid laying and particularly compacting of blends with low usefulness. Therefore, the steadiness of the blend is decreased on account of inadequate pressure. Blends with deficient machinability cause the coatings to have a non-homogenous structure. Likewise, blends with exceptionally high usefulness are by and large delivered with high-infiltration black-tops, which have low interior contact, and their solidness is low.

Impermeability: is dictated by the level of air hole. The interconnection of the holes in the blend and the association of the holes with the surface are the primary variables influencing the impermeability. The high level of void in the

blend configuration makes water and air go into the blend effectively and cause oxidation and accumulation of totals [34]. Recent research shows that this situation is still continuing in urban and forest roads [35-39].

5. Conclusions

Highway accept a basic employment in making travel less requesting and logically beneficial. This is an unfathomable help either for getting down to business or travel, similarly with respect to journeys including the carriage of stock. The expressway structure interfaces huge urban territories and rural systems all through the country. Has made the highway frameworks of extension conceivable, has given a helpful method to go for progressively worthwhile work openings, and enabled organizations to extend and develop all through the nation.

Highway gives the snappiest line from indicate A to B, suggesting that the people who must use this transport system ought to use the speediest and most direct course to pass by road. An average road system is fundamental for compelling improvement and headway in any country. At some point in the past emergency organizations were not open to the people who lived in remote zones in light of the way that there basically were not fitting ways. An extraordinary storm or a few slithers of snow may cost people living on soil boulevards in an emergency. By virtue of present day systems, there is no spot to accomplish today. Avenues accept a basic employment in the advancement and improvement of countries around the world.

6. References

[1] Shirley, C., & Winston, C. (2004). Firm inventory behavior and the returns from highway infrastructure investments. *Journal of Urban Economics*, *55*(2), 398-415.

[2] Bayraktar O.Y., Citoglu G.S, Caglar H., Caglar A., Arslan M., & Cetin M. (2018) The mechanical properties of the different cooling requirements of high-temperature applied plaster, Fresenius Environmental Bulletin 27(8): 5399-5409.

[3] Šelih, J., Kne, A., Srdić, A., & Žura, M. (2008). Multiple-criteria decision support system in highway infrastructure management. *Transport*, *23*(4), 299-305.

[4] Bayraktar O.Y., Citoglu G.S., & Abo Aisha A.E.S. (2019) The use of scrap tires in the construction sector, International Journal of Trend in Research and Development, Volume 6(1), 253-256. ISSN: 2394-9333, http://www.ijtrd.com/papers/IJTRD20299.pdf

[5] Chandra, A., & Thompson, E. (2000). Does public infrastructure affect economic activity?: Evidence from the rural interstate highway system. *Regional Science and Urban Economics*, *30*(4), 457-490.

[6] Bayraktar O.Y., Citoglu G.S., & Abo Aisha A.E.S. (2019) Performance research of lime based mortars, International Journal of Trend in Research and Development, Volume 6(1), 257-259. ISSN: 2394-9333, http://www.ijtrd.com/papers/IJTRD20300.pdf

[7] Bayraktar O.Y., Citoglu G.S., Belgin M.C., & Cetin M. (2019) Investigation of the mechanical properties of marble dust and silica fume substituted portland cement samples under high temperature effect, Fresenius Environmental Bulletin, 28(5):3865-3875.

[8] Noland, R. B., Graham, D. J., & Polak, J. W. (2009). Highway infrastructure investment and county employment growth: A dynamic panel regression analysis. *Journal of Regional Science*, *49*(2), 263-286.

[9] Brooks, R., & Cetin, M. (2012) Application of construction demolition waste for improving performance of subgrade and subbase layers, Int. J. Res. Rev. Appl. Sci 12 (3), 375-381

[10] Cetin, M. (2015). Chapter 55: Using Recycling Materials for Sustainable Landscape Planning. ST. Kliment Ohridski University Press, SOFIA. Book: Environment and Ecology at the Beginning of 21st Century. Eds: Recep Efe, Carmen Bizzarri, İsa Cürebal, Gulnara N. Nyusupova, ISBN:978-954-07-3999-1, pp.783-788.

[11] Cetin, M. (2015). Consideration of permeable pavement in landscape architecture, Journal of Environmental Protection and Ecology 16 (1), 385-392

[12] Swan, P. F., & Belzer, M. H. (2010). Empirical evidence of toll road traffic diversion and implications for highway infrastructure privatization. *Public Works Management & Policy*, *14*(4), 351-373.

[13] Houston, S. L., Houston, W. N., & Lawrence, C. A. (2002). Collapsible soil engineering in highway infrastructure development. *Journal of Transportation Engineering*, *128*(3), 295-300.

[14] Cetin, M. (2013). Chapter 27: Landscape Engineering, Protecting Soil, and Runoff Storm Water. InTech-Open Science-Open Minds. Book: Advances in Landscape Architecture-Environmental Sciences. Eds: Murat Ozyavuz, , ISBN 978-953-51-1167-2, pp.697-722.

[15] Cetin, M. (2013). Pavement design with porous asphalt, Temple University, Ph.D. Thesis, Philadelphia, USA.

[16] Maji, A., & Jha, M. (2007). Modeling highway infrastructure maintenance schedules with budget constraints. *Transportation Research Record: Journal of the Transportation Research Board*, (1991), 19-26.

[17] Cetin M. (2017). Change in Amount of Chlorophyll in Some Interior Ornamental Plants, Kastamonu University Journal of Engineering and Sciences 3(1):11-19, http://dergipark.gov.tr/download/issue-file/5600

[18] Çetin İ.Z., Cesur A., Keskin R., & Akarsu H. (2018) Bazı Peyzaj Bitkilerinde Klorofil Miktarının Değişimi: Samsun Örneği, Kastamonu University Journal of Engineering and Sciences 4(1):1-10, 2018, https://dergipark.org.tr/download/article-file/609695

[19] Mirzadeh, I., & Birgisson, B. (2015). Evaluation of highway projects under government support mechanisms based on an option-pricing framework. *Journal of construction engineering and management*, *142*(4), 04015094.

[20] Lakhmani, P., & Sikroria, R. (2012). Infrastructure Financing Instruments with a Special Emphasis on Highways and Roads. *International Journal of Management Research and Reviews*, *2*(9), 1668.

[21] Garza, J. M., Drew, D. R., & Chasey, A. D. (1998). Peer-reviewed paper Simulating Highway Infrastructure Management Policies. *Journal of Management in Engineering*, *14*(5), 64-72.

[22] Gharaibeh, N. G., Darter, M. I., & Uzarski, D. R. (1999). Development of prototype highway asset management system. *Journal of infrastructure systems*, *5*(2), 61-68.

[23] BSI (1990) British Standards Institution, Method for the determination of creep stiffness of bituminous aggregate mixtures subject to unconfined uniaxial loading, Draft for development DD-185, 1990.

[24] Button, J.W., Little, J.L., Kim, Y., & Ahmed, J., Mechanistic Evaluation of Selected Asphalt Additives, Proceedings of the Association of Asphalt Paving Technologists, 56, 1987.
[25] Rogue, R., Birgisson, B., Tia, M., Kim, B., & Cui, Z., Guidelines For Use of Modifiers in Superpave Mixtures: Evaluation of Ground-Tire-Rubber (GTR), Report 4910/4504/718/12, University of Florida, USA, 2004.
[26] Tunnicliff, D.G., A Review of Mineral Fillers. Proc. Association of asphalt paving technologists, 34, 214-236, 1962.
[27] Markow, M. J. (1995). Highway management systems: state of the art. *Journal of infrastructure systems*, *1*(3), 186-191.
[28] Kettinger, W. J. (1994). National infrastructure diffusion and the US information super highway. *Information & management*, *27*(6), 357-368.
[29] Kim, W. (1996). *A systems approach to transportation infrastructure management: development of a Highway Management System for the Virginia DOT* (Doctoral dissertation, Virginia Tech).
[30] Suhaibani, A., Mudaiheem, J., & Fozan, F., Effect of filler type and content on properties of asphalt concrete, effect of aggregates and mineral fillers on asphalt. 1991. Committee D-4 Symposium. San Diego.
[31] Mixture Performance, 1992. ASTM STP 1147, American society for testing and materials. Philadelphia.
[32] Hastak, M., & Baim, E. J. (2001). Risk factors affecting management and maintenance cost of urban infrastructure. *Journal of Infrastructure Systems*, *7*(2), 67-76.
[33] Goh, K. C., & Yang, J. (2013). Importance of sustainability-related cost components in highway infrastructure: perspective of stakeholders in Australia. *Journal of Infrastructure Systems*, *20*(1), 04013002.
[34] Woldesenbet, A., Jeong, H. D., & Park, H. (2015). Framework for integrating and assessing highway infrastructure data. *Journal of Management in Engineering*, *32*(1), 04015028.
[35] Sen, G., & Genc, A. (2018). Perceptions and expectations on forest management certification of foresters in state forest enterprises: a case study in Turkey. *Applied Ecology and Environmental Research*, 16(1), 867-891.
[36] Şen, G., Güngör, E., & Şevik, H. (2018). Defining the effects of urban expansion on land use/cover change: a case study in Kastamonu, Turkey. *Environmental Monitoring and Assessment*, 190(8), 454.
[37] Şen, G., & Genç, A. (2017). The definition of the problems in the forest management certification application process from forester's perspectives in Turkey. *Journal of Sustainable Forestry*, 36(4), 388-419.
[38] Şen, G., & Güngör, E. (2018). Analysis of land use/land cover changes following population movements and agricultural activities: a case study in northern Turkey. *Applied Ecology and Environmental Research*, 16(2), 2073-2088.
[39] Varol, T., Ertuğrul, M., Özel, H. B., Emir, T., & Çetin, M. (2018). The effects of rill erosion on unpaved forest road. *Applied Ecology and Environmental Research*, 17(1), 825-839.

Kastamonu University
Journal of Engineering and Sciences
e-ISSN 2667-8209
http://dergipark.gov.tr/kastamonujes

The Possibilities of Using Blue Spruce (*Picea pungens* Engelm) as a Biomonitor by Measuring the Recent Accumulation of *Mn* in Its Leaves

Mehmet Cetin *[, a], Oguzhan Cobanoglu [b]

[a] *Department of Landscape Architecture, Faculty of Engineering and Architecture, Kastamonu University Kastamonu, Turkey*
[b] *Department of Sustainable Agriculture and Natural Plant Resources, Institute of Science, Kastamonu University, Kastamonu, Turkey*

ARTICLE INFO

Received: May: 11.2019
Reviewed: May: 13. 2019
Accepted: May: 22. 2019

Keywords:
Manganese,
heavy metal,
biomonitor,
Picea pungens Engelm,
Leaves.

Corresponding Author:
E-mail: mcetin@kastamonu.edu.tr

ABSTRACT

Nowadays, air pollution has reached life-threatening levels in some cities, and worldwide, it has reached a level where millions of people lose their lives every year. Heavy metals (HMs), in particular, are among the significant components of air pollutants, as heavy metals are non-biodegradable and their concentration in the environment is constantly on the rise. They also tend to bio-accumulate. Therefore, identifying heavy metal concentrations in nature is of great importance in terms of identifying risky regions and risk levels. This study investigates the possibility of using the perennial Blue Spruce (*Picea pungens*) needles as a biomonitor and to measure the recent change in Mn concentrations in these organelles. As part of the study, the changes in the concentration of Mn levels according to the organelles ages and whether the sampled organelles were washed or unwashed were evaluated. The results of the study show that Mn concentration varies significantly depending on the organelle, its age, and whether its washed or unwashed.

Anahtar Kelimeler:
Mangan,
Ağır metal,
Biyomonitör,
Picea pungens Engelm,
Yapraklar.

ÖZ

Günümüzde hava kirliliği her yıl milyonlarca insanın sağlığını etkileyen en önemli çevre sorunlarından birisidir. Hava kirliliği etmenleri arasında ağır metaller biyobirikme eğiliminde olmaları, insan sağlığı açısından düşük konsantrasyonlarda bile toksik olmaları sebebiyle ayrı bir öneme sahiptir. Bundan dolayı ağır metallerin izlenmesi büyük önem taşımaktadır. Bu çalışmada da mavi ladin (*Picea pungens* Engelm) ibrelerinin yakın geçmişteki Mn konsantrasyonunun değişiminin izlenmesinde biyomonitor olarak kullanılabilme olanakları araştırılmıştır. Çalışma kapsamında Mn elementinin konsantrasyonunun, yıkanan ve yıkanmayan ibre, kabuk ve dal organlarında organ yaşına bağlı olarak değişimi değerlendirilmiştir. Çalışma sonuçları, Mn konsantrasyonunun organ, yıkanma ve organ yaşına bağlı olarak önemli ölçüde değiştiğini ortaya koymaktadır.

1. Introduction

Air pollution is one of the most important environmental problems in today's world. In addition to the continuous increase in the population across the globe, migration from rural to urban areas contributes heavily towards increasing pollution. Air pollution has become a problem that causes millions of people to die every year [1-18].

As mentioned previously, heavy metals play a dangerous part. While some heavy metals are beneficial to plants, (Fe, Cu, Zn, Mn, Mo) are essential for plant growth, (V, Co, Ni) stimulate plant growth), high concentrations of HMs have a toxic effect on both plants and other living things [19]. Therefore, monitoring HMs concentrations is extremely important.

When Mn, one of the most high-stress heavy metals, reaches people through the food chain, signs of toxicity are observed primarily in the respiratory system and in the brain. Symptoms of manganese intoxication include hallucinations, exhaustion, insomnia, weakness, amnesia, and nerve damage. Mn can also cause Parkinson's disease, lung embolism and bronchitis, while exposure to Mn toxicity in men may cause impotence [20].

Landscape plants that are most exposed to air pollution are the best indicator of this type of pollution. They show the progress of heavy metal concentration in the air by accumulating heavy metal pollution caused by fossil fuels especially in traffic intensive areas in their trunks, leaves and needles [8-12,14,16,21-22]. Therefore, instead of directly detecting heavy metal pollution, bioindicators or biomonitors are frequently used to measure pollution levels [16,22-34].

In this study, the possibility of using blue spruce (*Picea pungens* Engelm) needles as a biomonitor for monitoring the change of recent Mn concentration was investigated. Within the scope of the study, the change of the concentration of the Mn element in the wash and non-wash pointer, shell and branch organs depending on the age of the organ was evaluated.

2. Material and Method

The study was carried out on the side branches of a *Picea pungens* (Blue Spruce) tree from the city center of Ankara. The samples were taken by cutting the side branches of the Picea pungens tree, which is commonly used in landscaping, and brought to the laboratory. The branches were then cut and classified according to their age.

The classified samples were divided into two groups and washing was carried out in a group. In the washing process, the needle, shell and branches were first washed with plenty of water, then 1/3 of a large glass jar was filled with water and the pieces were thrown into the jar. The jar was rinsed with vigorous shaking for several minutes, and the process was repeated at least three times until the water was clear. After the water has started to maintain its clarity, this process was repeated three times with pure water to completely remove particulate matter adhering to the organs. Washed samples were spread on towel paper and lightly pressed again with the help of towel papers to remove excess water.

After washing a part of the organs, the needle, branch and shell parts were separated from each other. The shell samples were taken from the main part on the lateral branch and the branch samples from the lateral branches on the lateral branch. The bark samples were taken out of the branch by stripping and the branches were taken together with the more thin branches and the wood and the bark were not separated.

The samples were then left to dry for 15 days and were then dried in an oven at 45°C for one week. The dried samples were ground into powder and weighed 0.5 g and were placed in tubes designed for a microwave. 10 ml of 65% HNO3 was added to the samples. The prepared samples were then burned at 280 PSI in the microwave device and 20 minutes at 180 ºC. The tubes were removed from the microwave after the processes were completed and were allowed to cool. Cooled samples were added to 50 ml by adding deionized water. The prepared samples were read on the ICP-OES device at appropriate wavelengths after filtering through the filter paper. The data obtained were analyzed by using SPSS package program and variance analysis was applied to the data. The values were statistically analyzed by using Duncan test. The obtained data were simplified and interpreted.

3. Result and Discussion

The change in organ based on organ age was determined and the mean values on organ basis and F value obtained as a result of variance analysis, error rate and the groupings formed as a result of Duncan test are given in Table 1.

Table 1. Changes in Mn (ppm)

Age	Organ						F values	Error
	Needle		Bark		Branch			
	+	-	+	-	+	-		
1	43,46 c	34,28 a	40,89 b	83,35 f	54,01 e	50,70 d	16469,8	,000
2	40,26 b	88,80 f	23,71 a	58,92 e	41,67 c	49,51 d	35872,0	,000
3	39,01 a	50,19 c	52,10 d	63,90 e	47,50 b	66,93 f	4550,8	,000
4	74,93 e	168,8 f	21,72 a	39,96 b	57,77 d	46,76 c	333947,3	,000
5	50,40 c	80,46 e	18,61 a	59,87 d	50,58 c	48,51 b	41436,3	,000
6	54,65 c	97,01 e	35,78 a	80,20 d	50,30 b	54,75 c	20638,4	,000
7	88,14 d	117,2 e	73,71 b	77,61 c	128,05 f	46,86 a	14907,5	,000

When the values of the table are examined, it is seen that the change in Mn concentration of organ in all ages is statistically significant at 99.9% confidence level. When the mean values and the groupings formed as a result of the Duncan test are examined, the difference between the washed and unwashed samples is noteworthy. The values obtained in the samples washed in the shell are lower than the values obtained in the unwashed samples. In addition, when compared to the branch and shell samples, the values obtained are generally higher in the washed samples and the values obtained in the shell in the unwashed samples.

The change in the concentration of Mn according to organ was determined according to the age of the organ and the mean values on the basis of the organ and the F value obtained as a result of the analysis of variance, the error rate and the groupings formed as a result of Duncan test are given in Table 2.

Table 2. Change of Mn (ppm) Element by Year

Age	Organ					
	Needle		Bark		Branch	
	+	-	+	-	+	-
1	43,46 c	34,28 a	40,89 e	83,35g	54,01 d	50,70 d
2	40,26 b	88,80 d	23,71 c	58,92 b	41,67 a	49,51 c
3	39,01 a	50,19 b	52,10 f	63,90 d	47,50 b	66,93 f
4	74,93 f	168,84 g	21,72 b	39,96 a	57,77 e	46,76 a
5	50,40 d	80,46 c	18,61 a	59,87 c	50,58 c	48,51 b
6	54,65 e	97,01 e	35,78 d	80,20 f	50,30 c	54,75 e
7	88,14 g	117,24 f	73,71 g	77,61 e	128,05 f	46,86 a
F Values	14089,13	54421,35	52024,3	10057,90	24263,7	7765,5
Error	,000	,000	,000	,000	,000	,000

When the values of the table are analyzed, it is observable that the change of Mn concentration in all organs due to organ age is statistically significant at 99.9% confidence level. When the changes in the age of the organ are examined, it can be said that there is a general shot depending on the age. The change in bark and wood can be described as irregular. It is observed that the change in the Mn concentration on a year-on-year basis is generally horizontal, especially when there is no significant change in the branches. The Mn concentration in the unwashed branches ranged from 47.76 ppm to 66.93 ppm, while the Mn concentration in the washed branches ranged from 41.67 ppm to 54.01 ppm, except for the seven-year-old hands. However, the change in the hands is sometimes more than five times. The change of Mn concentration in terms of organ and organ age is given graphically (Figure 1).

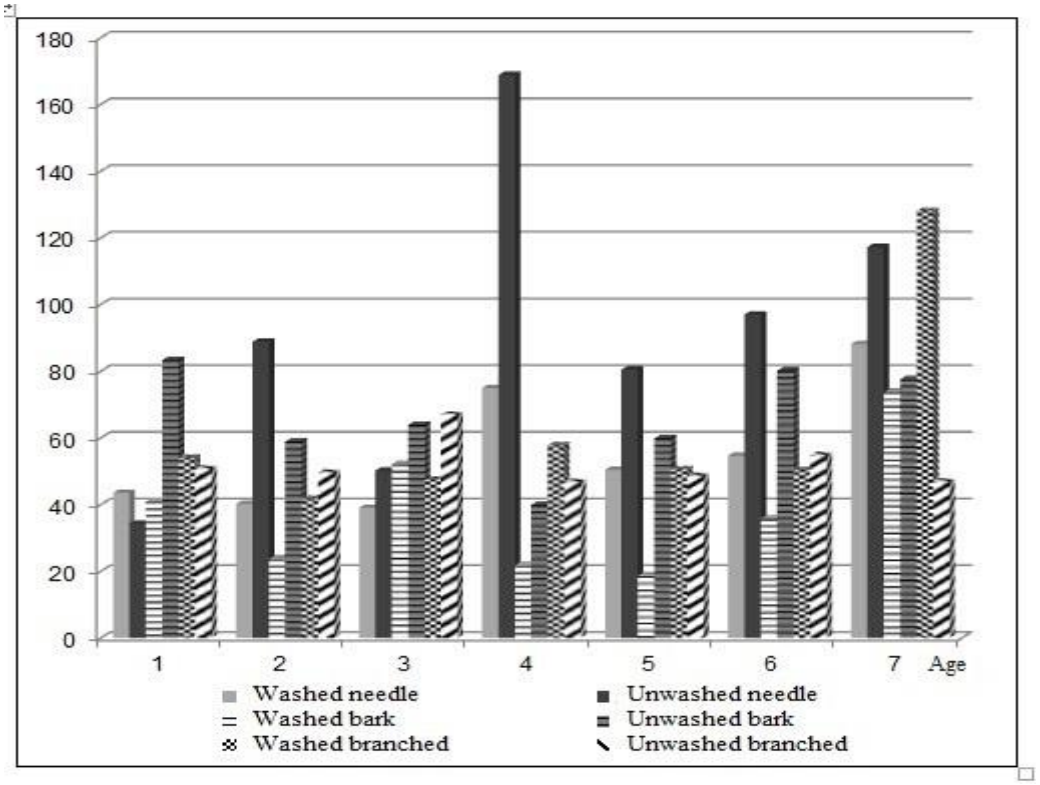

Figure 1. Graphic. Change of Mn concentration on organ and year basis

4. Conclusions

In the study, it was determined that the change of Mn concentration in all ages on organ basis was statistically significant at least at 95% confidence level. Variations in the element concentrations were evaluated according to the organ. In Mossi's study [35] , it was determined that the changes in the amount of elements in seven different types of leaves and branches, and that Cu, Ni, Pb, Cd and Ca concentrations were higher in the branches than in the leaves and Mn concentration was higher in the leaves than in the branches. Pınar [36] found that the difference between organs was 4.3 times in Cu, compared to leaf, seed and branch samples.

In heavy metal studies, the change of heavy metal concentrations depending on the organ is often the subject of studies. Mossi [35] leaf and branch, Turkyilmaz et al., [8-12] bark and wood, Erdem [37] and Sevik et al., [38] leaves, seeds and branches, Elfantazi et al. [39,40] Leaf and branch, Ozel [41] leaves, branches and fruits, Pınar [36] leaves, branches and seeds, Akarsu [42] have determined the differences between the inner shell, outer shell and the organs in the wood. There is not much work on leaf or needle age in studies to determine the heavy metal concentration up to now. In a study conducted on this subject Turkyilmaz et al., [8-12] *Pinus nigra*, *Pinus sylvestris*, *Abies bornmuelleriana* and *Picea pungens* species in one, two and three-year-old hands in the evaluation of changes in the concentration of some HMs in almost all values in relation to age, showed increased the amount of HMs. Similar results were obtained by Çobanoğlu [43] in his study on *Picea pungens*.

The change of HMs depending on the organ, the structure of the plant and organ as well as the structure of the HM, environmental conditions and all the interaction between them is a complex and yet not fully solved mechanism, and the information on this subject is limited [1-3, 13,14-18, 26, 31-33, 42, 44,45].

Zn, Mn, Cu and Mo are pivotal for the growth of the plants from the heavy metals reaching the plant root area, Co and Ni are required in some conditions. Al, V, As, Hg, Pb, Cd and Se are generally toxic [20]. Manganese toxicity in plants varies according to plant species. Manganese toxicity appears as brown spots on mature leaves in most plants. The areas where stains occur are fungus over time. It causes deformations of young leaves in plants such as beans and

cotton. Changes in Mn concentration in different plant species have been investigated. Celik et al., [46] *Robinia pseudoacacia*, Cesur [47] in *Cupressus arizonica*, Turkyilmaz et al., [8-12] *Tilia tomentosa*, *Eleagnus angustifolia*, *Prunus cerasifera* and *Ailanthus altissima*, Çobanoğlu [43] determined the change of Mn concentration in *Picea pungens*. Mn has also been studied in other studies related to heavy metal [48-51]. Recent studies with Ozel et al., worked Oak in Krikkale, Uludag Fir, and oriental plane found some resuls of it [52-58].

4. References

[1] Yucedag, C., Kaya, L.G. (2016). Hava Kirleticilerin Bitkilere Etkileri. Mehmet Akif Ersoy Üniversitesi Fen Bilimleri Enstitüsü Dergisi 7(1): 67-74.

[2] Yucedag, C., Kaya, L.G. (2017). Chapter 104. Recreational trend and demands of people in Isparta-Turkey, Book: Researches on Science and Art in 21 st Century Turkey. Eds: Hasan Arapgirlioglu, Atilla Atik, Robert L. Elliott, Edward Turgeon, Gece Publishing, ISBN: 978-605-180-771-3

[3] Yucedag, C., Kaya, L.G., Cetin, M. (2018). Identifying and assessing environmental awareness of hotel and restaurant employees' attitudes in the Amasra District of Bartin. Environmental Monitoring and Assessment 190(2): 60. DOI: https://doi.org/10.1007/s10661-017-6456-7

[4] Yucedag, C., Ozel, H.B., Cetin, M., Sevik, H., (2019). Variability in morphological traits of seedlings from five Euonymus japonicus cultivars. Environmental Monitoring and Assessment. 191 (5), 285. DOI: 10.1007/s10661-019-7464-6, https://link.springer.com/content/pdf/10.1007%2Fs10661-019-7464-6.pdf

[5] Varol T., Gormus S., Cengiz S., Ozel HB., Cetin M (2019). Determining Potential Planting Areas in Urban Regions. Environmental Monitoring and Assessment 191 (3), 157. DOI: 10.1007/s10661-019-7299-1, https://link.springer.com/content/pdf/10.1007%2Fs10661-019-7464-6.pdf

[6] Varol, T., Ertuğrul, M., Özel, H. B., Emir, T., Çetin, M. (2019). The effects of rill erosion on unpaved forest road. Applied Ecology and Environmental Research 17(1):825-839, http://www.aloki.hu/indvol17_1.htm

[7] Zeren, I., Cantürk, U. and Yaşar. M. O. (2017). Change of chlorophyll quantity in some landscaping plants. Journal of Bartin Faculty of Forestry, 19 (2): 174-182.

[8] Turkyilmaz, A, Sevik, H, Cetin, M. (2018). The use of perennial needles as biomonitors for recently accumulated heavy metals. Landsc Ecol Eng 14(1):115–120. https://doi.org/10.1007/s11355-017-0335-9

[9] Turkyilmaz, A., Sevik, H., Cetin, M., Ahmaida Saleh E.A. (2018). Changes in heavy metal accumulation depending on traffic density in some landscape plants. Pol J Environ Stud 27(5):2277-2284. https://doi. org/10.15244/pjoes/78620

[10] Turkyilmaz, A., Sevik, H., Isinkaralar, K., Cetin, M. (2018). Using Acer platanoides annual rings to monitor the amount of heavy metals accumulated in air. Environ Monit Assess 190:578. https://doi.org/ 10.1007/s10661-018-6956-0

[11] Turkyilmaz, A., Sevik, H., Isinkaralar, K, Cetin, M. (2018). Use of tree rings as a bioindicator to observe atmospheric heavy metal deposition, Environmental Science and Pollution Research, DOI: 10.1007/s11356-018-3962-2, https://doi.org/10.1007/s11356-018-3962-2

[12] Turkyilmaz, A., Cetin, M., Sevik, H., Isinkaralar, K., Ahmaida Saleh E.A. (2018). Variation of heavy metal accumulation in certain landscaping plants due to traffic density. Environment, Development and Sustainability. 1-14. DOI: https://doi.org/10.1007/s10668-018-0296-7, https://link.springer.com/article/10.1007%2Fs10668-018-0296-7

[13] Akarsu, H., Zeren Çetin, İ., Jawed, A.A., Abo Aisha A.E.S., Cesur A., and Keskin R (2019). Changes of Some Heavy Metal Concentrations Based on Organic and Traffic Density in Fraxinus excelsior L., International Journal of Engineering, Design and Technology 1(1): 24-30

[14] Aricak, B., Cetin, M., Erdem, R., Sevik, H., Cometen, H. (2019). The change of some heavy metal concentrations in Scotch pine (Pinus sylvestris) depending on traffic density, organelle and washing. Applied Ecology and Environmental Research 17(3): 6723-6734.

[15] Cetin M, Sevik H, Isinkaralar K. (2017). Changes in the Particulate Matter and CO_2 Concentrations Based on the Time and Weather Conditions: The Case of Kastamonu. Oxidation Communications, 40 (1-II), 477-485.

[16] Cetin, M., Kalayci Onac, A., Sevik, H., Sen, B. (2019). Temporal and regional change of some air pollution parameters in Bursa Air Quality, Atmosphere & Health (Air Qual Atmos Health) 12(3): 311-316. https://doi.org/10.1007/s11869-018-00657-6

[17] Cetin, M., Onac, A.K., Sevik, H., Canturk, U., Akpinar, H. (2018). Chronicles and geoheritage of the ancient Roman city of Pompeiopolis: a landscape plan. Arabian Journal of Geosciences. 11:798. DOI: 10.1007/s12517-018-4170-6. https://link.springer.com/article/10.1007/s12517-018-4170-6

[18] Cetin, M., Sevik, H., Yigit, N. (2018). Climate type-related changes in the leaf micromorphological characters of certain landscape plants. Environmental Monitoring and Asessmenet. 190: 404. https://doi.org/10.1007/s10661-018-6783-3

[19] Daghan, H., Uygur, V., Koleli, N., Arslan, M., & Eren, A. (2013). Effect of heavy metal applications on nitrogen, phosphorus and potassium intake in transgenic and non-transgenic tobacco plants. Journal of Agricultural Sciences, 19, 129-139.

[20] Sari, T. (2009). Investigation of some heavy metal pollution in the soil in Edirne and the surrounding areas of the highway (Master's thesis, Namik Kemal University). 53 page.

[21] Sevik, H., Cetin, M., Ozturk, A., Yigit, N., Karakus, O. (2019). Changes in micromorphological characters of Platanus orientalis L. leaves in Turkey. Applied Ecology and Environmental Research 17(3):5909-5921. DOI: http://dx.doi.org/10.15666/aeer/1703_59095921

[22] Cetin, M., Sevik, H., Yigit, N., Ozel H.B., Aricak, B., Varol, T. (2018) The variable of leaf micromorphogical characters on grown in distinct climate conditions in some landscape plants. Fresenius Environmental Bulletin, 27(5): 3206-3211.

[23]Cetin, M., Zeren, I., Sevik, H., Cakir, C., Akpinar, H. (2018). A study on the determination of the natural park's sustainable tourism potential. Environmental Monitoring and Assessment. 190(3): 167.https://doi.org/10.1007/s10661-018-6534-5

[24] Cetin, M., Sevik, H., Canturk, U., Cakir, C. (2018). Evaluation of the recreational potential of Kutahya Urban Forest. Fresenius Environmental Bulletin, 27(5):2629-2634.

[25] Cetin, M., Sevik, H., Saat, A. (2017). Indoor Air Quality: the Samples of Safranbolu Bulak Mencilis Cave. Fresenius Environmental Bulletin. 26(10): 5965-5970. http://www.prt-parlar.de/download_feb_2017/

[26] Jawed, A.A., Abo Aisha A.E.S. (2019). Usability of Horse Chestnut (Aesculus hippocastanum L.) as Biomonitor for Monitoring Some Heavy Metal Concentrations Caused by Traffic, International Journal of Engineering, Design and Technology 1(1): 16-23

[27] Kaya, L.G., Kaynakci-Elinc, Z., Yucedag, C., Cetin, M. (2018). Environmental outdoor plant preferences: a practical approach for choosing outdoor plants in urban or suburban residential areas in Antalya, Turkey. Fresenius Environmental Bulletin. 27(12):7945-7952.

[28] Cetin, M. (2015). Determining the bioclimatic comfort in Kastamonu City. Environmental Monitoring and Assessment, 187(10), 640, http://link.springer.com/article/10.1007%2Fs10661-015-4861-3

[29] Cetin, M. (2015) Evaluation of the sustainable tourism potential of a protected area for landscape planning: a case study of the ancient city of Pompeipolis in Kastamonu. International Journal of Sustainable Development & World Ecology, 22(6), 490-495, http://www.tandfonline.com/doi/abs/10.1080/13504509.2015.1081651?src=recsys&journalCode=tsdw20

[30] Cetin, M. (2015). Using GIS analysis to assess urban green space in terms of accessibility: case study in Kutahya. International Journal of Sustainable Development & World Ecology, 22(5), 420-424, http://www.tandfonline.com/doi/abs/10.1080/13504509.2015.1061066?journalCode=tsdw20

[31] Kaya, L.G., Cetin, M., Doygun, H. (2009). A holistic approach in analyzing the landscape potential: Porsuk Dam Lake and its environs, Turkey. Fresenius Environmental Bulletin 18(8): 1525-153.

[32] Kaya, L.G. (2009). Assessing forests and lands with carbon storage and sequestration amount by trees in the State of Delaware, USA. Scientific Research and Essays 4(10): 1100-1108.

[33] Cetin, M. (2017). Change in Amount of Chlorophyll in Some Interior Ornamental Plants, Kastamonu University Journal of Engineering and Sciences 3(1):11-19, http://dergipark.gov.tr/download/issue-file/5600

[34] Çetin İ.Z., Cesur A., Keskin R., Akarsu H. (2018). Bazı Peyzaj Bitkilerinde Klorofil Miktarının Değişimi: Samsun Örneği, Kastamonu University Journal of Engineering and Sciences 4(1):1-10, 2018, https://dergipark.org.tr/download/article-file/609695

[35] Mossi, M.M.M. (2018). Determination Of Heavy Metal Accumulation In Some Shrub Formed Landscape Plants, Kastamonu University, Institute of Science Department of Forest Engineering, PhD Thesis, Kastamonu, Turkey

[36] Pinar, P. (2019). The variation of heavy metal accumulation in some landscape plants due to traffic density. Kastamonu University Institute of Science, Master Thesis, Kastamonu, Turkey

[37] Erdem, T. (2018): The Change of Heavy Metal Concentrations in Some Plants due to Species, Organelles and Traffic Densities, Kastamonu University Institute of Science Department of Forest Engineering, Master Thesis, Kastamonu, Turkey

[38] Sevik, H., Ozel, H. B., Cetin, M., Özel, H. U., & Erdem, T. (2019). Determination of changes in heavy metal accumulation depending on plant species, plant organism, and traffic density in some landscape plants. Air Quality, Atmosphere & Health, 12(2):189-195. https://doi.org/10.1007/s11869-018-0641-x

[39] Elfantazi, M.F.M., Aricak, B. & Baba, F.A.M. (2018). Changes in Concentration of Some Heavy Metals in Leaves and Branches of Acer Pseudoplatanus Due to Traffic Density. International Journal of Trend in Research and Development, 5(2): 704-707.

[40] Elfantazi, M.F.M., Aricak, B., Ozer Genc, C. (2018). Concentrations in Morus Alba L. Leaves and Branches Due To Traffic Density. International Journal of Current Research. 10(05): 68904-68907.

[41] Ozel, S. (2019). The variation of heavy metal accumulation in some fruit tree organelles due to traffic density. Kastamonu University Institute of Science, Master Thesis, Kastamonu, Turkey

[42] Akarsu, H. (2019). Determination of heavy metal accumulation in atmosphere by being aid of annual rings. Kastamonu University Institute of Science, Master Thesis, Kastamonu, Turkey

[43] Çobanoğlu O. (2019). The possibilities of using blue spruce (picea pungens engelm) as a bio-monitor by measuring the recent accumulation of heavy metals in its leaves Kastamonu University Institute of Science, Master Thesis, Kastamonu, Turkey

[44]Uzu, G., Sobanska, S., Aliouane, Y., Pradere, P., & Dumat, C. (2009). Study of lead phytoavailability for atmospheric industrial micronic and sub-micronic particles in relation with lead speciation. Environmental Pollution, 157(4), 1178-1185.

[45] Shahid, M., Dumat, C., Khalida, S., Schreck, E., Xiong, T. & Nabeel N. K. (2017). Foliar heavy metal uptake, toxicity and detoxification in plants: A comparison of foliar and root metal uptake. Journal of Hazardous Materials, 325, 36-58.

[46] Celik, A., Kartal, A. A., Akdoğan, A., & Kaska, Y. (2005). Determining the heavy metal pollution in Denizli (Turkey) by using Robinio pseudoacacia L. Environment international, 31(1), 105-112.

[47] Cesur, A. (2019). Determination Of Heavy Metal Accumulation In Air Through Annual Rings: The Case of Cupressus arizonica Species, Kastamonu University Graduate School of Natural and Applied Sciences Department of Sustainable Agriculture and Natural Plant Resources. MSc. Thesis. 63 pages

[48] Alyemeni, M. N., & Almohisen, I. A. (2014). Traffic and industrial activities around Riyadh cause the accumulation of heavy metals in legumes: a case study. Saudi journal of biological sciences, 21(2), 167-172.

[49] Gunawardena, J., Ziyath, A. M., Egodawatta, P., Ayoko, G. A., & Goonetilleke, A. (2015). Sources and transport pathways of common heavy metals to urban road surfaces. Ecological Engineering, 77, 98-102.

[50] Sungur, A., Soylak, M., Yilmaz, E., Yilmaz, S., & Ozcan, H. (2015). Characterization of heavy metal fractions in agricultural soils by sequential extraction procedure: the relationship between soil properties and heavy metal fractions. Soil and Sediment Contamination: An International Journal, 24(1), 1-15.

[51] Yıldırım, G., & Tokalıoğlu, Ş. (2016). Heavy metal speciation in various grain sizes of industrially contaminated street dust using multivariate statistical analysis. Ecotoxicology and environmental safety, 124, 369-376.

[52] Yücedağ, C., & Özel, H. B. (2017). Variability of Leaf Characteristics in Seedlings of Pubescent Oak of Kırıkkale, Turkey. International Journal of Plant Soil Science, 17(5):1-7.

[53] Barış Özel, H., Ucun Özel, H., & Varol, T. (2015). Using Leaves of Oriental Plane (Platanus orientalis L.) to Determine the Effects of Heavy Metal Pollution Caused by Vehicles. Polish Journal of Environmental Studies, 24(6): 2569-2575.

[54] Yucedag, C., Ozel, H.B., Cetin, M., Sevik, H., (2019). Variability in morphological traits of seedlings from five Euonymus japonicus cultivars. Environmental Monitoring and Assessment. 191:285. DOI: 10.1007/s10661-019-7464-6, https://link.springer.com/content/pdf/10.1007%2Fs10661-019-7464-6.pdf

[55] Ucun Özel, H., & Özel, H. B. (2012). Investigation on Heavy Metal Pollution ın Uludag Fir Forests (Abies nordmanniana subsp. bornmülleriana MATTF) in the Bartın Region. Journal of Forestry Faculty of Kastamonu University, 12(31).

[56] Ertuğrul, M., Varol, T., & Özel, H. B. (2014). Climate changes in prospect for the West Black Sea Forests. Journal of Bartin Faculty of Forestry, 16(23), 35-43.

[57] Özel, H. B., & Ertekin, M. (2010). Investigation of Relationship between some climate factors and height increment in Black Pine (Pinus nigra Arnold. ssp. pallasiana (Lamb.) Holmboe) and Scotch Pine (Pinus sylvestris L.) afforestations in the Devrek-Akçasu District. Ecological Life Sciences, 5(4), 376-389.

[58] Ozel, H. B., & Ertekin, M. U. R. A. T. (2011). Growth models in investigating oriental beech (Fagus orientalis Lipsky.) juvenilities growth performance in the Western Black Sea in Turkey (Devrek-Akçasu Case Study). Romanian Biotechnological Letters, 16(1), 5850-5857.

.

Kastamonu University
Journal of Engineering and Sciences
e-ISSN 2667-8209
http://dergipark.gov.tr/kastamonujes

QTL Analysis Methods

Özge Şahin*, [a], Orhan Kavuncu[b]

[a] *Faculty of Biology, Institute of Evolution and Biodiversity, Münster University, Muenster, Germany*
[b] *Department of Genetics and Bioengineering, Faculty of Engineering and Architecture, Kastamonu University, Kastamonu*

ARTICLE INFO

Received: May:13.2019
Reviewed: May:14.2019
Accepted: May:22.2019

Keywords:
Quantitative trait loci (QTL),
QTL mapping,
QTL detecting,
Marker loci,
Linkage.

Corresponding Author:
*E-mail: sahinoz@ankara.edu.tr

ABSTRACT

In recent years, quantitative characters have settled to a quite important place among genetic studies. The inheritance of these traits is usually achieved by multiple gene expression and by the additive and interactive effects of these genes. Therefore, the analysis methods used to understand the genetic basis of quantitative traits may be more complex than those of qualitative traits. The loci on the chromosome at which the genes controlling the genetic architecture of the quantitative traits are located are called the quantitative trait loci (QTL). There are different methods for detecting and analyzing the presence of these loci. In addition, it is possible to map the QTLs with the help of the molecular markers as a developing method thanks to today's technology. In this review, the methods of diagnosing QTL and mapping studies were analyzed.

Anahtar Kelimeler:
Kantitatif özellik lokusları (QTL),
QTL haritalama,
QTL belirleme,
Belirteç lokus,
Bağlantı.

ÖZ

Son yıllarda kantitatif özellikler genetik çalışmalar içinde oldukça önemli bir yer teşkil etmeye başlamıştır. Bu özelliklerin kalıtımı genellikle birden fazla gen açılımı ve bu genlerin eklemeli ve interaktif etkisi ile gerçekleşmektedir. Bu sebeple de kantitatif özelliklerin genetik temelini anlamada kullanılan analiz yöntemleri, kalitatif özelliklerinkinden daha karmaşık olabilmektedir. Kantitatif özelliklerin genetik mimarisini kontrol eden genlerin kromozom üzerinde bulunduğu lokuslar kantitatif özellik lokusları (QTL) olarak isimlendirilmektedir. Bu lokusların varlığını tespit etmek ve analiz etmek için farklı yöntemler mevcuttur. Ayrıca günümüz teknolojisi sayesinde gelişen bir yöntem olarak moleküler belirteçler yardımıyla QTL haritalamak mümkündür. Bu derlemede, QTL varlığını teşhis etmeye ve haritalama çalışmalarına yönelik analiz yöntemleri incelenmiştir.

1. Quantitative Traits and QTL

Quantitative traits have long been involved in genetic studies as a major field. The most striking part of the variation observed between populations or populations in both experimental studies and field research is the part resulting from quantitative characters. A quantitative trait is defined as traits that vary in quantitative terms and that are constantly phenotypically distributed by definition. These traits are usually controlled by multiple genes. Some of these genes have a large effect, some of which have a small effect. In addition, these traits are under the influence of environmental factors as well as genetic factors.

Genes that control the genetic change of quantitative traits are called quantitative trait loci (QTL) [20]. QTL may consist of small effective genes, large effective genes, or both. Variations in these traits are generally controlled by segregating of many loci. Therefore, quantitative traits are sometimes defined as polygenic traits. However, inheritance of these traits cannot be studied by methods developed to study the inheritance of traits controlled by only a few genes. Genes that are effective on quantitative traits are also inherited according to Mendel's rules. In terms of those which have a major effect on them, segregation can be studied methods based on Mendel's rules. However, polygenic

inheritance cannot be studied by methods based on classical Mendelian rules because of many genes having small effects, plus environment that alter their effects; hence it is not possible to detect the phenotypic segregation rates according to the genotypes [12]. Therefore, if there are large effective genes, determining their location on the genome will provide significant benefits in terms of applying breeding methods such as indirect selection. Thus, the idea that these large effective genes and/or small effective gene blocks, which may be linearly aligned on the genome, can be determined by their linkage to specific marker loci, led to the use of QTL definition from the 1990s [20], unlike the poligen definition. QTL is also referred to as large-effect gene sequences which are investigated to be related to one or more marker loci with small-effect genes.

When examining quantitative traits, it should be known that environmental differences play a significant role in the phenotypic variation of these traits. Most quantitative traits are controlled by multiple genes and environmental factors as mentioned above. Therefore, the change in the polygenic structure and the environment makes the studies on quantitative traits more difficult than studies on monogenic traits. These traits are genetically complex, although they are easy to measure as phenotypes and therefore the expression of complex traits are used by some researchers [11]. Because of its polygenicity and its sensitivity to environmental changes, it is necessary to use statistical tools to examine the genetic architecture of these traits in large populations.

In parallel with the developments in the field of molecular biology and biotechnology, analysis methods for QTL have been developed since the 1990s. Thanks to these developments and studies at the molecular level, the possibility of utilizing DNA sequences called genetic markers has emerged in determining the effect of QTLs and their settlements. The respective positions of the markers in the marker maps can be determined by the recombination events observed throughout the genome. The segregating marker samples may provide information on quantitative traits such as the number of linked QTLs and chromosomal locations and the effectivity of each QTL by virtue of phenotype and pedigree information. A description containing all QTL information is also referred to as the genetic structure of the quantitative trait of interest. The study about the genetic structures of quantitative traits using molecular markers means that QTL mapping is actually used by the relationship between marker loci and quantitative traits [24]. Therefore, using the possible relationship between the molecular markers and the quantitative trait interested, QTL is called QTL mapping to predict their position in the genome and predict QTL effects [20].

Identifying each gene separately and knowing the presence of QTL will enable many useful applications to be implemented. First, this may improve the effect of selective breeding for low-remodeling (ie, more affected by environmental differences) and for traits that can only be observed in single sex. Another important aspect is that transgenic technology can be applied to quantitative traits in the future. In addition, the identification of alleles that cause susceptibility to common multifactorial diseases such as heart disease or diabetes in the medical field can help in the development of some methods for prevention [2]. Considering the benefits that can be achieved through studies on the inheritance of quantitative traits, it can be said that in the future genetic researches on QTL will increase. For this reason, in this paper, methods for determining the presence and location of QTLs were reviewed.

2. QTL Mapping Methods

The experimental set-ups designed to predict the effect of QTL and its location on the genetic maps are based on two fairly recent mapping studies for single genes and methods of estimating the linkage disequilibrium between marker locus alleles and QTL alleles.

Required thing for QTL mapping is the variation in the quantitative traits of the linkage map of the polymorphic marker loci that covers the entire genome sufficiently or within the allel groups of marker alleles.

2.1 Marker loci

In recent years, the development of DNA marker technologies has contributed to the investigation of the genetic structures of living things and to the mapping of agriculturally important genes, including QTLs. In addition, markers serve as an important and powerful tool in the scientific world in many aspects such as analysis of evolutionary relations. Molecular markers may be genes on the DNA, or any genetic coding function, ie, DNA sequences that have no function or function as phenotypes.

An ideal marker should have some features. The first of these is the high level of polymorphicity. Accordingly, individuals or populations should have different alleles in marker loci. Another desirable feature is that the marker is abundant to cover the entire genome. It should also be neutral in relation to the quantitative trait of interest and

associated with the breeding success of the species. Finally, a marker should be codominant to help distinguish all possible genotypes in the locus. However, this last item does not always have to be fulfilled, because dominant or recessive markers can also be used successfully in the experimental desings.

The analyzes that can be carried out with molecular markers are listed as follows [5]: Selection by means of marker (Marker Assisted Selection, MAS), QTL analyzes, genetic mapping, gene isolation strategies, characterization of gene sources, phylogenetic analysis, identification of culture types and determination of genetic kinship, determination of parents. For example, the identification of subgroups of living species, such as mutant species, has been studied extensively with some techniques such as RFLP (Restriction Fragment Length Polymorphism), RAPD (Random Amplified Polymorphic DNA), SSR (Simple Sequence Repeat Polymorphism). In addition, in recent years, DNA Microarray technology with thousands of genes at the same time to learn the relationship with each other in the field of many areas of molecular biology and genetic research is being done extensively [25].

The identification of the mutation that affects the quantitative traits of interest is quite difficult, as there may be a large number of genes and many potential variants within each gene. Therefore, the first step here is to determine the locations of genes of interest through genome mapping [9]. Genetic markers have an important role in genome mapping. These markers are mapped by the help of their linkage analysis.

The presence of molecular markers and the chromosome maps made with their help enable the identification of elements such as large effective genes and small effective gene levels of the genetic structure that control quantitative traits. Due to the quantitative properties are affected by a large number of genes, it should be known where these genes are in the genome. By applying the method known as QTL analysis in a suitable population, the location of the relevant genes in the specific chromosomal region can be determined. In addition to this, the magnitude of the effects can be predicted and whether the gene effect is additive or dominant can be detected [5].

2.2 QTL mapping

It is possible to detect QTLs position and identify them by analyzing the expression of marker genes and the phenotypic value of interest in the population. QTL mapping is the analysis of the offspring by the selection and crossing of parents of different phenotypes in terms of one or more quantitative traits, and the detection of a possible linkage between known marker loci and QTL.

The term QTL was first proposed by Geldermann [3]. QTL detection was developed approximately 90 years ago after Sax's work [18]. The study of Sax on the relationship between seed size differences in seed bean (*Phaseolus vulgaris*) and the seed coating model and pigmentation has been one of the initial studies of the linkage between QTL and genes that affect a quantitative trait. Then Sax's experiments were repeated on *Drosophila melanogaster* by Mather [15]. Thoday [21] proposed the idea of using single locus markers to identify and map genetic regions that control variation in quantitative traits.

QTL mapping has quite simple principle. What is required is just two lines having different phenotypes of the quantitative traits studied and a linkage map for some polimorphic marker loci. The lines are crossed to get the F_1 offsipring and then it has to get the backcrossed and/or F_2 offspring. The data is then classified according to a marker locus (or some marker loci) and compared statistically if they are different means fort the quantitative trait. If there is a significant difference it is decided that the QTL and marker loci are linked [16, 17].

2.2.1 Single marker mapping

This method independently searches each of the markers without taking into account their position and sequence. Haley and Knott [4] and Martinez and Curnow [14], independently of each other, introduced the regression method analysis with the help of information on neighboring markers. Weller [22] and Weller *et al.* [23] developed mixed model analysis to find QTL by using single marker information in hybridization between inbreeding and outbreeding populations. A mixed model approach for QTL mapping in unrelated populations is also reported by Jansen *et al.* [7].

The single marker mapping shows which marker has a linkage with the quantitative trait of interest and thus indicates the presence of possible QTL. The H_0 hypothesis (control hypothesis) is that the mean value of the property of interest is independent of the marker. If the test statistic is greater than the significant value, this indicates that the QTL is linked to the marker. Hypothesis controls using t-test, ANOVA and simple linear regression approaches for

differences in phenotypic averages may be misleading in predicting the frequency of recombination between QTL or marker and QTL, which are predicted to be close to each other, although they are all similar.

QTL discovery with a single marker approach is a simple protocol in which statistical analysis software packages can be implemented and has the potential to identify many important markers. When considering these statistical results, you need to think carefully about two important issues. The first of these is the sample size. The higher the number of individuals studied, the more reliable the phenotypic mean and variance is estimated. Large sample sizes allow for the possibility to observe recombination events and more accurate estimation of parameters. Thus, the possibility of detecting QTL increases. The second important issue is the problems in multiple tests. They occur during the investigation of multiple markers by independent statistical tests. This may increase the level of statistical significance as determined by the investigator, which may lead to false-positive QTL.

2.2.2 Interval mapping

Interval mapping is an approach developed to determine which of the QTLs in the map can be in a previously prepared map of the marker locus. The most commonly used statistical method in this approach is the maximum likelihood method. Maximum likelihood (ML) methods are widely used in QTL mapping. Linear models use only marker averages, and use many information about the co-distribution of ML, marker and quantitative trait. Therefore, ML requires the use of statistical models with more intensive probability calculations. One approach can be seen in the interval mapping indicated by Eric Lander and David Botstein [10]. In this mapping, a predicted genetic map is used to find the location of QTL. Intervals defined for sequential markers are investigated and the probability of QTL being located in the interval investigated is tested using statistical methods. In the interval mapping defined by Lander and Botstein, single QTLs against each sequential marker in the genome are tested statistically. Test results are expressed as LOD (Logarithms of odd) scores. As the statistical values calculated from the samples taken from the default population with control hypotheses are generally very large, the logarithm of these values is taken to compare them easily [8]. This logarithm is called LOD scores.

Interval mapping investigates a systematic, linear model where sequential genetic markers are tested for the same H_0 hypothesis and the same probability form is used for each increment. In addition, the combined LOD scores represent a LOD profile versus the genetic map. The placement of the maximum LOD profile has the potential to display multiple or fictitious QTLs when using a single QTL model. Deciding the peaks indicating single QTLs is related to the determination of statistical significance results. Because this probability is often a function of the mixture of normal distributions when it is maximized under both control and alternative hypothesis, test statistics may be insufficient in observing standard statistical distributions. It is therefore difficult to specify a QTL in this case. Instead, the composite interval mapping method discussed below is proposed.

2.2.3 Composite interval mapping

Composite interval mapping method is defined by Zhao-Bang Zeng in 1993 [26]. In the same year Ritsert Jansen identified multiple QTL mapping and achieved the same result in reducing the number of models considered [6]. Both methods have the same idea that interval mapping includes additional markers as cofactors to aim at reducing variation of other QTLs in the genome. Both approaches have limitations. These can be studied in one-dimensional studies in comparison to genetic maps, and the research is difficult in cases where epistatic QTL effects are high. In addition, there is a risk of taking a large number of markers in the model as cofactors, and care should be taken to protect the information that is appropriate for the correct prediction of the QTL effect.

2.2.4 Multiple QTL mapping

The concept of planning for the placement of multiple QTLs is more powerful than single QTL, because these approaches have the potential to distinguish between QTLs that are connected and/or interacting. The effect of two or more QTL alleles is difficult to be predicted when the interaction occurs. It is not possible to see this effect in single QTL analysis. The goal is to investigate whether the effect of a new potential QTL with another QTL is in interaction and the new QTL segregates from the other independently. One of the many interesting situations may be the loss of the expression of the trait with a special combination of the multiple QTL's alleles. Another problem in the study for multiple QTL mapping is to think about each position in the genome at the same time. Therefore, the position of a QTL that behaves independently, QTL connected to another QTL or QTL that interacts with other QTL can be detected.

QTLs which are in the interaction are a field of special interest, because they can show specific regions in the genome. Otherwise, they may be related to quantitative traits using one-dimensional research.

QTLs in the interaction are open despite their multiple positions. However, it is difficult to consider that there are many potential QTLs and their interaction with numerous statistical models and difficult calculations. On the other hand, an approach can be presented as follows: First of all, all QTLs must be placed. Then a statistical model should be created for these QTLs and their interactions. Then, the model should be continued by removing the others from the model and remaining important interactions. Due to the computational density of a multidimensional research, it is impossible to investigate simultaneously and it is called semi-simultaneous research. Such approaches have the potential to work in many cases. However, it is limited to the QTL pool that passes the first QTL analysis, and it is unlikely that QTL epistatic effects are not properly established. Research through all potential models is a problem known as model selection and remains an active field of study in the field of theoretical statistics.

The importance of models developed for multiple QTLs is well understood for the linked QTL and plays an important role in the prediction and location of epistatic QTL. In the successful use of multiple QTLs, the limiting feature is not to write equations for the model, but not to define the best of many model subsets. Counting all possible QTL models that are considered suitable for the genetic structure such as linkage, epistasis in the experiment is a very difficult task. Accurate and fast simultaneous multidimensional researchs and their comparisons across most of the possible models allow decision on the most appropriate model for future research. One of the approaches to investigate the optimal multiple QTL genotype is to use genetic algorithms. Application of genetic algorithms to multiple QTL problems is one of many useful approaches. Because this application allows the sampling of QTL models corresponding to unequal QTL numbers and can be used in multidimensional investigation of a genome in conjunction with the QTL mapping methodology. In addition to this, distinguishing between the covariance caused by the linkage disequilibrium between QTLs and the variance from the epistatic (interactive) effect is waiting as an important problem.

Sen and Churchill proposed an approach for covariants, non-normal distribution traits, epistatic QTL and multiple simultaneous investigations in addition to the above mentioned challenges [19]. This approach divided the QTL problem into two different parts: the relationship between QTLs and the relationship between the quantitative trait and QTL. Separation of these two independent relationships intensely predicts unknown QTL genotypes. It then allowed different models to be searched and compared with the information obtained from QTL genotypes. The approach of dividing the problem into two parts is not new. In 1993, Jansen dealt with this issue. After estimating QTL genotypes, Sen and Churchill [19] described all possible QTL models using an approach that allows different models of various QTL numbers. The QTL genotypes calculated independently from QTL effects and locations reduced the epistasis and related QTL cases, because the state of the QTL genotype and the number of QTL are known before their effects and interactions are estimated.

3. Result and Discussion

There are two approaches to identifying a gene to be accepted as QTL in a specific genomic region. These are changings of positional cloning and QTL which is in the same region with the candidate locus.

Positional cloning requires the map position of the locus of interest at 0.3 cM. The reason of taking 0.3 cM is the average length that a vector research can carry [2]. This requires screening for high stability meiotic mapping in experimental organisms as well as polymorphic markers in random mating populations in the region where there is a strong linkage disequilibrium between the quantitative trait phenotype and QTL. Although everything seems clear in this respect, it is difficult to define the gene of interest and decide whether the polymorphisms are related to alleles or other effects. This method is suitable for loci identified by the broad effects of mutant alleles and is used to identify single loci that affect human diseases. From a medical point of view, the importance of loci with smaller effects will increase in the future. Therefore, it is important to develop this application in order to analyze QTLs at the single locus level.

The most common strategy used to go from the mapped region to the gene is the candidate gene approach. With this approach, many loci with known genetic function are identified and cloned from the unknown locus regions on the map. Therefore, the linkage between the molecular polymorphism and phenotype in each candidate locus in the region is investigated.

Exploring QTL in previous years was aimed at many scientific researches and was a targeted goal. Today, QTLs which determine many traits and the location of QTLs in multiple interactions are aimed to be found with the help of advanced statistical analysis. In addition to many statistical methods Bayesian approaches may alternatively be used in the estimation of some parameters involved in genome analyses [13]. More research is carried out by developing technologies and these researches bring together more information. Therefore, this information allows us to better understand central dogma, which includes replication, transcription and translation stages. Quantitative variation can be observed in each stage of central dogma [1]. When this variation information is combined with appropriate statistical significance, it can be seen how a genome works in a unique way. When one considers the ideas about emerging technologies and methodologies, it is accepted that a single technological progress or statistical method cannot be a solution to genomic problems. Instead, a combination of many techniques and analyzes will contribute to the solution.

4. References

[1] W. R. Doerge, "Mapping and analysis of quantitative trait loci in experimental populations," Nature, vol. 3, pp. 43-52, Jan. 2002. DOI: 10.1038/nrg703

[2] D. S. M. Falconer and T. F. C. Mackay, "Quantitative trait loci" in Introduction To Quantitative Genetics, 4th ed., Essex, England, 1996, pp. 356-377.

[3] H. Geldermann, "Investigations on inheritance of quantitative characters in animals by gene markers I. methods," Theoretical and Applied Genetics, vol. 46, no. 7, pp. 319-330, 1975.

[4] C.S. Haley and S.A. Knott, "A simple regression method for mapping quantitative trait loci in line crosses using flanking markers," Heredity, vol. 69, pp. 315-324**,** 1992.

[5] B. İşçi, "Asmada QTL (kantitatif karakter lokus) analizi," Anadolu (Journal of Aegean Agricultural Research Institute), vol. 18, no. 2, pp. 11-37, 2008.

[6] R. C. Jansen, "Interval mapping of multiple quantitative trait loci," Genetics, vol. 135, pp. 205-211, Sep. 1993.

[7] R. C. Jansen, D. L. Johnson and J. A. M. Van Arendonk, "A mixture model approach to the mapping of quantitative trait loci in complex populations with an application to multiple cattle families," Genetics, vol. 148, pp. 391-399, Jan. 1998.

[8] O. Kavuncu, "İstatistik Teorisi ve Teorik Dağılımlar", Ankara, Turkey, 1995.

[9] H. Kozanoğlu and İ. Oğuz, "Importance of DNA markers in animal breeding and genetics," in II. International Symposium on Molecular Diagnosis and Applications, İzmir, Turkey, May 10-14, 2004, pp. 75-80.

[10] E. S. Lander and D. Botstein, **"**Mapping Mendelian factors underlying quantitative traits using RFLP linkage maps," Genetics, vol. 121, pp. 185-199, Jan. 1989.

[11] E. S. Lander and N. J. Schork, "Genetic dissection of complex traits," Focus, vol. 4, no. 3, pp. 442–458, 2006.

[12] M. Lynch and B. Walsh, "Quantitative trait loci" in Genetics and Analysis of Quantitative Traits. Sunderland, USA, 1998, pp. 319-532.

[13] A.O. Maraghi, "A Bayesian generalized linear model approach to quantitative trait loci (QTL) detection of litter size in mice," Ph.D. dissertation, Dept. Animal Sci., Ankara Univ., Ankara, Turkey, 2011.

[14] O. Martinez and R. N. Curnow, "Estimating the locations and the sizes of the effects of quantitative trait loci using flanking markers," Theoretical and Applied Genetics, vol. 85, pp. 480-488**,** 1992.

[15] K. Mather, "Variation and selection of polygenic characters," Journal of Genetics, vol. 41, pp. 159-193, 1941.

[16] J. A. M. Arendonk and H. Bovenhuis, "Designs and Methods to Detect QTL for Production Traits Based on Mapped Genetic Markers," Poultry Genetics, Breeding and Biotechnology, W. M. Muir and S. E. Aggrey, Ed., Cambridge, USA, 2003, pp. 439-465.

[17] N. Yi and S. Xu, "Designs and Methods to Detect QTL for Production Traits Based on Random Genetic Models," Poultry Genetics, Breeding and Biotechnology, W. M. Muir and S. E. Aggrey, Ed., Cambridge, USA, 2003, pp. 465-497.

[18] K. Sax, "The association of size differences with seed co at pattern and pigmentation in *Phaseolus vulgaris*," Genetics, vol. 8, pp. 552-560, 1923.

[19] S. Sen and G. A. Churchill, "A statistical framework for quantitative trait mapping," Genetics, vol. 159, pp. 371-387, Sep. 2001.

[20] S. D. Tanksley, "Mapping polygenes," Annual Review of Genetics, vol. 27, pp. 205-233, 1993.

[21] J. M. Thoday, "Location of polygenes," Nature, vol. 191, pp. 368-370, Jul. 1961.

[22] J. I. Weller, "Maximum likelihood techniques for the mapping and analysis of quantitative trait loci with the aid of genetic markers," Biometrics, vol. 42, no. 3, pp. 627-640, Sep. 1986.

[23] J. I. Weller, Y. Kashi and M. Soller, "Power of daughter and granddaughter designs for determining linkage between marker loci and quantitative trait loci in dairy cattle," Journal of Dairy Science, vol. 73, pp. 2525–2537, 1990.

[24] S. Xu, "QTL analysis in plants," Methods in Molecular Biology: Quantitative Trait Loci: Methods and Protocols, vol. 195, pp. 283-310, 2002.

[25] H. E. Yurter, "Gen ekspresyon analizinde microarray teknolojisinin kullanımı," DEU Tıp Fakültesi Dergisi Özel Sayısı, pp. 41-48, 2001.

[26] Z. B. Zeng, "Theoretical basis for separation of multiple linked gene effects in mapping quantitative trait loci," Genetics, vol. 90, pp. 10972-10976, Dec. 1993.

Kastamonu University
Journal of Engineering and Sciences
e-ISSN 2667-8209
http://dergipark.gov.tr/kastamonujes

Synthesis of New Thiacalix[4]arene Based Azo Dyes and Analysis of Absorption Spectrums

İzzet Şener[*,a], Güngör Canbulat[b], Nesrin Şener[c], Mahmut Gür[d]

[a] *Food Engineering Department, Faculty of Engineering and Architecture, Kastamonu University, Kastamonu, Turkey*
[b] *Science Institute, Pamukkale University, Denizli, Turkey*
[c] *Department of Chemistry, Faculty of Art and Science, Kastamonu University, Kastamonu, Turkey*
[d] *Department of Forest Industrial Engineering, Faculty of Forestry, Kastamonu University, Kastamonu, Turkey*

ARTICLE INFO

Received: May:17.2019
Reviewed: May:17.2019
Accepted: June:13.2019

Keywords:
Azo Dyes,
Azo Thiacalixarene.

Corresponding Author:
[*]*E-mail: isener@kastamonu.edu.tr*

ABSTRACT

In this study, firstly a novel thiacalix[4]arene functionalized from the phenolic oxygen side was synthesized. Then, a series of dyes were synthesized by linking the heterocyclic groups to the novel thiacalix[4]aren through a diazotization reaction. The azo dyes were characterized by UV-Vis, FT-IR and ^{1}H-NMR spectroscopic techniques. Furthermore, effect of solvent and acid-base upon the absorption spectra of the azo dyes were investigated.

Anahtar Kelimeler:
Azo Boyaları,
Azo Tiyakaliksaren

ÖZ

Bu çalışmada ilk olarak fenolik oksijen tarafından işlevselleştirilmiş yeni bir tiakaliks [4] aren sentezlendi. Daha sonra, heterosiklik grupların, tiyakaliks[4]arene diazolama reaksiyonu yoluyla bağlanarak, bir seri boya sentezlendi. Azo boyaları UV-Vis, FT-IR ve 1H-NMR spektroskopik teknikleri ile karakterize edildi. Ayrıca, azo boyaların absorpsiyon spektrumları üzerine çözücü ve asit baz etkisi araştırıldı.

1. Introduction

Being half of the dyes used in textiles, Azo dyes have been known for many years. In recent years, it has been reported that dyes obtained by the use of heterocyclic compounds exhibit very good light, washing, and bleaching fastness related to yellow-orange color range. There are many examples related with the synthesis of heteroaryl azo dyes and their usage as a dyestuff for synthetic fabrics [1-5].

Within the macrocyclic compounds family, calixarene derivatives have also been synthesized in the field of heterocyclic dyes because of that azo groups make a significant chromogenic contribution to calixarenes [6-7]. The modification of the calix skeleton involve rearrangement through the methylene bridges among the phenol units by heteroatoms such as nitrogen, oxygen, sulfur [8]. Sone et al. synthesized p-*tert*-butylthiacalix[4]arene for the first time, in which sulfur are replaced to CH_2 groups of p-*tert*-butylcalix[4]arene [9-10]. It was reported that oxidation of bridging sulfur afforded sulfinyl- and sulfonylcalix arenes, which showed intrinsic metal ion selectivity determined by the hardness and softness of the ion [11]. Furthermore, thiacalixarenes are applied to many fields such as molecule/ion Carrier [12], catalyzer [13], electrode [14], liquid membrane [15], sensor [16]. Morever, the dyes derived from thiacalixarene are also available for other purposes in the literature. For example; thiacalixarene diazonium salts were converted to *p*-azo-thiacalixarene derivatives at room temperature with high yield. At the same time, the study claimed that tetra-amine-derived thiacalixarene can be obtained through reduction at the *p*-position [17]. In another

comprehensive study, the acyloin and heteroaryl azo derivatives of the thiacalix[4]arene were synthesized and the properties of the cations were examined [18].

Studies to date show that future studies will be based on the functioning of the azothiacalix[4]arene, which is a subclass of calix[n]arenes. In particular, host-guest interaction with metal ions will facilitate the use of these compounds as sensors and electrodes. For all these reasons, in this study, a novel thiacalix[4]aren functionalized from the phenolic oxygen side was synthesized at the first stage. Then, a series of dyes were synthesized by linking the heterocyclic groups to the novel thiacalix[4]aren through a diazo reaction. The azo dyes were characterized by UV-vis, FT-IR and ^{1}H-NMR spectroscopic techniques.

2. Material and Methods

The used devices are as follows: Evaporator (Heidolph 4000 Efficient), melting point device (Stuart SMP-30), oven (NFe FN-120), balance (Radwag AS-220), mantle heater (Thermo Scientific), magnetic stirrer (VELP Scientifica). UV-vis measurements and FT-IR analyzes of the synthesized compounds were performed using Shimadzu UV-1601 UV-visible and Perkin Elmer FT-IR spectrophotometers. ^{1}H-NMR spectra were taken with Bruker Ultra Shield Plus 400 MHz. The chemicals were obtained from high purity Merck, and Sigma-Aldrich brands.

In this study, *p*-tert-butylthiacalix[4]arene (1) was synthesized in accordance with the literature [19]. Thiacalix[4]arene (2) was obtained by eliminating the tertiary butyl groups of this compound [12]. The compound was then reacted with *p*-nitrobenzylbromide to obtain 25,27-bis-(4-nitrobenzyloxy)-26,28- thiacalix[4]arene (3). The nitro groups on this compound were reduced and 25,27-bis-(4-aminobenzyloxy)-26,28- dithiacalix[4]arene (4) was producted. This compound was reacted with a series of coupling compounds to obtain the new azothiacalix[4]arene derivatives **(Scheme 1)**.

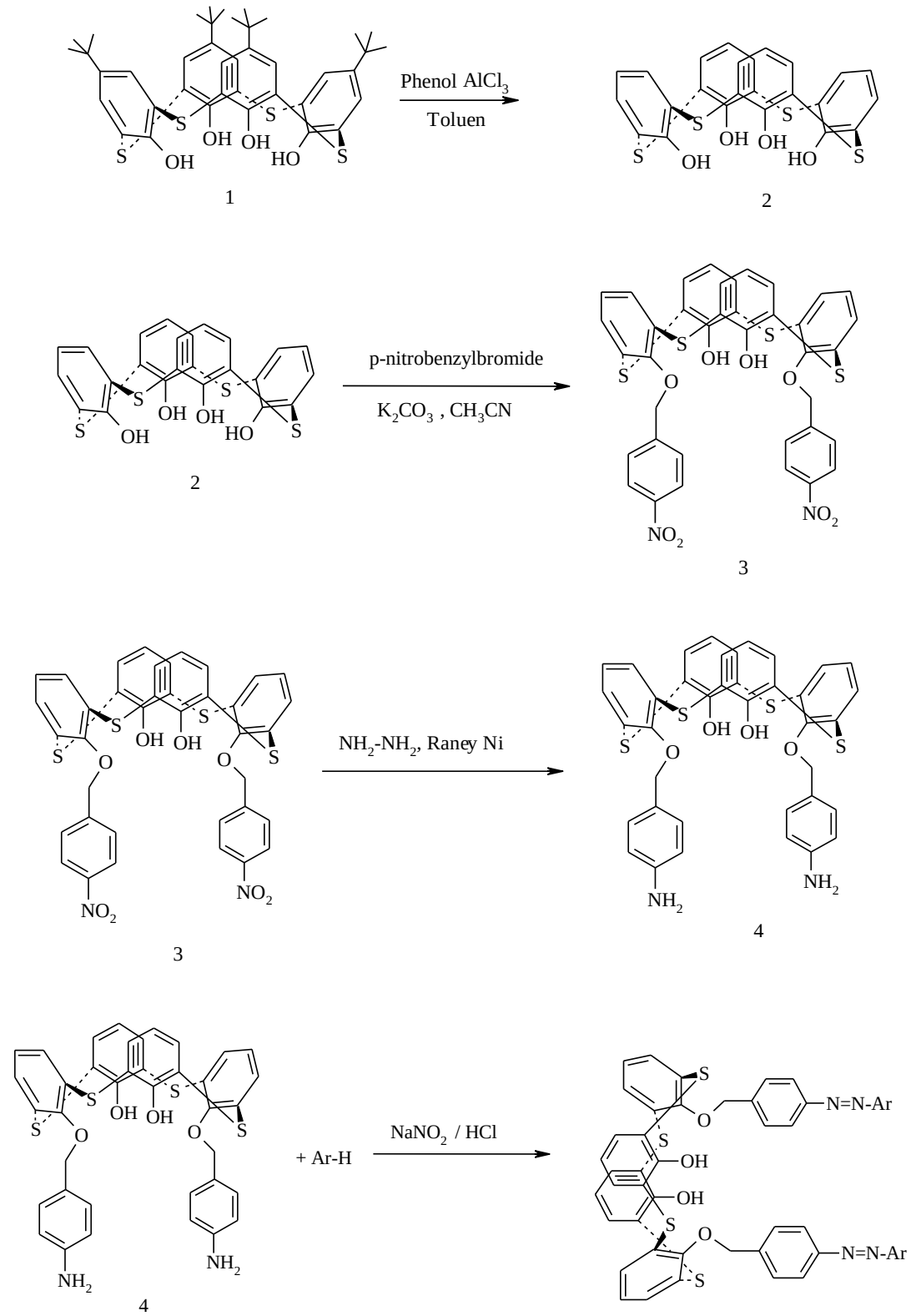

Scheme 1. General Synthesis Route.

Synthesis of 25,27-bis-(4-nitrobenzyloxy)-26,28 dihydroxythiacycline [4]arene (3)

A 500 mL two necked flask was charged with a reaction mixture of 2.756 g (5.55 mmol) of thiacalix [4] arene, 0.767 g (5.55 mmol) of K_2CO_3 and 300 mL of acetonitrile and heated for 30 minutes. 2,398 g (11,1 mmol) of *p*-nitrobenzylbromide was added to the reaction mixture and boiled for 24 hours. The white reaction mixture is taken up in the evaporator and the solvent is evaporated. 1 N 100 mL HCl is added and a suspension is obtained. The insoluble material was removed by filtration and washed sequentially with methanol and distilled water. The dried material is crystallized from chloroform **(Scheme 2).**

Yield: 2,05 g, 48%; **mp:** 225 ºC **FT-IR,** ν_{max} (cm^{-1}): 3385(-OH); 3060 (Arom.C-H); 2950 (Aliphatic C-H); 1512,1346 (-NO_2); 1001 (C-O) ^{1}H-NMR (DMSO-d_6), δ(ppm): 5,51 (s, 4H, -CH_2); 6,81, 7,09, 7,79 (m, 12H, calix aromatic C-H); 7,61, 8,21 (d, 8H, Arom.C-H); 7,88 (s, 2H, -OH).

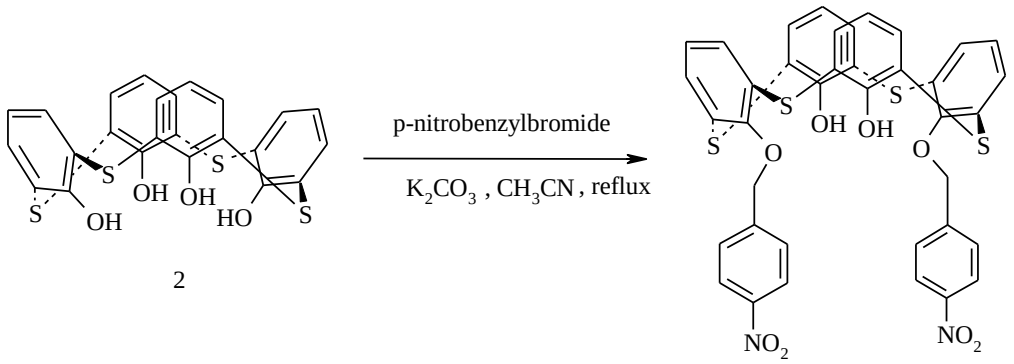

2 3

Scheme 2. Synthesis of *25,27-bis*-(4-nitrobenzyloxy)-26,28-dihydroxythiacalix[4]arene

Synthesis of 25,27-bis-(4-aminobenzyloxy)-26,28-dihydroxythiacalix[4]arene (4)

2.02 g (2.64 mmol) of 25,27-bis-(4-nitrobenzyloxy)-26,28-dihydroxythiacalix[4]arene, 2.87 g of Raney Nickel, 130 mL of ethanol and 260 mL of THF were added to a 500 mL flask, 5,33 mL of $N_2H_4.H_2O$ was added slowly to the stirred flask at room temperature. After boiling for 12 hours, 2.66 mL of $N_2H_4.H_2O$ was slowly added dropwise to the green mixture and the color turned blue. After further boiling for 24 hours, the green reaction mixture is cooled and filtered through bilayer filter paper. The green material is crystallized from chloroform **(Scheme 3)**.

Yield: 1.242 g, 67%; **mp:** 330 ºC (decomp.) **FT-IR,** ν_{max} (cm^{-1}): 3423 (-OH); 3325 (-NH_2); 3007 (Arom. C-H); 2919 (Aliphatic C-H); 1066 (C-O) ^{1}H-NMR (DMSO-d_6), δ(ppm): 3,82, 5,26 (s, 4H, -CH_2); 6,20, 8,75 (m, 20 H, Arom.C-H); 11,25 (s, 2H, -OH); 13,01, 15,05 (s, 4H, -NH_2).

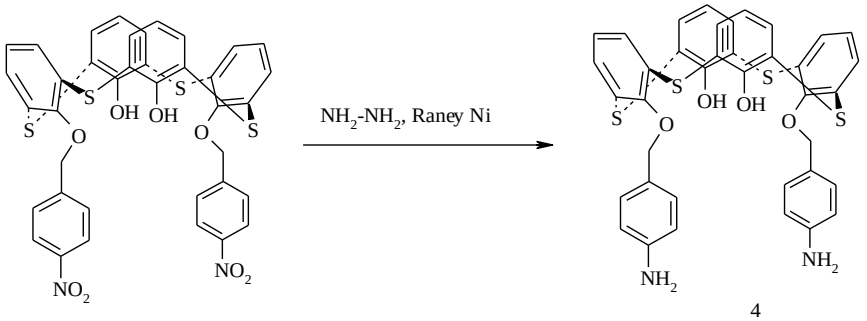

3 4

Scheme 3. Synthesis of 25,27-bis- (4-aminobenzyloxy) -26,28-dihydroxy-thiacalix[4]arene compound.

Synthesis of 25,27-bis-[4- (2'-hydroxynaphthol-1-yl-azo) benzyloxy]-26,28-dihydroxy thiacalix[4]arene (4a)

0,1 g (0.14 mmol) of 25,27-bis- (4-aminobenzyloxy)-26,28 dihydroxythiacalix[4]arene dissolved in DMF and 0.2 mL of HCl were added in an ice-water bath. In another beaker, a solution of 0.022g (0.35mmol) $NaNO_2$ with the lowest possible water was added dropwise to the reaction mixture in an ice water bath and stirred for 2 hours. On the other hand, a basic solution of 0.40 g (0.28 mmol) of 2-naphthol, for using as a coupling component, with NaOH, was prepared and added dropwise to the beaker from which the diazonium salt was prepared. Stir in ice-water bath for 2 hours. After this time, saturated sodium acetate solution was added to add the mixture to pH = 7 and pure water was added. The precipitate formed was filtered and dried. The red material was crystallized from DMSO **(Scheme 4).**

Yield: 0,102 g, 70,9%; **mp:** 230-240 ºC **FT-IR,** ν_{max} (cm^{-1}): 3266 (-OH); 3060 (Arom.C-H); 2923 (Aliphatic C-H); 1678, 1596 (N=N); 1090 (C-O). ^{1}H-NMR (DMSO-d_6), δ(ppm): 4.76-4.80 (s, 4H, -CH_2); 6.61-8.81 (m, 32H, Arom.C-H); 11.20, (s, 2H, -OH); 9.80 (s, 2H, -OH).

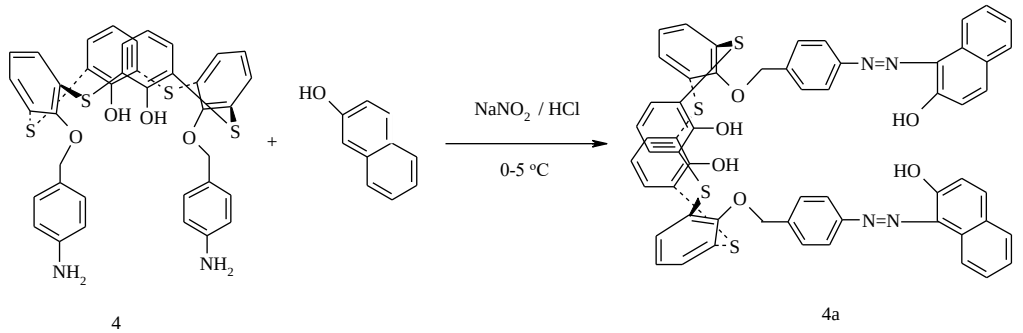

4 4a

Scheme 4. Synthesis of 25,27-bis-[4-(2-hydroxy-butanol-1-yl-azo) benzyloxy]-26,28-dihydroxy thiacalix[4]arene **(4a).**

Other compounds **(4b-4h**) in the study were also synthesized according to this procedure (**Scheme 5)**.

Synthesis of 25,27-bis-[4-(2 ', 4'-dihydroxyquinolin-3'-yl-azo) benzyloxy]-2,28-dihydroxy thiacalix[4]arene (4b)

Yield: 0,076 g, **51,1%; mp:** 280-290 ºC **FT-IR,** ν_{max} (cm^{-1}): 3264 (-OH); 3059 (Arom.C-H); 2926 (Aliphatic C-H); 1678, 1596 (N=N); 1090 (C-O). ^{1}H-NMR (DMSO-d_6), δ(ppm): 4.91 (s, 4H, -CH_2); 7.05-8.94 (m, 28H, Arom.C-H); 11.65 (s, 2H, -OH) , 9.90(s, 2H, -OH).

Synthesis of 25,27-bis-[4- (8'-hydroxyquinolin-7'-yl-azo) benzyloxy]-26,28-dihydroxy thiacalix[4]arene (4c)

Yield: 0,087 g, **60,3%; mp:** 280-288 ºC **FT-IR,** ν_{max} (cm^{-1}): 3268 (-OH); 3064 (Arom.C-H); 2926 (Aliphatic C-H); 1678, 1607 (N=N); 1090 (C-O). ^{1}H-NMR (DMSO-d_6), δ(ppm): 4.90 (s, 4H, -CH_2); 7.14-8.84 (m, 30H, Arom.C-H); 11.05 (s, 2H, -OH), 9.80(s, 2H, -OH).

Synthesis of 25,27-bis-[4-(4'-hydroxy-coumarin-3-yl-azo) benzyloxy]-26,28-dihydroxy thiacalix[4]arene (4d)

Yield: 0,065 g, **43,6%; mp:** 275-285 ºC **FT-IR,** ν_{max} (cm^{-1}): 3267 (-OH); 3059 (Arom.C-H); 2926 (Aliphatik C-H); 1678, 1607 (N=N); 1090 (C-O). ^{1}H-NMR (DMSO-d_6), δ(ppm): 4.88 (s, 4H, -CH_2); 7.12-8.89 (m, 28H, Arom.C-H); 12.85 (s, 2H, -OH), 11.10 (s, 2H, -OH).

Synthesis of 25,27-bis-[4-(7'-hydroxy-4'-methylcoumarin-8'-yl-azo)benzyloxy]-26,28- dihyroxythiacalix[4] arene (4e)

Yield: 0,050 g, **32,7%; mp:** 295-300 ºC **FT-IR,** ν_{max} (cm^{-1}): 3266 (-OH); 3059 (Arom.C-H); 2926 (Aliphatic C-H); 1678, 1597 (N=N); 1090 (C-O). ^{1}H-NMR (DMSO-d_6), δ(ppm): 6.18 (s, 2H, -CH); 4.91 (s, 4H, -CH_2); 7.05-9.06 (m, 24H, Arom.C-H); 11.10 (s, 2H, -OH) , 10.05 (s, 2H, -OH).

Synthesis of 25,27-bis- [4-(3-methyl-5'-pyrazolon-4-yl-azo) benzyloxy]-26,28-dihyroxythiacalix[4]arene (4f)

Yield: 0,052 g, **39,7%; mp:** 285-295 ºC, **FT-IR,** ν_{max} (cm^{-1}): 3265 (-OH); 3059 (Arom.C-H); 2922 (Aliphatic C-H); 1677(N=N); 1090 (C-O). ^{1}H-NMR (DMSO-d_6), δ(ppm): 4.79 (s, 4H, -CH_2); 2.25 (s, 6H, -CH_3); 6.50-8.15 (m, 20H, Arom.C-H); 8.15 (s, 2H, -OH); 9.57 (s, 1H, -NH).

Synthesis of 25,27-bis-[4-(4'-hydroxy-6'-methyl-2-pyrid-3-yl-azo)benzyloxy]-26,28- dihyroxythiacalix[4]arene (4 g)

Yield: 0,049 g, **35,3%; mp:** 292-307 ºC **FT-IR,** ν_{max} (cm^{-1}): 3265 (-OH); 3060 (Arom.C-H); 2926 (Aliphatic C-H); 1677 (N=N); 1090 (C-O). ^{1}H-NMR (DMSO-d_6), δ(ppm): 5.85 (s, 2H, -CH); 4.75 (s, 4H, -CH_2); 2.54 (s, 6H, -CH_3); 6.60-7.85 (m, 20H, Arom.C-H); 10.42 (s, 2H, -OH), 9.80 (s, 2H, -OH).

Synthesis of 25,27-bis-[4-(3-methyl-1'-phenyl-5'-pyrazolon-4-yl-azo) benzyloxy]-26,28- dihyroxythiacalix[4]arene (4h)

Yield: 0,073 g, **47,7%; mp:** 220-230 ºC **FT-IR,** ν_{max} (cm^{-1}): 3268 (-OH); 3060 (Arom.C-H); 2922 (Aliphatic C-H); 1677, 1594 (N=N); 1090 (C-O). ^{1}H-NMR (DMSO-d_6), δ(ppm): 6.05 (s, 2H, -CH); 4.79 (s, 4H, -CH_2); 2.25 (s, 6H, -CH_3); 6.60-7.25 (m, 30H, Arom.C-H); 8.15 (s, 2H, -OH).

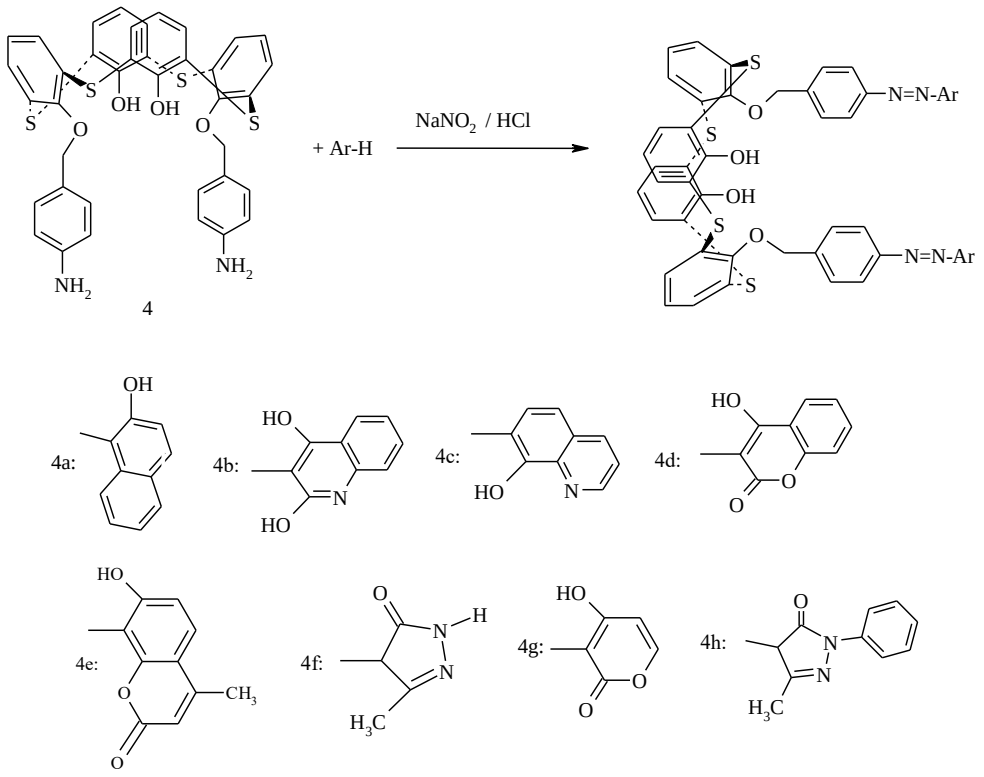

Scheme 5. General Reaction Scheme of Synthesized Compounds

Absorption Study:

In this part of our study, the effects of the substituents, different solvents and the pH of the medium on the colors of the azo dyes obtained were investigated. The change in maximum absorption wavelengths in these solvents was examined. The concentrations in each solvent are different due to the resolution. Protic solvents can form hydrogen bonds with the electron pair of the carbonyl group oxygen. In this case, while reducing the n energy level, π * energy level does not bring a change occurs.

Solvent Effect:

Visible absorption spectra of the synthesized azo dyes were obtained in six different solvents (DMSO, DMF, MeCN, MeOH, AcOH, $CHCl_3$).

Acid-Base Effect:

In this part of our study, the UV-visible region spectra of the dyes were taken by adding HCl and KOH in methanol to examine the absorption spectra of the compounds in acidic and basic environment.

3. Result

In the results of FT-IR spectrums, the broad bands resulting from O-H stretching vibrations were seen in the range of 3423-3264 cm^{-1}. The bands in the range of 3026-3064 cm^{-1} were assigned to aromatic C-H stretching vibrations, aliphatic C-H stretching vibrations were also identified at the range of 2962-2913 cm^{-1}. The peaks at the range of 1678-1594 cm^{-1} corresponded to N=N stretching and bending vibrations azo bridges. The peaks associated to C-O bonds were seen at 1090- 1001 cm^{-1}. The peaks at 3325 cm^{-1} were associated to $-NH_2$ stretching vibration only for compound 4. The peaks associated to NO_2 bonds were seen at 1512-1346 cm^{-1} only for compound 3 **(Table 1).**

Table 1: Values of FT-IR spectra of compounds.

Compound	FT-IR, υ_{max} (cm^{-1})						
	-OH	**$-NH_2$**	**Arom. C-H**	**Aliphatic C-H**	**N=N**	**NO_2**	**C-O**
1	3323		3026	2962			1087
2	3270		3062	2913			1063
3	3385		3060	2950		1512 1346	1001
4	3423	3325	3007	2919			1066
4a	3266		3060	2923	1678-1596		1090
4b	3264		3059	2926	1678-1596		1090
4c	3268		3064	2926	1678-1607		1090
4d	3267		3059	2926	1678-1607		1090
4e	3266		3059	2926	1678-1597		1090
4f	3265		3059	2922	1677		1090
4g	3265		3060	2926	1677		1090
4h	3268		3060	2922	1677-1594		1090

^{1}H-NMR spectral results for compounds 1, 2 and 3 were found to be consistent with the literature. And then the peak of OH proton for Compound 4 was observed at 11.25 ppm. While aromatic protons belonging to this structure were

observed between 6,20 and 8,75 ppm, aliphatic protons were observed at 3,82 and 5,26 ppm. The amine protons in the compound were seen at 13.01 and 15.05 ppm (**Table 2)**.

When the NMR results obtained for the synthesized dyes were examined, the peaks of OH protons were seen between 8.12-11.65 ppm. Aromatic protons were obtained between 6.50-9.06 ppm and aliphatic protons were obtained between 2.25-6.18 ppm. The proton of the imine was observed at 9.57 ppm only for the compound 4f (**Table 2)**.

The integration rates obtained from the NMR results are proportional to the structures of the synthesized compounds.

Table 2: Values of ^{1}H-NMR spectra of compounds.

Compound	**^{1}H-NMR δ(ppm)**			
	Ar-OH	**Arom. C-H**	**Aliphatic C-H**	**-NH_2, -NH**
1	9,63 (s, -OH)	7,67 (s, 8H, Arom.C-H)	1,25 (s, 36H, tert-buthyl)	
2	9,45 (-OH)	8,50-8,42 (m, 12H, Arom.C-H)		
3	7,88 (s,2H,-OH)	6,81, 7,09, 7,79 (m, 12H, Arom.C-H); 7,61, 8,21 (d,d, 8H Arom.C-H)	5,51 (s, 4H, -CH_2)	
4	11,25 (s, 2H,-OH)	6,20, 8,75 (m, 20H, Arom.C-H)	3,82, 5,26 (s, 4H, -CH_2)	13,01, 15,05 (s, 4H, -NH_2)
4a	11.20, (s, 2H,-OH), 9.80 (s, 2H,-OH)	6.68-8.81 (m, 32H, Arom.C-H)	4.76-4.80 (s, 4H, -CH_2)	-
4b	11.65 (s, 2H,-OH), 9.90 (s, 2H,-OH)	7.05-8.94 (m, 28H, Arom.C-H)	4.91 (s, 4H, -CH2)	-
4c	11.05, 9.80 (s, 4H,-OH	7.14-8.84 (m, 30H, Arom.C-H)	4.90 (s, 4H, -CH_2)	-
4d	11.10, 12.85 (s, 4H,-OH	7.12-8.89 (m, 28H, Arom.C-H)	4.88 (s, 4H, -CH_2)	-
4e	11.10, 10.05 (s, 4H,-OH	7.05-9.06 (m, 24H, Arom.C-H)	6.18, (s, 2H, -CH), 4.91 (s, 4H, -CH_2)	-
4f	8.12 (s, 2H,-OH	6,50- 8,15 (m, 20H, Arom.C-H)	5.89 (s,1H,CH),4.79 (s, 2H, -CH_2), 2.25 (s,3H,CH_3)	9.57 (s,1H,NH)
4g	10.42,9.80 (s, 2H,OH)	6,60- 7,85 (m, 20H, Arom.C-H)	5.85 (s,1H,CH),4.75 (s, 2H, -CH_2), 2.54 (s,3H,CH_3)	-

4h	8.15 (s, 2H,OH)	6,60- 8,25 (m, 30H, Arom.C-H)	6.05 (s,1H,CH),4.79 (s, 2H, -CH_2), 2.25 (s,3H,CH_3)	-

When the absorption values of the compounds in different solvents are taken into consideration in the spectra taken in DMSO, the compound 4a shows a double maximum, while the other compounds show a single maximum. The spectra of compounds 4a, 4c are observed at long wavelengths. When the spectrum in DMF is examined, it is observed that the compound 4c gives a double maximum while the others have a single maximum. 4a is seen at long wavelength, and 4c at short wavelength. In the spectra in acetonitrile, the compound 4a gives a double maximum while the others have a single maximum. The 4a and 4c compounds are seen at long wavelength and the 4b compound at short wavelength. When the spectrum in methanol is examined, it is observed that all compounds give a single maximum. 4a and 4d compound at short wavelength. When the spectrum in acetic acid is examined, it is observed that the compound 4a gives a double maximum, while the compound 4e does not give a maximum and the other compounds have a single maximum. 4a, 4c compounds at long wavelength, and 4b, 4d, 4f and 4g compounds at short wavelength. When the spectrum in chloroform is examined, it is observed that the compound 4a gives a double maximum while the others have a single maximum. 4a, 4d and 4f compounds at long wavelength and 4b and 4c compounds at shorter wavelength. According to these results, it can be said that the compounds are not in a single tautomeric form and may exist in different tautomeric forms (**Table 3)**.

Table 3: Values of UV-vis. spectra of compounds.

Compound	DMSO	DMF	Acetonitrile	Methanol	Acetic acid	Chloroform
4a	409 478 518 s	412 478 s 518 s	397 469 510 s	411 477 s	385 490 516 s	397 481 514 s
4b	422	417	421 398 s	423 394 s	432 395 s	434 394 s
4c	411 461 s 491 s	459 490 433 s	401 455 s	446	392 457 s	434 392 s
4d	419	414	405	415 389 s	421 388 s	363 389 s 429 s
4e	405	404	392	389	371 s	370
4f	411	409	403	405	411 370 s	354 421 s
4g	410	409	401	403	409 389 s	385
4h	403	402	396	396	396	397

S: Shoulder

When the spectrum in methanol + HCl is examined, the 4a and 4d compounds give a double maximum, while the 4c and 4e compounds do not give a maximum and the others have a single maximum. 4a is observed at long wavelength and 4b at short wavelength. The compounds 4a, 4c, 4d, 4g and 4h show hipsochromic shift when compared to the spectra taken in methanol, while the 4b and 4f compounds do not change much. When the HCl of 4e compound in methanol was added, it changed to hypsochromic shift and turned into short wavelength shoulder. When the spectra in methanol + HCl are examined in general, it is observed that λmax values are hipsochromic shift according to the spectra taken in methanol. When the spectrum in methanol + KOH is examined, it is observed that all compounds have a single

maximum. Shoulders of 4a, 4b, 4d and 4h are seen at long wavelength. Compared to the spectra taken in methanol, other compounds except for 4b and 4c were observed to have been subjected to a bichocromic shift. When the spectra in methanol + KOH are examined in general, it can be concluded that λmax values have been subjected to the batochromic shift according to the spectra taken in methanol (**Table 4**).

Table 4: Values of UV-vis. spectra of compounds in acidic and basic solvents.

Compound	Methanol	Methanol + KOH	Methanol + HCl
4a	411 477 s	431 456 s	376 482 513 s
4b	423 394 s	388 452 s	426 394 s
4c	446	436	417
4d	415 389 s	426 495 s	390 421
4e	389	437	 378 s
4f	405	427	422
4g	403	437	357
4h	396	396 428 s	393

S: Shoulder

The colors from the left to right of the 4a, 4b, 4c, 4d, 4e, 4f, 4g, 4h azo dyes we synthesize are shown below (**Figure 1)**.

Figure 1. Color scale of synthesized compounds

The color states of the compound 4a at 25 ºC at different pH values are shown below. In the acidic environment, the shades of orange color shift to purple hues in the basic environment (**Table 5 and Figure 2)** .

Table 5. Colors of compound 4a at different pH values.

1	2	3	4	5	6	7	8	9	10	11	12
2,70	2,79	2,88	2,98	3,44	8,15	9,23	10,3	11,55	12,09	12,37	12,48

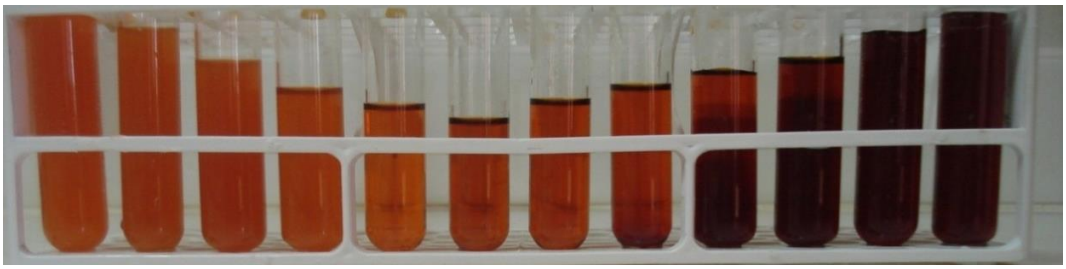

Figure 2. Solvents of compound 4a at different pH values

4. Discussion and Conclusion

Obtained from the analysis results; the synthesized dyes have different tautomeric structures. As shown in **Scheme 6**, several of the possible tautomeric forms on the compound 4a are shown. Of these, diketo-dihydrazo, dienol-diazo, keto-hydrazo-enol-azo are given. Apart from these, there are different representations of these tautomers and anionic and cationic tautomers.

In the structures containing the hydroxyl group in the FT-IR spectrum of the synthesized compounds, the peaks observed in the -OH group and the absence of any peaks of the carbonyl group indicate that the compound may be present in the solid dienol-diazo tautomeric form.

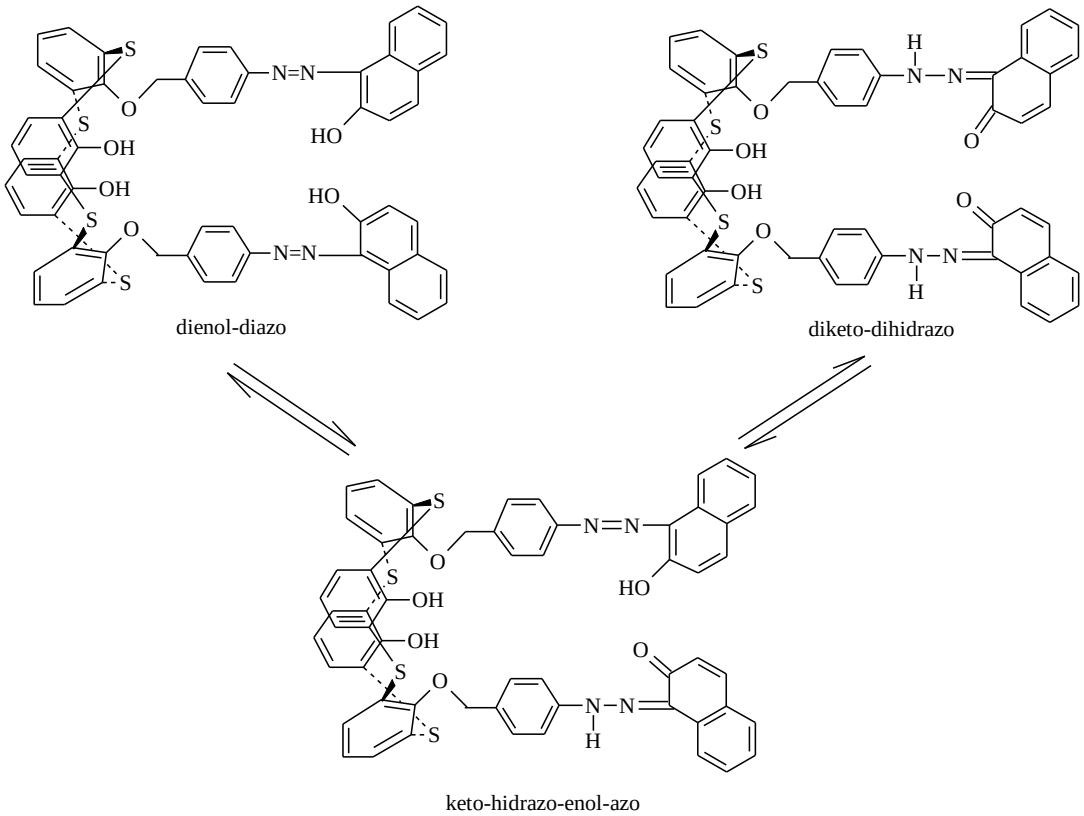

Scheme 6. Possible tautomeric structures of compound **4a**.

As a result, eight different dyes of thiacalix[4]arene were successfully synthesized and macrocyclic chemistry was introduced into new compounds.

5. References

[1] A. Whitaker, J. Soc. Dyers Colour, 1995, vol. 111, pp. 66–72.

[2] M.S. Yen, I.J. Wang, Dyes Pigm., "A facile syntheses and absorption characteristics of some monoazo dyes in bis-heterocyclic aromatic systems part I: syntheses of polysubstituted-5-(2-pyrido-5-yl and 5-pyrazolo-4-yl)azo-thiophene derivatives" 2004, vol. 62, pp. 173–180.

[3] M.S. Yen, I.J. Wang, Dyes Pigm., "A facile syntheses and absorption characteristics of some monoazo dyes in bis-heterocyclic aromatic systems: part II: syntheses of 4-(p-substituted) phenyl-2-(2-pyrido-5-yl and 5-pyrazolo-4-yl)azo-thiazole derivatives" 2004, vol. 63, pp. 1–9.

[4] N. Ertan, Dyes Pigm. "Synthesis of some hetarylazopyrazolone dyes and solvent effects on their absorption spectra" 2000, vol. 44, pp. 41–48.

[5] F. Karcı and N. Ertan, Dyes Pigm., "Hetarylazo disperse dyes derived from 3-methyl-1-(3′,5′-dipiperidino-s-triazinyl)-5-pyrazolone as coupling component" 2002, vol.55, pp. 99–108.

[6] A. T. Peters, "Chisowa E. Colour-constitution relationships in 2-acylamino-4-N, Ndiethylaminobenzene disperse dyes" Dyes and Pigments, 1993, vol. 22(4), pp. 223-38.

[7] H. Hartmann, M. Schulze, R. Guenter, "Nucleophilic substitution in arylazo phenols e a simple route for preparing chloro-substituted azobenzenes" Dyes and Pigments, 1991, vol. 15(4), pp. 255-62.

[8] Kon et al. "Synthesis of p-tert-butylthiacalix [n] arenes (n= 4, 6, and 8) from a sulfur-bridged acyclic dimer of p-tert-butylphenol" Tetrahedron Letters, 2002, vol. 43.12 pp. 2231-2234.

[9] Sone et al. Abstract Book of Workshop on Calixarenes and Related Compounds, p. PS/B-36, 2–4 June 1993, Fukuoka, Japan.

[10] Sone et al. "Synthesis and properties of sulfur-bridged analogs of p-tert-Butylcalix[4]arene" Tetrahedron,1997, vol. 53, pp. 10689-10698.

[11] Iki, et al. "Selective oxidation of thiacalix[4]arenes to the sulfinyl- and sulfonylcalix[4]arenes and their coordination ability to metal ions" Tetrahedron Lett., 1998, vol. 39, pp. 7559-7562.

[12] Akdaş et al., "Thiacalixarenes: Synthesis and structural analysis of thiacalix[4]arene and of p-tert-butylthiacalix[4]arene" Tetrahedron Letters, 1998, vol: 39, pp. 2311-2314.

[13] Proto et al., "Ethylene polymerization promoted by dinuclear titanium p-tert-butylthiacalix[4]arene complexes" European Polymer Journal, 2009, vol.45, pp. 2138-2141.

[14] Ali et al., "Comparison study of evaporated thiacalix[4]arene thin films on gold substrates as copper ion sensing" Thin Solid Films , 2006, vol: 495 , pp. 368-371.

[15] Zaghbani et al., "Selective thiacalix[4]arene bearing three amide groups as ionophore of binary Pd(II) and Au(III) extraction by a supported liquid membrane system" Separation and Purification Technology, 2007, vol: 57, pp. 374-379.

[16] Zlatuskova et al., "Novel anion receptors based on thiacalix[4]arene derivatives" Tetrahedron Letters, 2004, vol. 60, pp. 11383-11390.

[17] Lhotak et al., "Diazo coupling: an alternative method for the upper rim amination of thiacalix[4]arenes" Tetrahedron Letters, 2002, vol. 43, pp. 3665-3668.

[18] Chakrabarti et al., "Synthesis and cation binding properties of new arylazo- and heteroarylazotetrathiacalix[4]arenes" Tetrahedron, 2006, vol: 62, pp. 1150-1157.

[19] Kumagai et al., "Facile synthesis of p-tert-butylthiacalix[4]arene by the reaction of p-tert-butylphenol with elemental sulfur in the presence of a base" Tetrahedron Letters, 1997, vol: 38, pp. 3971-3972.